

## A Monolithic Switching Regulator with 100 $\mu$ V Output Noise

"Silence is the perfectest herald of joy ..."

Jim Williams

### INTRODUCTION

Size, output flexibility and efficiency advantages have made switching regulators common in electronic apparatus. The continued emphasis on these attributes has resulted in circuitry with 95% efficiency that requires minimal board area. Although these advantages are welcome, they necessitate compromising other parameters.

#### Switching Regulator "Noise"

Something commonly referred to as "noise" is a primary concern. The switched mode power delivery that permits the aforementioned advantages also creates wideband harmonic energy. This undesirable energy appears as radiated and conducted components commonly labeled as "noise." Actually, switching regulator output "noise" is not really noise at all, but coherent, high frequency residue directly related to the regulator's switching.<sup>1</sup> Figure 1 shows typical switching regulator output noise. Two distinct characteristics are present. The slow, ramping output ripple is caused by finite storage capacity of the regulator's output filter components. The quickly rising spikes are associated with the switching transitions. Figure 2 shows another switching regulator output. In this case the ripple has been eliminated by adequate filtering and linear postregulation, but the wideband spikes remain. It is these fast spikes that cause so much difficulty in systems. Their high frequency content often corrupts associated circuitry, degrading performance or even disabling operation. Noise gets into adjacent circuitry via three paths. It is conducted out of the regulator output lead, it is conducted

back to the driving source ("reflected" noise) and it is radiated. The multiple transmission paths combine with the high frequency content to make noise suppression difficult. Unconscionable amounts of bypass capacitors, ferrite beads, shields, Mu-metal and aspirin have been expended in attempts to ameliorate noise-induced effects.

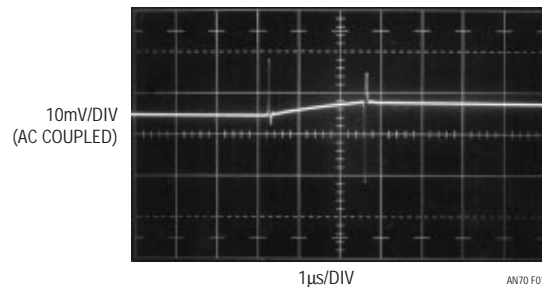


Figure 1. Typical Switching Regulator Output "Noise." Wideband Spikes Are Difficult to Suppress, Causing System Interference Problems. Ripple Component Has Low Harmonic Content, Is Relatively Easily Filtered

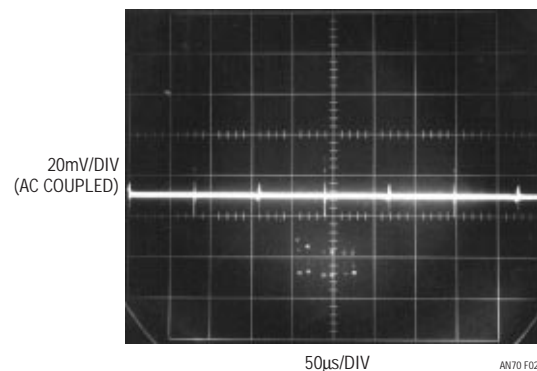


Figure 2. Linear Regulator Eliminates Ripple, but Wideband Spikes Remain. Peak-to-Peak Amplitude Exceeds 30mV (Just Visible Near 2nd, 5th and 8th Vertical Graticule Divisions)

Note 1. Noise contains no regularly occurring or coherent components. As such, switching regulator output "noise" is a misnomer. Unfortunately, undesired switching related components in the regulated output are almost always referred to as "noise." As such, although technically incorrect, this publication treats all undesired output signals as "noise." See Appendix B, "Specifying and Measuring Something Called Noise."

# Application Note 70

Alternate approaches involve synchronizing switching regulator operation to the host system or turning off switching during critical system operation (an “interrupt driven” power supply). Another approach places critical system operations between switch cycles, literally running between electronic rain drops.<sup>2</sup>

The difficulty of debugging a noise-laden system and the compromises involved in synchronized approaches could be eliminated with a low noise switching regulator. An inherently low noise switching regulator is the most attractive approach because it eliminates noise concerns while maintaining system flexibility.

## A Noiseless Switching Regulator Approach

The key to an inherently low noise regulator is to minimize harmonic content in the switching transitions. Slowing down the switching interval does this, although power dissipated during the transition causes some efficiency loss. Reducing switch repetition rate can largely offset the

losses, resulting in a reasonably efficient design with small magnetics and the desired low noise. Noise reduction by restricting harmonic generation has been employed before, although the implementations were complex and narrowly applicable.<sup>3</sup> A monolithic approach, broadly usable over a range of magnetics and applications, is described here.

## A Practical, Low Noise Monolithic Regulator

Figure 3 describes the LT<sup>®</sup>1533, a monolithic regulator designed for low noise switching supplies. Figure 4 details the pin functions. Figure 3’s functional blocks show a fairly conventional push-pull architecture with a major exception. The push-pull approach has good magnetics utilization (power transfer is always occurring in the transformer; the core does not store energy) and pulls current

Note 2: See References 2 and 3 for details and practical examples of these techniques.

Note 3: See Appendix A, “A History of Low Noise DC/DC Conversion.” See also References 4 through 10.

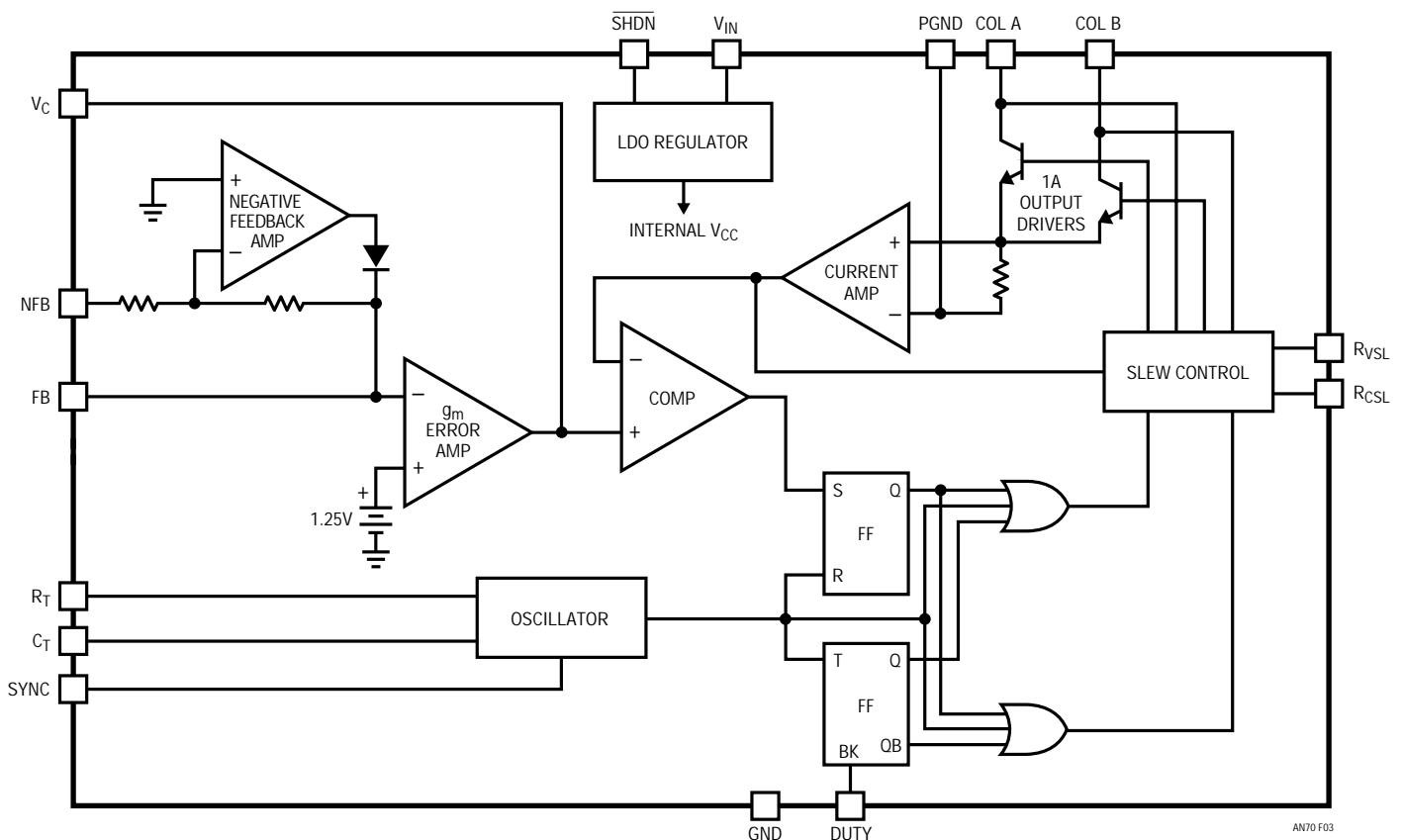


Figure 3. LT1533 Simplified Block Diagram. 1A Slew-Controlled Output Stages Provide Low Noise Switching

COL A, COL B: Output transistor collectors which switch out-of-phase.

DUTY: Grounding this pin forces the outputs to switch at a 50% duty cycle. This pin must float if not used.

SYNC: Used to synchronize to an external clock. Float or tie to ground if unused.

$C_T$ : Oscillator timing capacitor.

$R_T$ : Oscillator timing resistor.

FB: Used for positive output voltage sensing.

NFB: Used for negative output voltage sensing.

GND: Analog ground pin.

PGND: High current ground return. Should be returned to ground via  $\approx 50\text{nH}$  ( $\approx 1''$  of PC trace or wire, or a small ferrite bead). See Appendix F or schematic (Figures 5 and 26) notes for details. In some package options, this pin may be internally connected to "GND" pin.

$V_C$ : Frequency compensation node.

SHDN: Normally high. Grounding this pin shuts the part down.  $I_{\text{SHDN}} = 20\mu\text{A}$ .

$R_{\text{CSL}}$ : Current slew control resistor.

$R_{\text{VSL}}$ : Voltage slew control resistor.

$V_{\text{IN}}$ : Input supply pin. 2.7V to 30V range. Undervoltage lockout at 2.55V.

Figure 4. LT1533 Short Form Pin Function Descriptions

continuously from the source. The even, continuous current drain from the source eliminates the fast, high peak currents required by flyback and other approaches. The source sees a benign load and is not corrupted. The switches also receive nonoverlapping drive, ensuring they do not conduct simultaneously. Simultaneous conduction

would cause excessive, quickly rising currents, degrading efficiency and generating noise.

The design's most significant aspect is the output stage. Each 1A power transistor operates inside a broadband control loop. The voltage across each transistor and the current through it are sensed and the loop controls slew rate of each parameter. The voltage and current slew rates are independently settable by external programming resistors. This ability to control the switching's rate-of-change makes low noise switching regulation practical. Operating the switching transistors in a local loop permits predictable, wide range control over a variety of situations.<sup>4</sup> Figure 5 is a 40kHz, 5V to 12V converter using the LT1533 in a push-pull, "forward" configuration. The feedback resistor's ratio produces a 12V output. A two-section LC filter provides high ripple attenuation, although a single section will give good performance. It is particularly noteworthy that high frequency noise content (as opposed to the 40kHz fundamental related ripple) is unaffected by output filter characteristics. This is so simply because there is so little high frequency energy developed in this circuit. If there's nothing there, it doesn't need to be filtered!

L2 provides compensation for the output current control loop. In practice, L2 may be a length of PC trace, a small inductor, a coiled section of wire or a ferrite bead. See Appendix F, "Magnetics Considerations" for complete discussion.

Note 4: Patent pending.

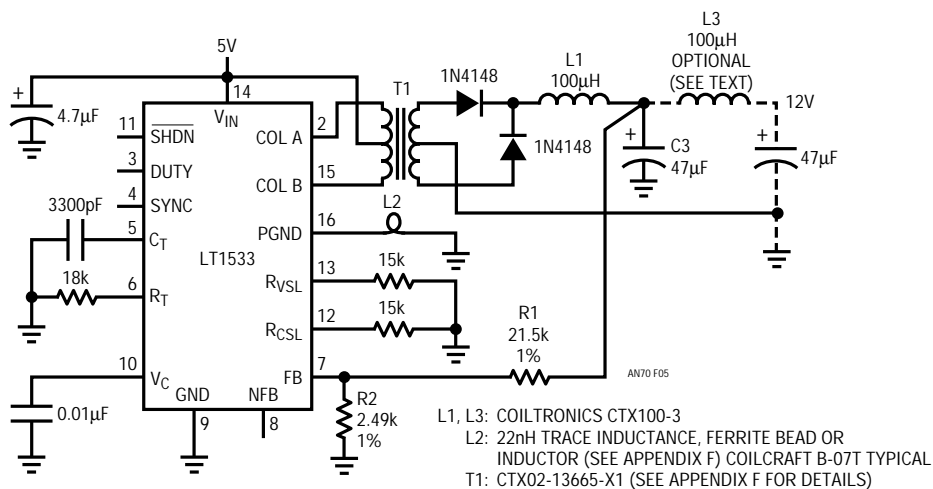


Figure 5. 100µV Noise 5V-to-12V Converter. Output LC Section May Be Deleted If Low Frequency Ripple Is Acceptable

# Application Note 70

## Measuring Output Noise

Measuring the LT1533's unprecedented low noise levels requires care.<sup>5</sup> Figure 6 shows a test setup for taking the measurement. Good connection and signal handling technique combined with judicious instrumentation choice should yield a 100 $\mu$ V noise floor in a 100MHz bandwidth. This corresponds to the noise of a 50 $\Omega$  resistor in a 100MHz bandwidth.

Before measuring regulator output noise, it is good practice to verify test setup performance. This is done by running the test setup with no input. Figure 7 shows a noise base line of 100 $\mu$ V in a 100MHz bandwidth, indicating the instrumentation is operating properly. Measuring Figure 5's noise involves AC coupling the circuit's output into the test setup's input. Figure 8 shows this. Coaxial connections must be maintained to preserve measurement integrity.<sup>6</sup> Figure 9's waveforms detail circuit operation. Traces A and C are switching transistor collector voltages, B and D are the respective transistor currents. The test setup's output, representing circuit output noise, is Trace E. Wideband spiking and ripple, just visible in the noise floor, is inside 100 $\mu$ V, even in a 100MHz bandpass.<sup>7</sup>

This is spectacularly good performance and is, in fact, actually better than the photo shows. Removing all probes from the breadboard leaves only Trace E's coaxial connection. This eliminates any possible ground loop-induced error.<sup>8</sup> Figure 10's trace shows 40kHz ripple with about the same amplitude as in Figure 9. Switching related spikes, just faintly outline in the noise, are reduced.

Measurement bandwidth is reduced to 10MHz in Figure 11, attenuating test fixture amplifier noise. Switching and ripple residue amplitude and shape do not change, indicating no signal activity beyond this frequency. Figure 12's

Note 5: Equipment selection and measurement techniques are detailed in Appendix B, "Specifying and Measuring Something Called Noise." See also Appendix C, "Probing and Connection Techniques for Low Level, Wideband Signal Integrity."

Note 6: Again, see Appendices B and C for extended treatment of these and related issues.

Note 7: It is common industry practice to specify switching regulator noise in a 20MHz bandpass. There can be only one reason for this, and it is a disservice to users. See Appendix B for tutorial on observed noise versus measurement bandwidth.

Note 8: See Appendix C for related discussion and techniques for triggering oscilloscopes without invasively probing the circuit.

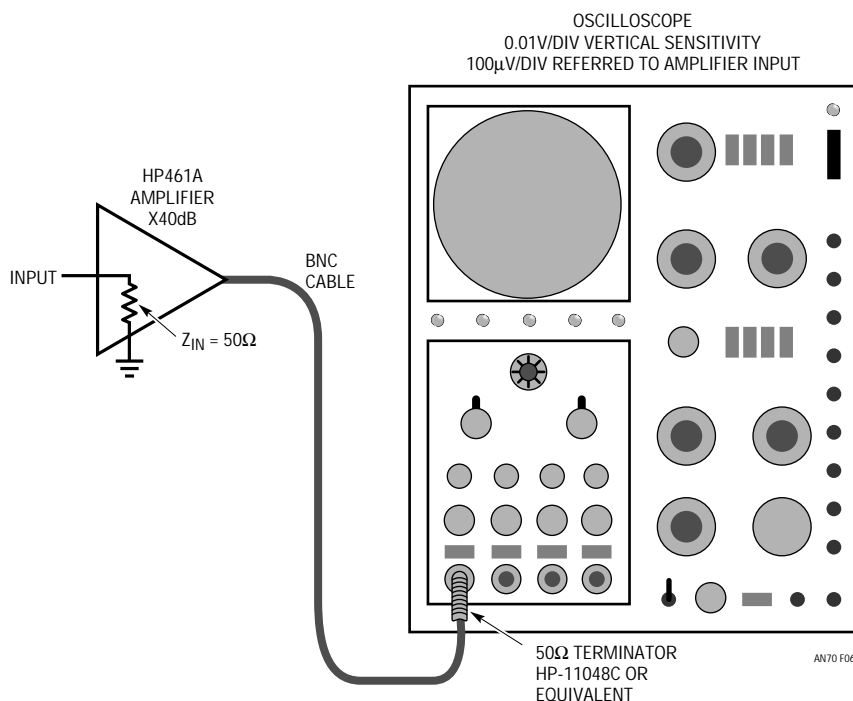


Figure 6. Test Setup Noise Baseline Is 100 $\mu$ V<sub>p-p</sub> in 100MHz Bandwidth. Performance Is 50 $\Omega$  Resistor Noise Limited. BNC Cable Connections and Terminations Provide Coaxial Environment, Ensuring Wideband, Low Noise Characteristics

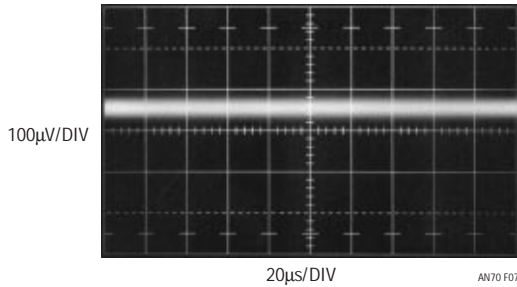


Figure 7. Oscilloscope Verifies Test Setup 100µV Noise Floor in 100MHz Bandwidth. Indicated Noise Is That of a 50Ω Resistor

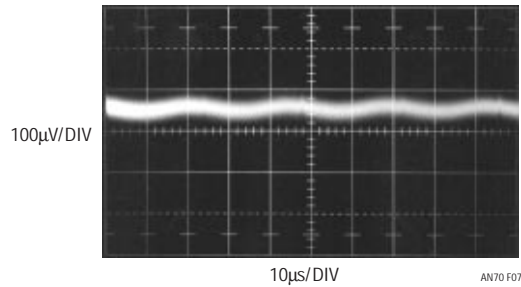


Figure 10. Removing Probes from Figure 9's Test Eliminates Ground Loops, Slightly Reducing Observed Noise. Switching Artifacts Are Just Discernible Above Noise Floor

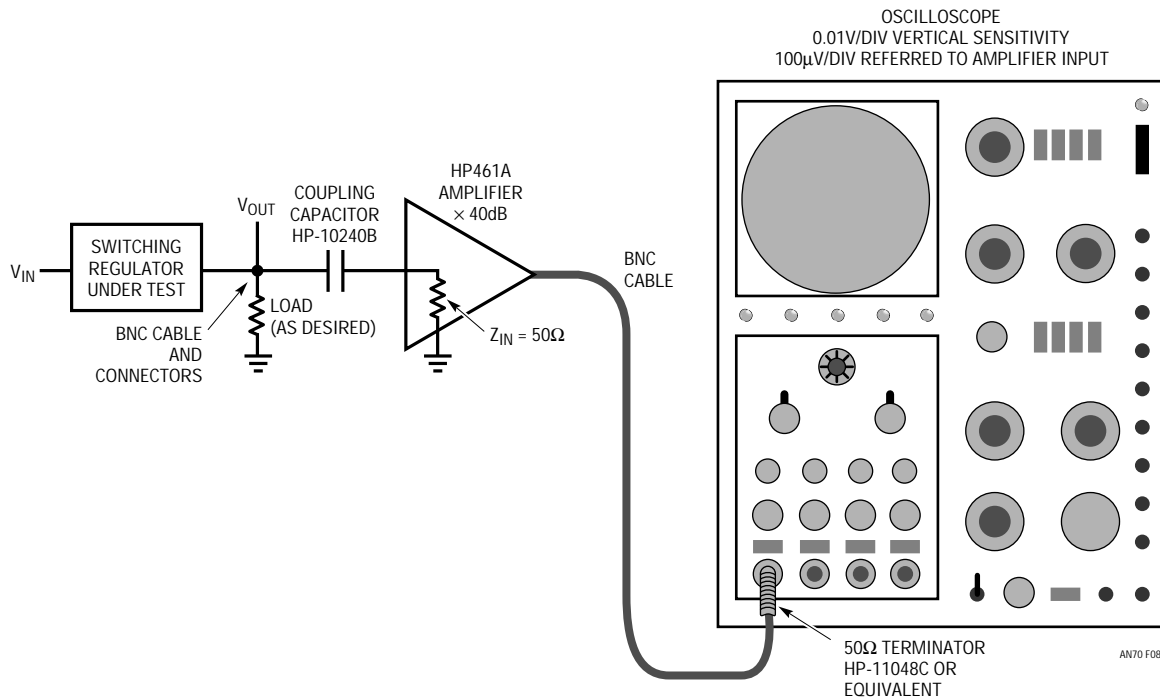


Figure 8. Connecting Figure 5's Circuit to the Test Setup. Coaxial Connections Must Be Maintained to Preserve Measurement Integrity

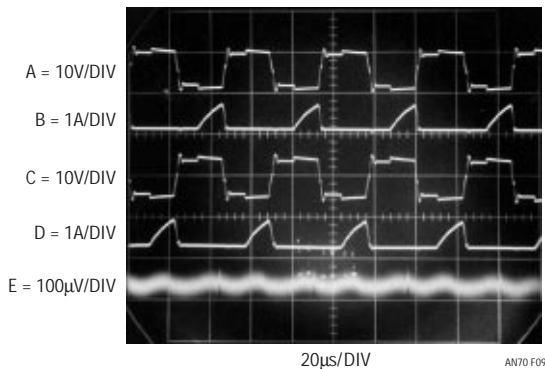


Figure 9. Waveforms for Figure 5 at 100mA Loading. Traces A and C Are Voltage; B and D are Current, Respectively. Switching Transition's Noise Signature Appears in Trace E, the Circuit's Output Noise

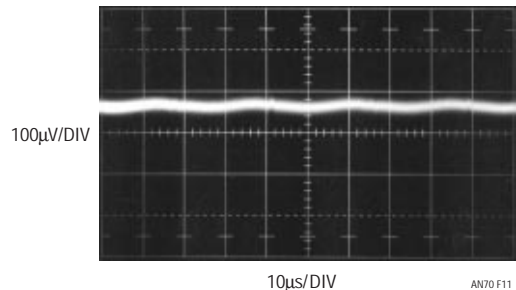


Figure 11. Reducing Measurement Bandwidth to 10MHz Attenuates Amplifier Noise. Switching Residue Characteristics Remain Unchanged, Indicating No Signal Activity Beyond This Frequency



# Application Note 70

horizontal expansion of Figure 10 returns to 100MHz bandpass. The switching spike appears in the center screen region. At 2 $\mu$ s/division sweep, there is no wide-band activity observable. Figure 13, a 10MHz bandpass version of Figure 12, retains all signal information, further suggesting no signal power beyond 10MHz.

Figure 14 is the noise floor of an HP4195A spectrum analyzer in a 500MHz sweep. When Figure 5's circuit is AC coupled into the analyzer, the output (Figure 15a) is essentially identical. The analyzer is unable to detect switching-induced noise in a 500MHz bandpass. Some 40kHz fundamental-related components are detectable in Figure 15b's 1MHz wide plot, although the rest of the sweep is analyzer noise limited. Additional filtering or a linear postregulator could eliminate the 40kHz ripple-related residue if desired.

The preamplified oscilloscope is a more sensitive tool for these measurements because its triggered operation has the advantage of synchronous detection. This is demonstrable by free running the preamplified oscilloscope sweep; the switching-related components are indistinguishable in the noise background.

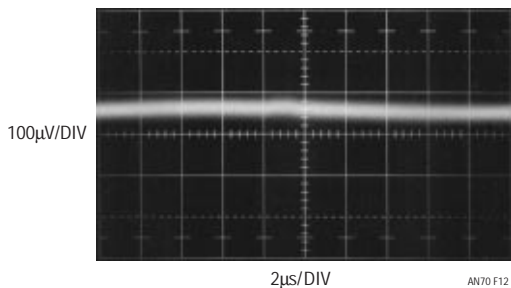


Figure 12. Horizontal Expansion of Figure 10 Shows No Wideband Components. Switching Originated Noise Appears in Center Screen Region

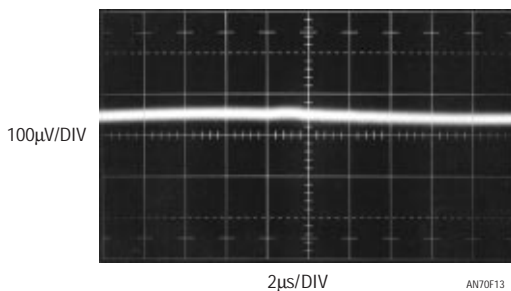


Figure 13. A 10MHz Band Limited Version of Figure 12. As Before, Signal Information Is Retained, Although Amplifier Noise Is Reduced. Results Indicate No Signal Power Beyond 10MHz

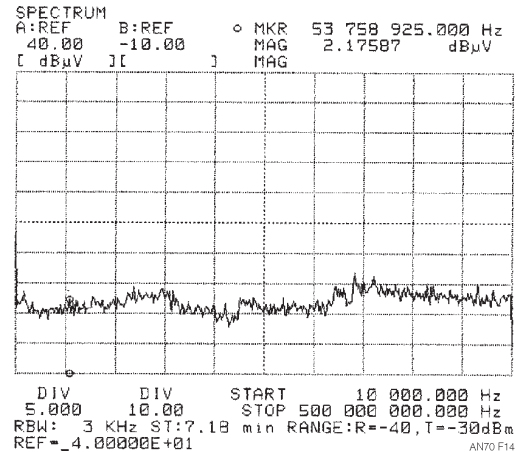


Figure 14. Noise Floor of Test Fixture and HP-4195A Spectrum Analyzer in a 500MHz Sweep

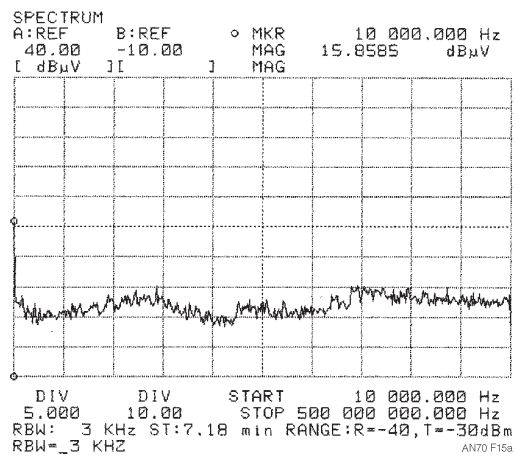


Figure 15a. Figure 5's Circuit Connected to the Spectrum Analyzer Produces Essentially Identical Results to Figure 14. Circuit's Noise Is Undetectable

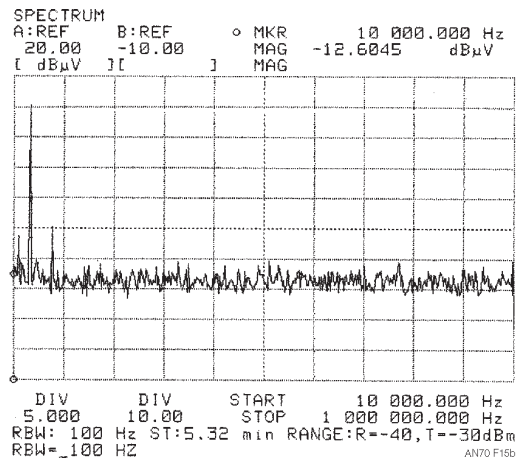


Figure 15b. Reducing Analyzer Sweep to 1MHz Width Reveals 40kHz Related Components. Remainder of Plot Is Analyzer Noise Floor Limited, Even in Sensitive 455kHz Band

Figure 16 studies ripple at the first LC filter section output. The ripple's 40kHz fundamental is clearly seen, although no wideband spikes are visible. Figure 17 horizontally expands Figure 14's time scale, but high frequency harmonics and spikes are not observable.

Low frequency noise is rarely a concern, although Figure 18 shows it is inside 50 $\mu$ V in a 10Hz to 10kHz bandpass. Input current noise is usually of more interest. Excessive "reflected" noise can corrupt the regulator's driving source, causing system level interference. Figure 19 shows Figure 5's input current as DC with a small, 40kHz fundamental-related sinusoidal component. There is no high frequency content, and the sinusoidal variations are easily handled by the driving source.

## System-Based Noise "Measurement"

In the final analysis, the effect of switching regulator output noise on the system it is powering is the ultimate test. Appendix K, "System-Based Noise "Measurement," presents results when the LT1533 is used to power a 16-bit A/D converter.

## Transition Rate Effects on Noise and Efficiency

In theory, simply setting transition rate to low values will achieve low noise. Practically, such an approach, while workable, wastes power during transitions, lowering efficiency. A good compromise sets transition time at the fastest rate permitting desired noise performance. The LT1533's slew adjustments allow easy determination of this point. Figure 20's photographs dramatically demonstrate the relationship between transition time and output noise for Figure 5's circuit. The sequence shows >5:1 noise reduction as switch transition time slows from 100ns (20a) to 1 $\mu$ s (20d). Figure 20d's displayed noise is actually lower, as the probing-induced error caused by monitoring the switch corrupts the measurement.<sup>9</sup>

Figure 21 graphically summarizes Figure 20's information. Significant noise reduction coincides with descending transition slew time until about 1.3 $\mu$ s. Little additional noise benefit occurs beyond this point. Figure 22 shows efficiency fall-off with slew time. There is a 6% penalty between 100ns and 1.3 $\mu$ s, the same region where noise performance improves by a factor of 5 (per previous

Note 9: See Appendix C, "Probing and Connection Techniques for Low Level, Wideband Signal Integrity" for guidance.

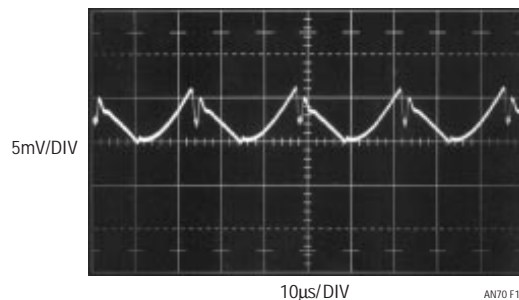


Figure 16. Ripple at Figure 5's First LC Output Has No Wideband Spikes

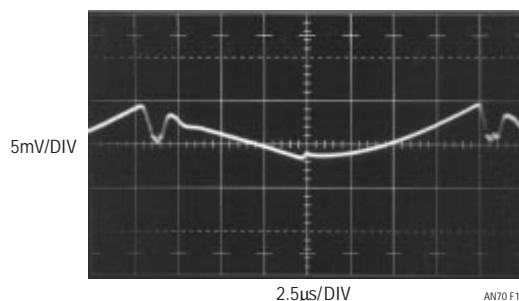


Figure 17. Time Expansion of Previous Figure. No High Frequency Content Is Visible

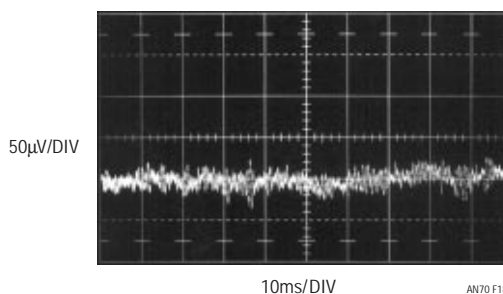


Figure 18. Low Frequency Noise in a 10Hz to 10kHz Bandpass

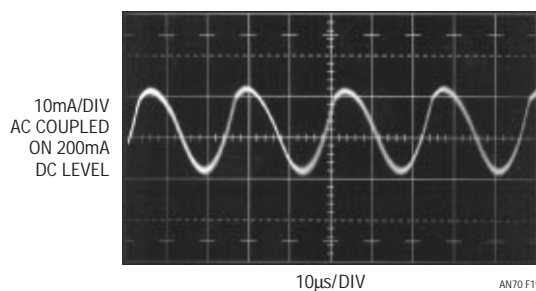


Figure 19. Figure 5's Small Sinusoidal Input Current Variations Contain No High Frequency Content and Are Easily Absorbed by Input Supply

# Application Note 70

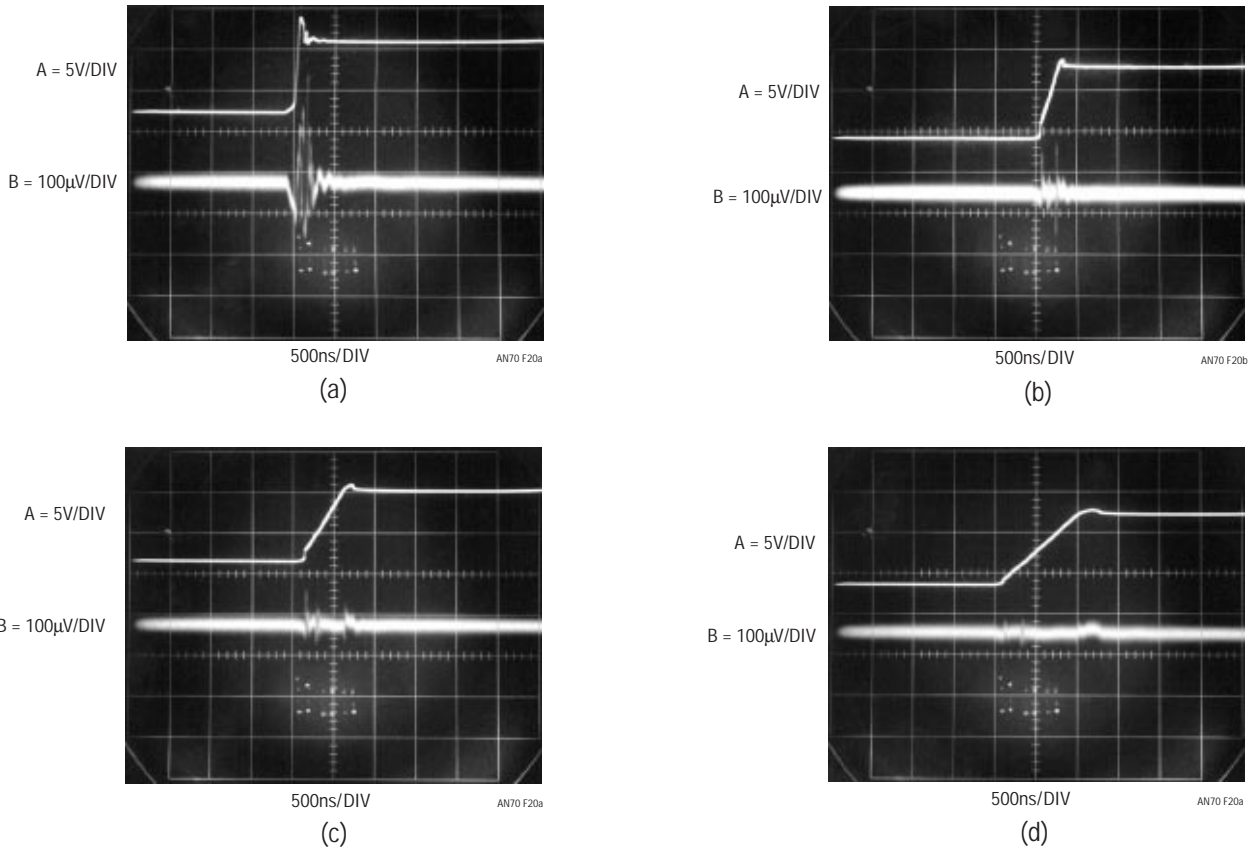


Figure 20. Output Noise (Trace B) vs Different Switch Slew Rates (Trace A). Highest Slew Rate (Figure a) Causes Largest Noise. Retarding Slew Rate (Figures b and c) Decreases Noise Until Lowest Noise Performance Is Achieved (Figure d)

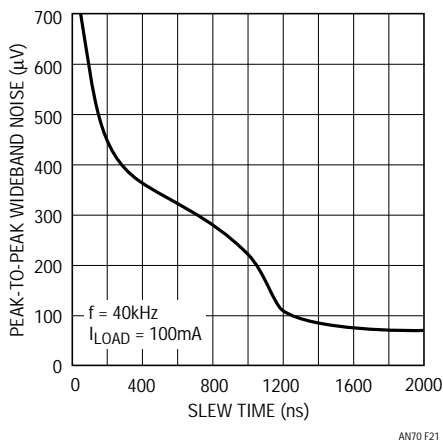


Figure 21. Figure 5's Noise vs Slew Time at 40kHz Switching Frequency. Noise Reduction Beyond 1.3µs Is Minimal

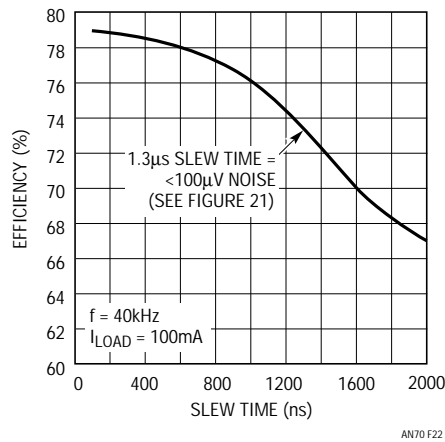


Figure 22. Figure 5's Efficiency Drops 6% as Slew Time Extends to 1.3µs. Operation Beyond This Point Gains Little Noise Performance (See Previous Curve) with 6% Efficiency Penalty

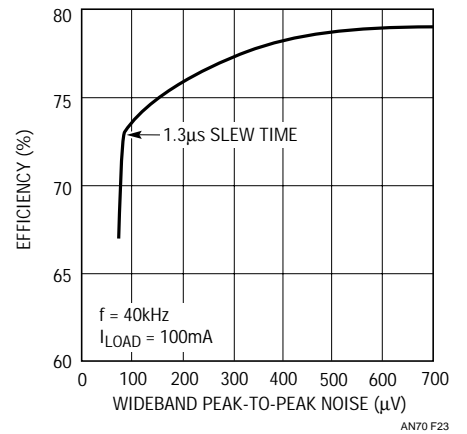


Figure 23. Efficiency vs Noise for Figure 5. Data Shows Significant Efficiency Fall-Off for Noise Below 80µV



figure). There is an additional 6% penalty beyond 1.3 $\mu$ s, although no significant noise reduction occurs (again, per Figure 21). As such, operation in this region is undesirable. Figure 23 clearly shows the inflection point in the efficiency versus noise trade-off.<sup>10</sup>

## Negative Output Regulator

The LT1533 has a separate feedback input that directly accepts negative inputs.<sup>11</sup> This permits negative outputs without the usual discrete level shifting stage. Figure 24's 5V to -12V converter is similar to Figure 5's circuit, except that the negative output is fed back to the negative feedback input. The feedback scale factor change is necessitated by the higher effective reference voltage. In all other respects, the circuit (and its performance) is similar to Figure 5.

## Floating Output Regulator

Figure 25's isolation stage permits a fully floating, regulated output. The LT1431 shunt regulator compares a portion of the output to its internal reference and drives the optoisolator with the error signal. The optoisolator's collector output biases the LT1431's V<sub>C</sub> pin, closing a feedback loop to regulate circuit output. The 0.22 $\mu$ F capacitor stabilizes the loop and the 240k $\Omega$  resistor biases the optoisolator into a favorable operating region. This circuit's operation and characteristics are similar to Figure 5 with the added benefit of the isolated output.

## Floating Bipolar Output Converter

Grounding the LT1533's "DUTY" pin and biasing FB forces the device into its 50% duty cycle mode. Figure 26's output is full wave rectified with respect to T1's secondary center tap, producing bipolar outputs. The forced 50% duty cycle combined with no feedback means the outputs are unregulated, proportioning to T1's drive voltage. An output inductor is usually not required, as in Figure 5's "forward" converter. At the very highest output currents, some inductance may be necessary to limit inrush current. If this is not done, the circuit may not start. Typically, linear regulators provide regulation.<sup>12</sup>

Figure 26's waveforms appear in Figure 27. Collector voltage (Traces A and C) and current (Traces B and D) are shown, along with the indicated output noise (Trace E). In this case linear regulators and an output filter are in use. In Figure 28 all probes except the coaxial output connection are removed. This eliminates probing induced parasitics,<sup>13</sup> allowing a higher fidelity signal presentation. Here, the switching residuals are barely detectable in the noise floor. Removing the optional output filter (Figure 29) allows linear regulator contributed noise and switching spikes to rise, but noise is still below 300 $\mu$ V<sub>p-p</sub>.

Note 10: The noise and efficiency characteristics appearing in Figures 20 to 23 were generated at the bench in about ten minutes. All you CAD modeling types out there might want to think about that.

Note 11: See Figure 3's Block Diagram.

Note 12: See Appendix E, "Selection Criteria for Linear Regulators."

Note 13: See Appendix C, "Probing and Connection Techniques for Low Level, Wideband Signal Integrity," for relevant discussion.

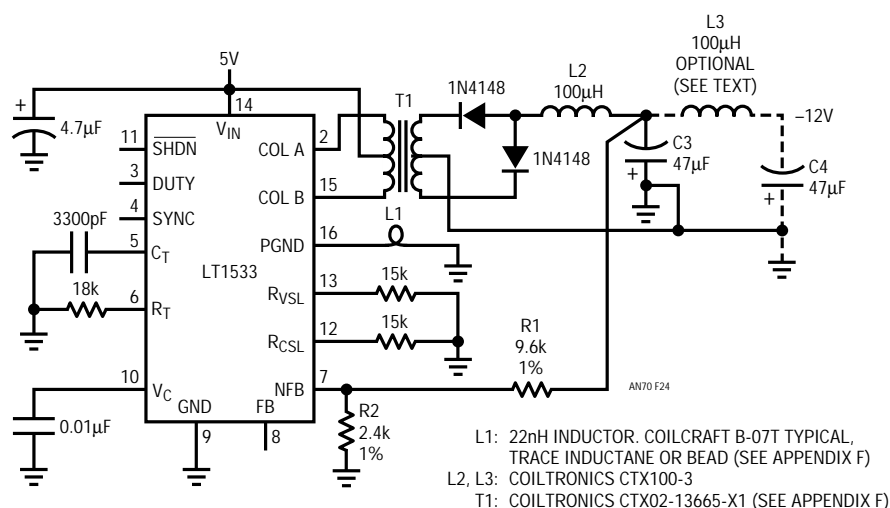


Figure 24. A Negative Output Version of Figure 5. LT1533's Negative Feedback Input Requires Minimal Configuration Changes. Noise Performance Is Identical to Positive Output Version

# Application Note 70

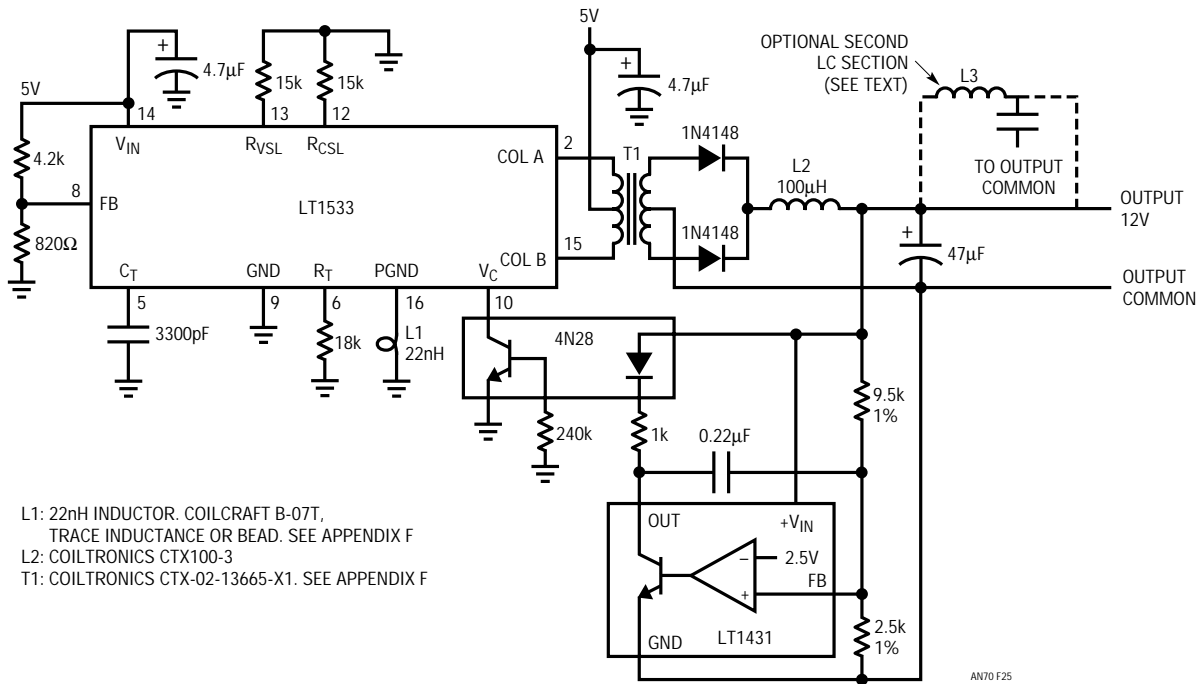


Figure 25. An Optoisolated Output Variant of Figure 5. Loop Closure to  $V_C$  Pin Bypasses LT1533 Error Amplifier, Enhancing Loop Stability. Noise Performance is Maintained.

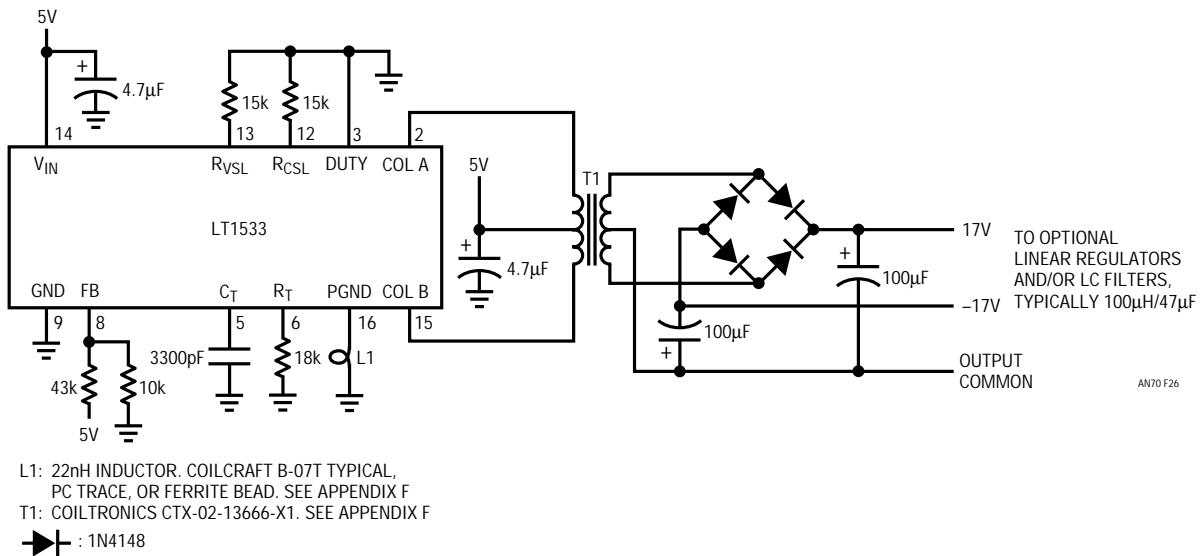


Figure 26. A Bipolar, Floating Output Converter. Grounding "DUTY" Pin and Biasing FB Puts Regulator into 50% Duty Cycle Mode. Floating, Unregulated Outputs Proportion to T1's Center Tap Voltage. Linear Regulators Are Optional

As in Figure 5's case, spectrum analyzer measurements are instrument limited. Figure 30 shows the analyzer's noise floor in a 500MHz sweep when monitoring the unpowered Figure 26's breadboard. In Figure 31, the breadboard is powered, but analyzer output is noise limited and essentially indistinguishable from the unpowered case. Similarly, Figure 32's 1MHz wide "power-on" plot is identical to Figure 33's noise floor limited "power-off" sweep. Note that linear postregulation is in use and the 40kHz fundamental components are not detectable. Figure 5's circuit did not have linear postregulation and 40kHz fundamental residue appeared in Figure 15b.

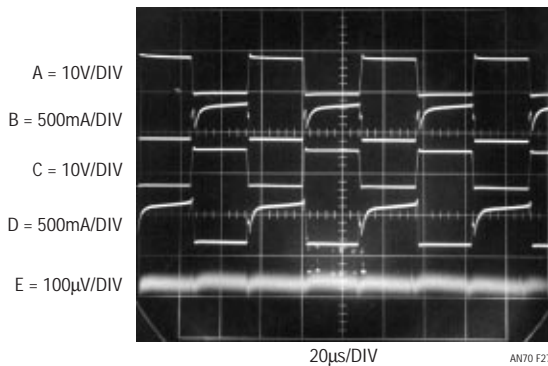


Figure 27. Waveforms for the Floating Output Converter at 100mA Loading. Linear Postregulator and Optional LC Filter Are Employed. Slew-Controlled Collector Voltage (Traces A and C) and Current (Traces B and D) Produce Output (Trace E) with Under 100µV Noise

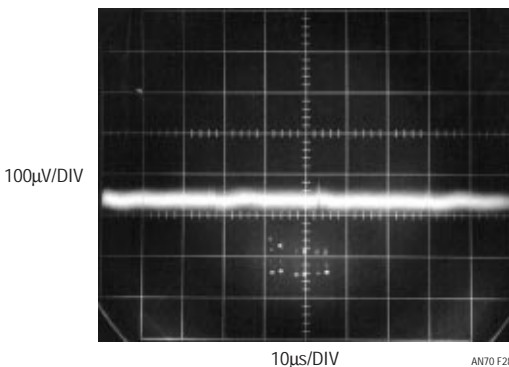


Figure 28. Removing All Probes Except Coaxial Output Connection Reveals Figure 27's True Noise Figure. Switching Residue Is Just Detectable in Amplifier Noise

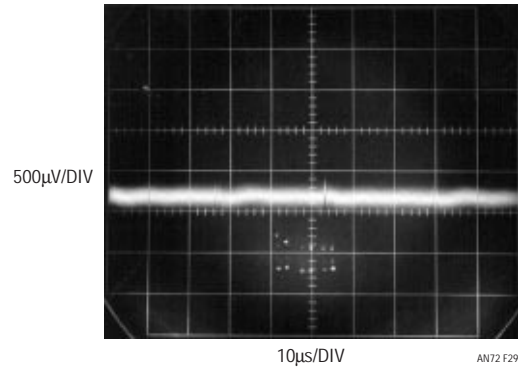


Figure 29. Removing Optional LC Filter Causes Linear Regulator-Contributed Noise and Switching Spikes to Rise. Peak-to-Peak Noise Is Still <300µV

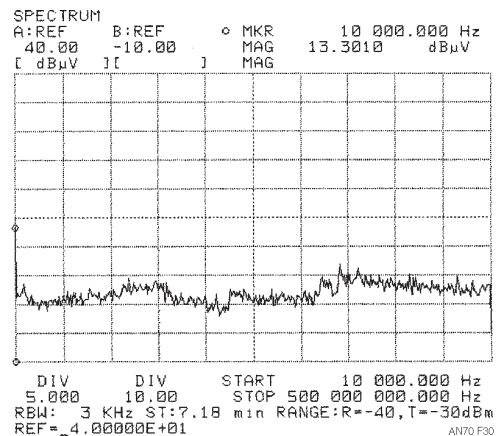


Figure 30. HP4195A Analyzer's Noise Floor in a 500MHz Sweep When Connected to Unpowered Figure 26

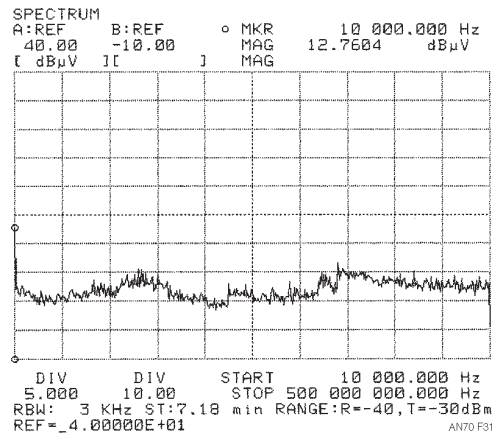


Figure 31. Figure 26's "Power-On" Output Noise Is Undetectable in Analyzer's Noise Floor Limited 500MHz Sweep

# Application Note 70

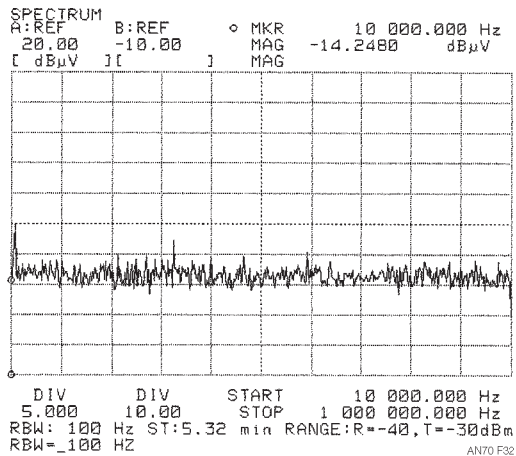


Figure 32. Linear Postregulation Eliminates 40kHz Fundamental-Related Components in 1MHz Sweep

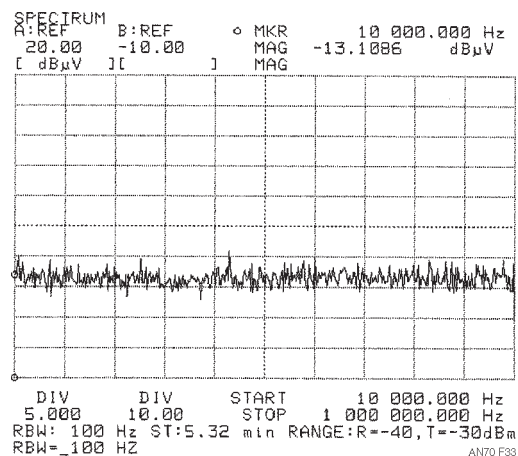


Figure 33. Turning Circuit Power Off Verifies Figure 32's Plot Is Analyzer Noise Floor Limited. Sweep Results Are Identical to Figure 32's "Power-On" Data

## Battery-Powered Circuits

The basic configurations may be battery-powered for use in portable apparatus. Figure 34, similar to Figure 5, runs from  $2.7V_{MIN}$  (e.g., three NiCd batteries), producing 12V output. This design induces no noise-based error when powering a fast 16-bit A/D converter, something almost no DC/DC converter can do. Appendix K contributes compelling testimony to this somewhat boastful claim.

Figure 35 also operates from three NiCd cells, producing a 9V output. This design achieves  $100\mu V$  output noise, qualifying it as the electronic equivalent of a 9V battery.

## Performance Augmentation

In some cases it may be desirable to augment LT1533 performance characteristics. Usually, this involves additional circuitry, and may necessitate trading off performance in one area to gain the desired benefit.

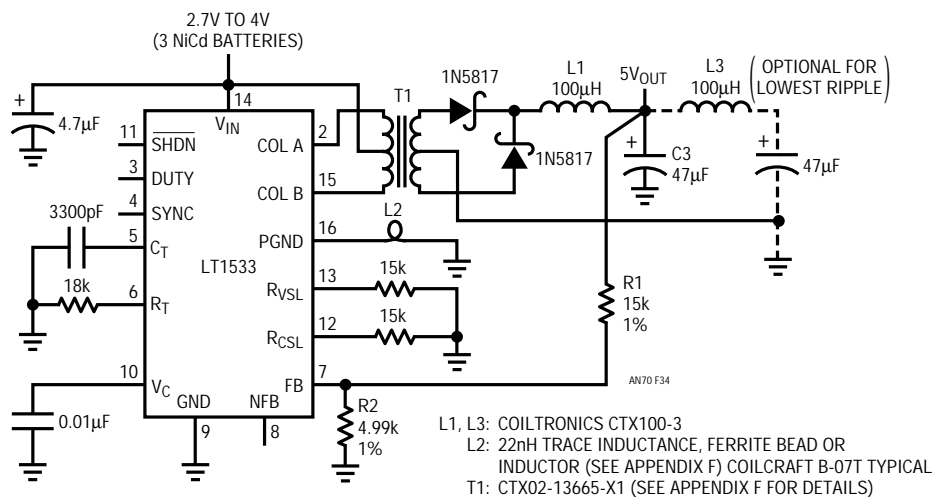


Figure 34. Circuit Delivers 5V from Three NiCd Batteries, Has  $100\mu V$  Wideband Output Noise. This Design Contributes No Noise-Based Error When Powering a 16-Bit A/D Converter (See Appendix K)

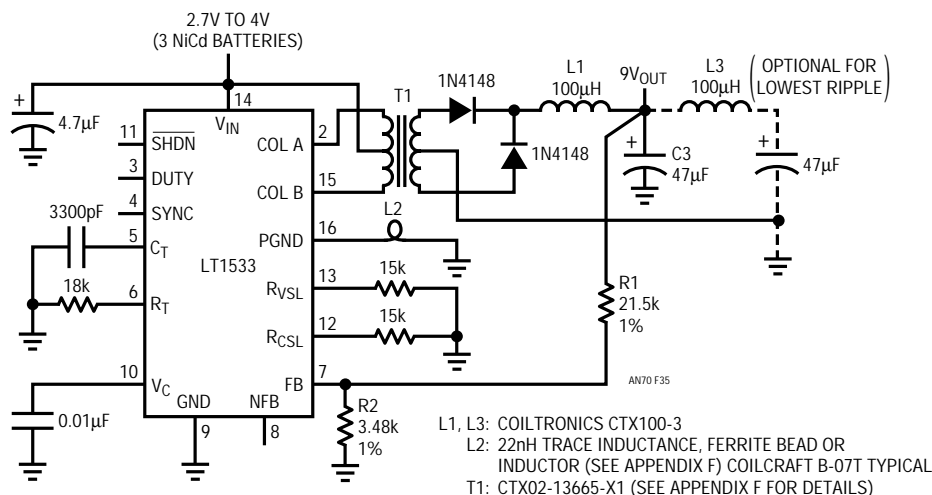


Figure 35. Electronic Equivalent of 9V Battery Operates from Three NiCd Cells. Output Noise Is Below 100µV

## Low Quiescent Current Regulator

The LT1533 has a quiescent current of about 6mA. Figure 36's circuit reduces this figure to 100µA by running an on-off control loop around the device. The control loop replaces the normal error amplifier, achieving regulation by switching the IC in and out of shutdown in accordance with loop demands.

Comparator C1 compares a scaled version of the output with its internal reference and biases the regulators shutdown pin. Loop hysteresis is obtained by utilizing the phase shift (e.g., time delay) of the output LC components. In a normal continuously closed loop this phase shift must be minimized and compensated. In this case it promotes the desired hysteretic control characteristic. Local AC positive feedback at C1 ensures clean transitions. Figure 37 shows the loop at work. When circuit output drops below the regulation point, C1's output (Trace A) goes high. This enables the regulator and it responds with a burst of drive (Trace B) to the transformer. The output is restored and C1 goes low until the next cycle. During C1's low time the regulator is shut down, resulting in the extremely low quiescent current noted. The loop's on-off control characteristic causes low frequency output noise related to LC tank ring. Trace C shows 600µV peaks, although no wideband components are observable.

## High Voltage Input Regulator

The LT1533's IC process limits collector breakdown to 30V. A complicating factor is that the transformer swings to 2x supply. Thus, 15V represents the maximum allowable input supply. Many applications require higher voltage inputs and Figure 38 uses a cascoded<sup>14</sup> output stage to achieve such high voltage capability. This 24V-to-50V converter is reminiscent of previous circuits, except that Q1 and Q2 appear. These devices, interposed between the IC and the transformer, constitute a cascoded high voltage stage. They provide voltage gain while isolating the IC from their large collector voltage savings.

Normally, high voltage cascodes are designed to simply supply voltage isolation. Cascoding the LT1533 presents special considerations because the transformers instantaneous voltage and current information must be accurately transmitted, albeit at lower amplitude, to the LT1533. If this is not done, the regulator's slew control loops will

Note 14: The term "cascoding," derived from "cascade to cathode," is applied to a configuration that places active devices in series. The benefit may be higher breakdown voltage, decreased input capacitance, bandwidth improvement, etc. Cascoding has been employed in op amps, power supplies, oscilloscopes and other areas to obtain performance enhancement. The origin of the term is clouded and the author will mail a magnum of champagne to the first reader correctly identifying the original author and publication.



# Application Note 70

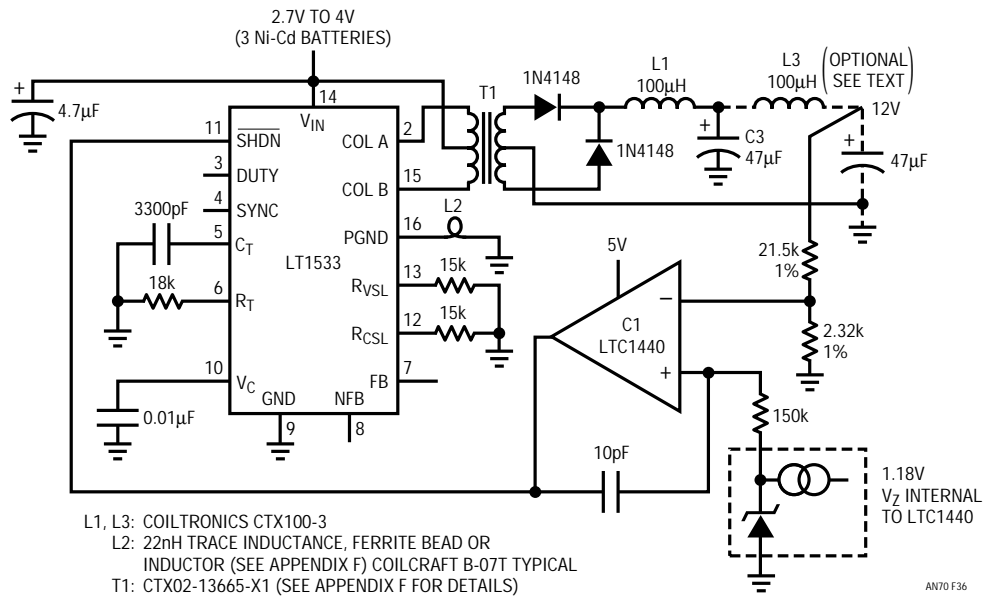


Figure 36. Hysteretic "Burst Mode™" Loop Lowers Quiescent Current to 100µA While Maintaining Low Output Noise

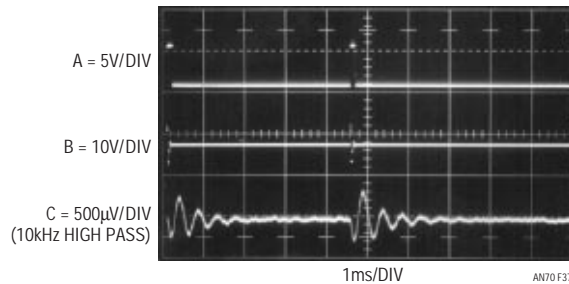


Figure 37. Operating Waveforms for the Low Quiescent Current Converter. Comparator Output (Trace A) Restores Output Voltage by Turning LT1533 On (Trace B). Output Noise Shows LC Ringing (Trace C), Although High Frequency Content Is Negligible

Burst Mode is a trademark of Linear Technology Corporation.

not function, causing a dramatic output noise increase. The AC compensated resistor dividers associated with the Q1-Q2 base collector biasing serve this purpose. Q3 and associated components provide a stable DC termination for the dividers. Figure 39 shows waveforms for Q1's operation (Q2 is identical, although of opposing phase). Trace A is Q1's emitter, Trace B its base and Trace C the collector. T1's ring-off obscures the fact that waveform fidelity is maintained through the cascode, although inspection reveals this to be the case. Additional testimony is given by circuit output noise (Trace D), which measures about 100 $\mu$ V peak.

## 24V-to-5V Low Noise Regulator

Figure 40 extends Figure 38's cascoding technique in a step-down design.<sup>15</sup> Inputs from 20V to 50V are converted to a 5V/2A capacity output. Q3 and Q4 protect the regulators  $V_{IN}$  pin from the high input voltages. The cascode must accommodate 100V transformer swings. In this instance MOSFETs (Q1-Q2) are utilized, although the divider technique is necessarily retained. RC gate damper networks prevent transformer swings coupled via gate-channel capacitance from corrupting the cascode's waveform transfer fidelity. Figure 41 shows that resultant cascode response is faithful, even with 100V swings. Trace A is Q1's source, with Traces B and C its gate and drain, respectively. Under these conditions, at 2A output, noise is inside 400 $\mu$ V peak. Note that Q3 and Q4 protect the regulator from excessive input voltages.

## 10W, 5V to 12V Low Noise Regulator

Figure 42 boosts the regulator's 1A output capability to over 5A. It does this with simple emitter followers (Q1-Q2). Theoretically, the followers preserve T1's voltage and current waveform information, permitting the LT1533's slew control circuitry to function. In practice, the transistors must be relatively low beta types. At 3A collector current their beta of 20 sources  $\approx$ 150mA via the Q1-Q2 base paths, adequate for proper slew loop operation.<sup>16</sup> The follower loss limits efficiency to about 68%. Higher input voltages minimize follower-induced loss, permitting efficiencies in the low 70% range.

Figure 43 shows noise performance. Ripple measures 4mV (Trace A) using a single LC section, with high frequency content just discernible. Adding the optional second LC section drops ripple below 100 $\mu$ V (Trace B), and high frequency content is seen (note  $\times$ 50 vertical scale factor change) to be inside 180 $\mu$ V.

## 7500V Isolated Low Noise Supply

A final form of performance augmentation is extremely high voltage isolation. This is often required in situations where circuitry must withstand high common mode voltage effects. Figure 44 is similar to Figure 25's isolated supply, except that it has 7500V (peak) breakdown capability. Transformer and optoisolator changes permit this. The remaining operating and performance characteristics are identical to Figure 25.

Note 15: This circuit was developed from a design by Jeff Witt of Linear Technology Corporation.

Note 16: Operating the slew loops from follower base current was suggested by Bob Dobkin of Linear Technology Corporation.



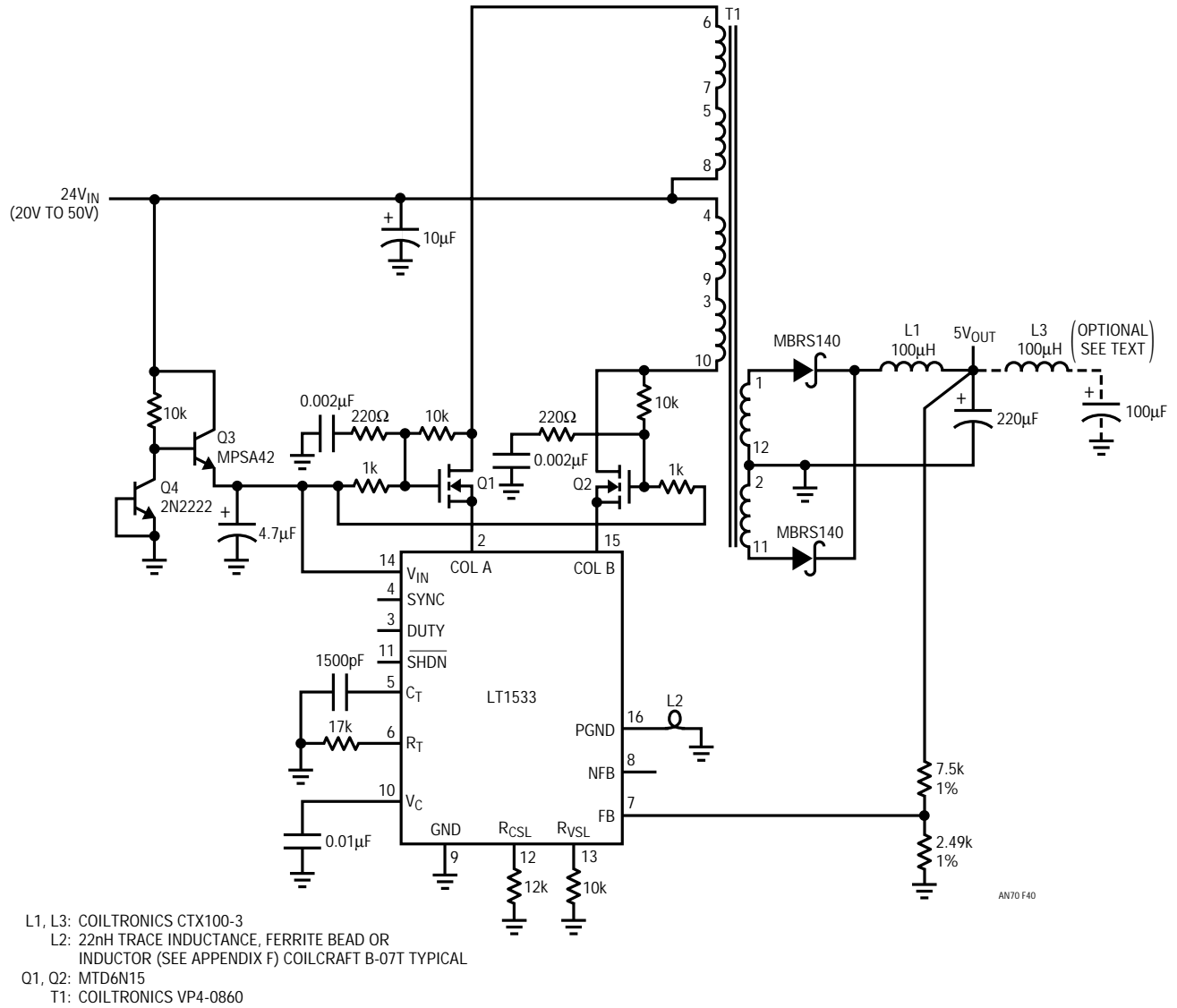


Figure 40. A Low Noise 24V-(20V<sub>IN</sub> to 50V<sub>IN</sub>)-to-5V Converter. Cascoded MOSFETs Withstand 100V Transformer Swings, Permitting LT1533 to Control 5V/2A Output

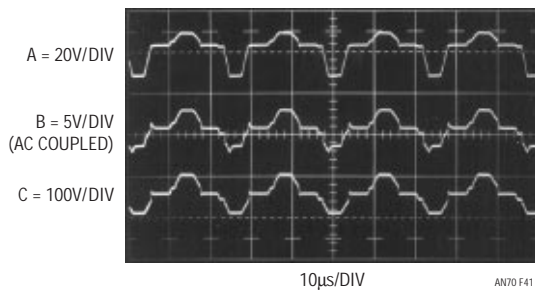


Figure 41. MOSFET-Based Cascode Permits Regulator to Control 100V Transformer Swings While Maintaining Low Noise 5V Output. Trace A Is Q1's Source, Trace B Q1's Gate and Trace C the Drain. Waveform Fidelity Through Cascode Permits Proper Slew Control Operation

# Application Note 70

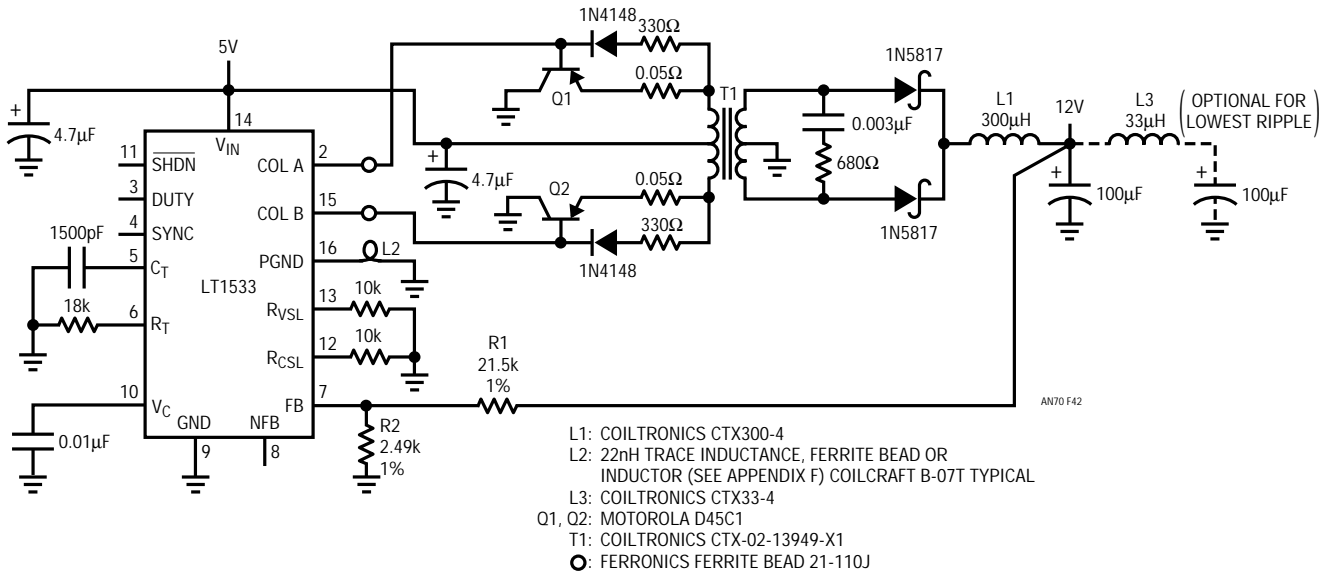


Figure 42. A 10W Low Noise 5V-to-12V Converter. Q1-Q2 Provide 5A Output Capacity While Preserving LT1533's Voltage/Current Slew Control. Efficiency Is 68%. Higher Input Voltages Minimize Follower Loss, Boosting Efficiency Above 71%

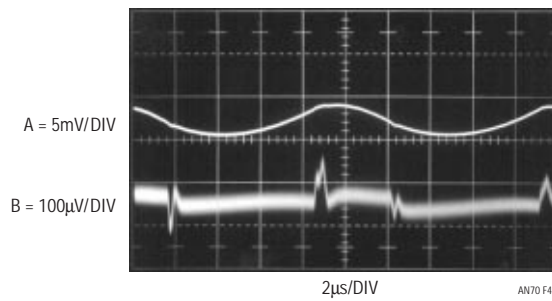


Figure 43. Waveforms for Figure 42 at 10W Output. Trace A Shows Fundamental Ripple with Higher Frequency Residue Just Discernible. Optional LC Section Produces Trace B's 180µV<sub>p,p</sub> Wideband Noise Performance





# Application Note 70

---

## REFERENCES

1. Shakespeare, William, "Much Ado About Nothing," II, i, 319, 1598-1600.
2. Williams, Jim, "Design DC/DC Converters to Catch Noise at the Source," *Electronic Design*, October 15, 1981, page 229.
3. Williams, Jim, "Conversion Techniques Adapt Voltages to Your Needs," *EDN*, November 10, 1982, page 155.
4. Tektronix, Inc. "Type 535 Operating and Service Manual," CRT Circuit, 1954.
5. Tektronix, Inc. "Type 454 Operating and Service Manual," CRT Circuit, 1967.
6. Tektronix, Inc. "7904 Oscilloscope Operating and Service Manual," Converter-Rectifiers, 1972.
7. Hewlett-Packard Co. "1725A Oscilloscope Operating and Service Manual," High Voltage Power Supply, 1980.
8. Arthur, Ken, "Power Supply Circuits," High Voltage Power Supplies, Tektronix Concept Series, 1967.
9. Williams, Jim and Huffman, Brian, "Some Thoughts on DC/DC Converters," Low Noise 5V to  $\pm 15V$  Converter and Ultralow Noise 5V to  $\pm 15V$  Converter, pages 1 to 5, Linear Technology Corporation Application Note 29, 1988.
10. Williams, Jim and Huffman, Brian, "Precise Converter Designs Enhance System Performance," *EDN*, October 13, 1988, pages 175 to 185.
11. Tektronix, Inc. "Type 1A7A Differential Amplifier Instruction Manual," Check Overall Noise Level Tangentially, pages 5-36 and 5-37, 1968.
12. Williams, Jim, "High Speed Amplifier Techniques," Linear Technology Corporation Application Note 47, 1991.
13. Witt, Jeff, "The LT1533 Heralds a New Class of Low Noise Switching Regulators," *Linear Technology*, Vol. VII, No. 3, August 1997, Linear Technology Corporation.
14. Morrison, Ralph, "Noise and Other Interfering Signals," John Wiley and Sons, 1992.
15. Morrison, Ralph, "Grounding and Shielding Techniques in Instrumentation," Wiley-Interscience, 1986.
16. Sheehan, Dan, "Determine Noise of DC/DC Converters," *Electronic Design*, September 27, 1973.
17. Hewlett-Packard Co. "HP-11941A Close Field Probe Operation Note," 1987.
18. Terrien, Mark, "The HP-11940A Close Field Probe: Characteristics and Application to EMI Troubleshooting," RF and Microwave Symposium, available from Hewlett-Packard Co.
19. Pressman, A.I., "Switching and Linear Power Supply, Power Converter Design," Hayden Book Co., Hasbrouck Heights, New Jersey, 1977.
20. Chryssis, G., "High Frequency Switching Power Supplies, Theory and Design," McGraw Hill, New York, 1984.

## APPENDIX A

## A HISTORY OF LOW NOISE DC/DC CONVERSION

Why are batteries low noise power sources? Why do 60Hz AC power line derived linear regulators have low output noise? As with most innocent questions, thoughtful answers provide surprising insights. These sources have low output noise because they have low harmonic energy content. A 60Hz fundamental driven supply produces some harmonic activity, but power becomes very small well inside 1kHz. A battery is even better.

These conclusions set a direction towards designing low noise DC/DC converters. If the goal is low noise, the key is reduction of harmonic energy, in particular, wideband harmonics. This simple guideline is central to LT1533 operation, although refinements are necessary for a generally applicable IC.

## History

The notion of minimizing harmonics in DC/DC conversion to get low output noise is not new. Oscilloscopes have used this technique to generate high voltage CRT accelerating potentials without degrading instrument operation.<sup>1</sup> Designing a 10,000V output DC/DC converter that does not disrupt a 500MHz, high sensitivity vertical amplifier is challenging.

Figure A1 shows the CRT DC/DC converter from a Tektronix 454 oscilloscope. Q1430, configured as a modified Hartley power oscillator, drives T1430. T1430's output is multiplied by the diode-capacitor tripler, producing 12,000V. Feedback to Q1414 is summed against a 75V derived reference, closing a regulation loop around the power oscillator.

The sine wave transformer drive (see waveforms in the figure) has low harmonic content, resulting in the desired low conducted and radiated noise. This approach is not very efficient—Q1430 operates in its linear region—but the power loss is acceptable in a 125W instrument.

Tektronix 7000 series oscilloscopes used a resonant, off-line converter to power the entire instrument. As before, CRT high voltage was generated separately (see Footnote

1). Figure A2, a partial schematic of a Tektronix 7904 power converter, shows a series resonant network, L1237-C1237 in the Q1234-Q1241 drive path. This results in sine wave drive to output transformer T1310, despite Q1234-Q1241's rectangular waveshape. Feedback (not shown) closes a loop around this stage, stabilizing its operating point. The resonant, sine wave transformer drive provides the desired low noise characteristics with good efficiency.

A less specific example appears in LTC Application Note 29. Figure A3, a partial schematic of Application Note 29's Figure 4, shows a sine wave oscillator (A1 based) driving a power amplifier (A3 and Q2 to Q6). L3, the output transformer, provides voltage boosted secondary drive to linear regulators (not shown). This brute force approach provides a converter with extraordinarily low noise, but is complex and inefficient. Q4 and Q5, operating in their linear regions, dissipate considerable power, and efficiency is 30%.

Figure A4's approach, also from AN29's Figure 1, achieves better efficiency. The partial schematic shows source followers driven from 100Ω-0.003μF edge slow-down networks. This slows down the transistor's transitions, resulting in harmonic reduction and low noise. Unfortunately, the drive scheme is complex and somewhat inflexible, requiring bootstrapped voltages to fully switch the transistors on and off. Additionally, a transformer change would require drive rework to maintain efficiency and low noise characteristics. Finally, the dynamic voltage and current control in the transistors is passively determined and not very well controlled.

The LT1533 uses closed-loop control<sup>2</sup> around its output stages to tightly control voltage and current slewing. This allows a variety of circuits and magnetics to be easily accommodated, resulting in a true general purpose solution. Text Figure 3 and the associated discussion provide more LT1533 operating details.

Note 1: Ancillary benefits include eliminating a complex and expensive high voltage winding in the main power transformer, avoidance of long, high voltage wire runs and space and weight savings.

Note 2: Patent pending.







# Application Note 70

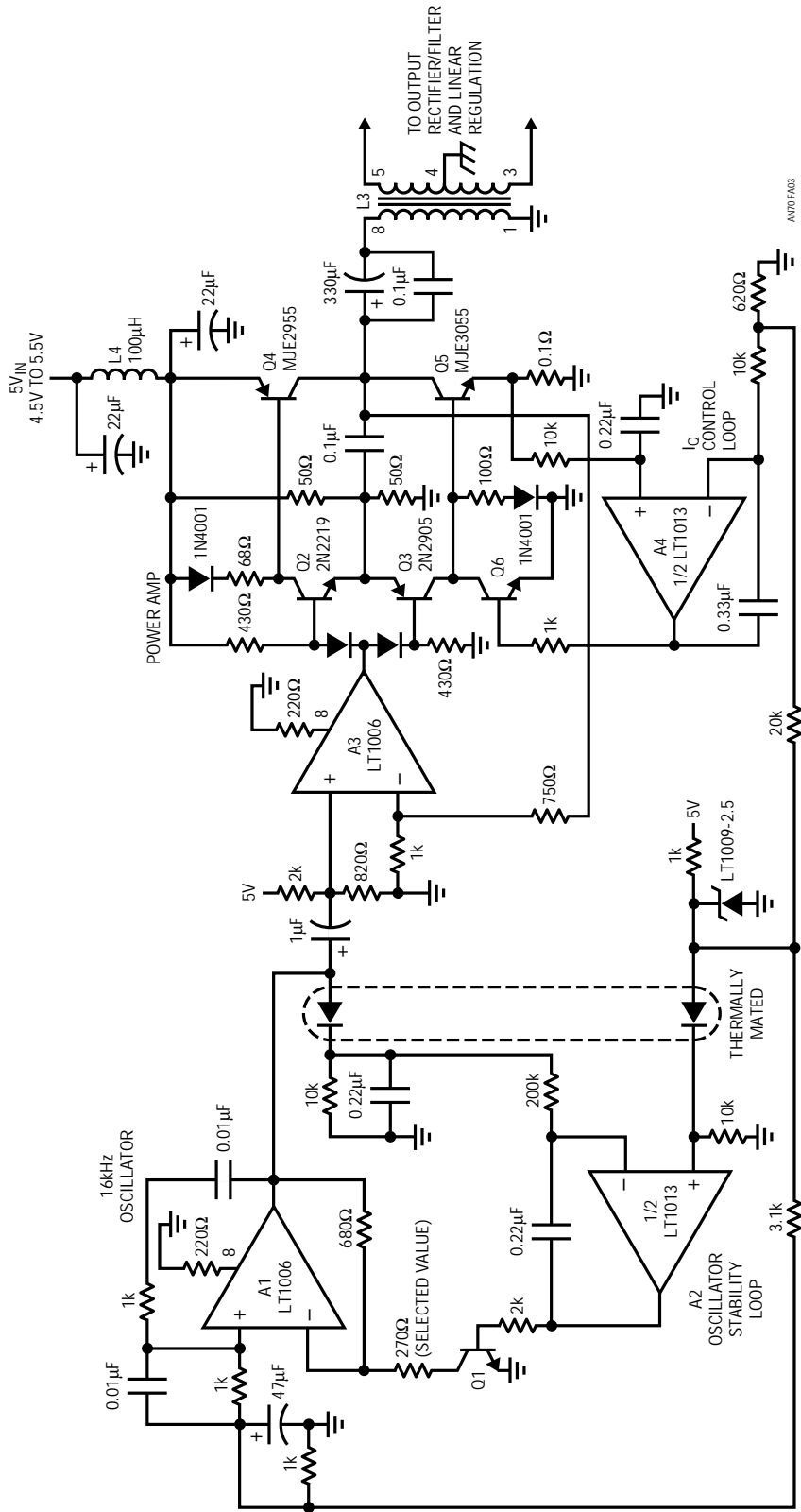


Figure A3. Sine Wave-Based DC/DC Converter Appeared in LC Application Note 29. Output Noise Is Low, but Circuit Is Complex and Inefficient



# Application Note 70

---

## APPENDIX B

### SPECIFYING AND MEASURING SOMETHING CALLED NOISE

Undesired output components in switching regulators are commonly referred to as “noise.” The rapid, switched mode power delivery that permits high efficiency conversion also creates wideband harmonic energy. This undesirable energy appears as radiated and conducted components, or “noise.” Actually switching regulator output “noise” isn’t really noise at all, but coherent, high frequency residue directly related to the regulator’s switching. Unfortunately, it is almost universal practice to refer to these parasitics as “noise,” and this publication maintains this common, albeit inaccurate, terminology.<sup>1</sup>

#### Measuring Noise

There are an almost uncountable number of ways to specify noise in a switching regulator’s output. It is common industrial practice to specify peak-to-peak noise in a 20MHz bandpass.<sup>2</sup> Realistically, electronic systems are readily upset by spectral energy beyond 20MHz, and this specification restriction benefits no one.<sup>3</sup> Considering all this, it seems appropriate to specify peak-to-peak noise in a verified 100MHz bandwidth. Reliable low level measurements in this bandpass require careful instrumentation choice and connection practices.

Our study begins by selecting test instrumentation and verifying its bandwidth and noise. This necessitates the arrangement shown in Figure B1. Figure B2 diagrams signal flow. The pulse generator supplies a subnanosecond rise time step to the attenuator, which produces a <1mV version of the step. The amplifier takes 40dB of gain ( $A = 100$ ) and the oscilloscope displays the result. The “front-to-back” cascaded bandwidth of this system should be about 100MHz ( $t_{rise} = 3.5ns$ ) and Figure B3 reveals this to be so. Figure B3’s trace shows 3.5ns rise time and about

100 $\mu$ V of noise. The noise is limited by the amplifier’s 50 $\Omega$  noise floor.<sup>4</sup>

Figure B4’s presentation of text Figure 5’s output noise shows barely visible switching artifacts (at vertical graticule lines 4, 6 and 8) in the 100MHz bandpass. Fundamental ripple is seen more clearly, although similarly noise floor dominated. Restricting measurement bandwidth to 10MHz (Figure B5) reduces noise floor amplitude, although switching noise and ripple amplitudes are preserved. This indicates that there is no signal power beyond 10MHz. Further measurements as bandwidth is successively reduced can determine the highest frequency content present.

The importance of measurement bandwidth is further illustrated by Figures B6 to B8. Figure B6 measures a commercially available DC/DC converter in a 1MHz bandpass. The unit appears to meet its claimed 5mV<sub>P,P</sub> noise specification. In Figure B7, bandwidth is increased to 10MHz. Spike amplitude enlarges to 6mV<sub>P,P</sub>, about 1mV outside the specification limit. Figure B8’s 50MHz viewpoint brings an unpleasant surprise. Spikes measure 30mV<sub>P,P</sub>—six times the specified limit!<sup>5</sup>

---

Note 1: Less genteelly, “If you can’t beat ‘em, join ‘em.”

Note 2: One DC/DC converter manufacturer specifies *RMS* noise in a 20MHz bandwidth. This is beyond deviousness and unworthy of comment.

Note 3: Except, of course, eager purveyors of power sources who specify them in this manner.

Note 4: Observed peak-to-peak noise is somewhat affected by the oscilloscope’s “intensity” setting. Reference 11 describes a method for normalizing the measurement.

Note 5: Caveat Emptor.



Figure B1. 100MHz Bandwidth Verification Test Setup.  
Note Coaxial Connections for Wideband Signal Integrity

# Application Note 70

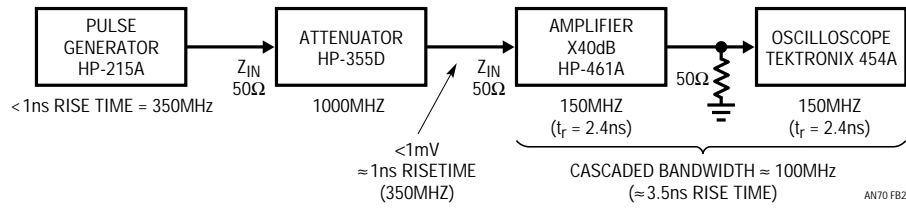


Figure B2. Subnanosecond Pulse Generator and Wideband Attenuator Provide Fast Step to Verify Test Setup Bandwidth

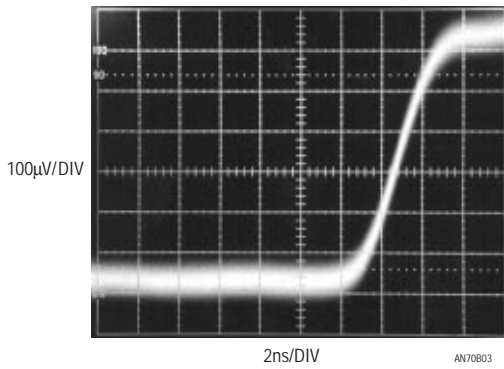


Figure B3. Oscilloscope Display Verifies Test Setup's 100MHz (3.5ns Rise Time) Bandwidth. Baseline Noise Derives from Amplifier's 50Ω Input Noise Floor

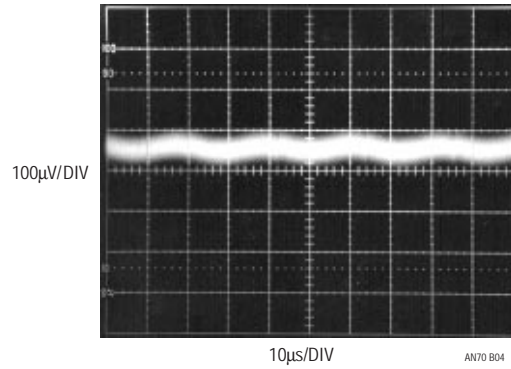


Figure B4. Text Figure 5's Output Switching Noise Is Just Discernible in A 100MHz Bandpass

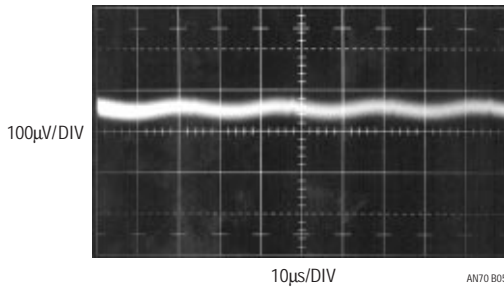


Figure B5. 10MHz Band Limited Version of Preceding Photo. All Switching Noise Information Is Preserved, Indicating Adequate Bandwidth

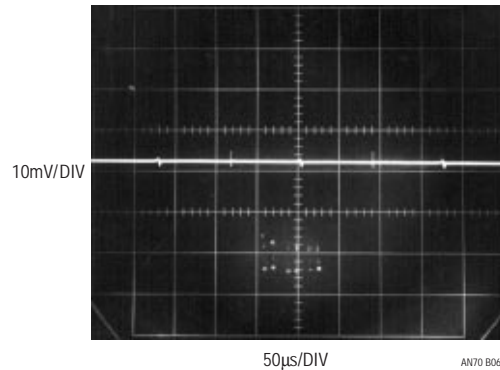


Figure B6. Commercially Available Switching Regulator's Output Noise in a 1MHz Bandpass. Unit Appears to Meet Its 5mV<sub>p-p</sub> Noise Specification



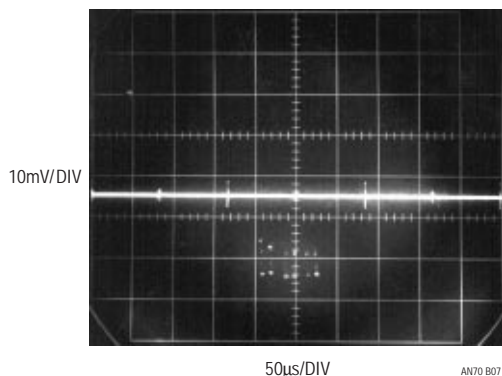


Figure B7. Figure A6's Regulator Noise in a 10MHz Bandpass. 6mV<sub>P-P</sub> Noise Exceeds Regulator's Claimed 5mV Specification

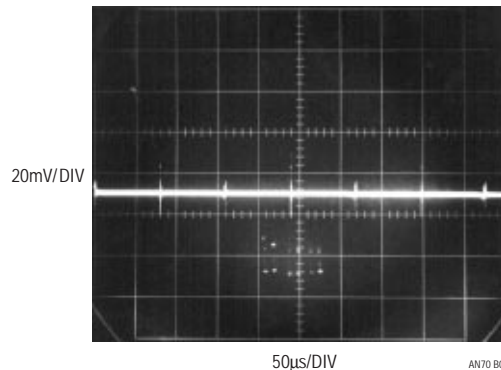


Figure B8. Wideband Observation of Figure A7 Shows 30mV<sub>P-P</sub> Noise—Six Times the Regulator's Specification!

## Low Frequency Noise

Low frequency noise is rarely a concern, because it almost never affects system operation. Text Figure 5's low frequency noise is shown in Figure B9. It is possible to reduce low frequency noise by rolling off control loop bandwidth (e.g., via a 0.68µF feedback capacitor across R1 and V<sub>C</sub> value of 2000pF in text Figure 5). Figure B10 shows about a five times improvement when this is done, even with greater measurement bandwidth. A possible disadvantage is loss of loop bandwidth and slower transient response.

## Preamplifier and Oscilloscope Selection

The low level measurements described require some form of preamplification for the oscilloscope. Current generation oscilloscopes rarely have greater than 2mV/DIV sensitivity, although older instruments offer more capability. Figure B11 lists representative preamplifiers and oscilloscope plug-ins suitable for noise measurement. These

units feature wideband, low noise performance. It is particularly significant that the majority of these instruments are no longer produced. This is in keeping with current instrumentation trends, which emphasize digital signal acquisition as opposed to analog measurement capability.

The monitoring oscilloscope should have adequate bandwidth and exceptional trace clarity. In the latter regard high quality analog oscilloscopes are unmatched. The exceptionally small spot size of these instruments is well-suited to low level noise measurement.<sup>6</sup> The digitizing uncertainties and raster scan limitations of DSOs impose display resolution penalties. Many DSO displays will not even register the small levels of switching-based noise.

Note 6: In our work we have found Tektronix types 454, 454A, 547 and 556 excellent choices. Their pristine trace presentation is ideal for discerning small signals of interest against a noise floor limited background.

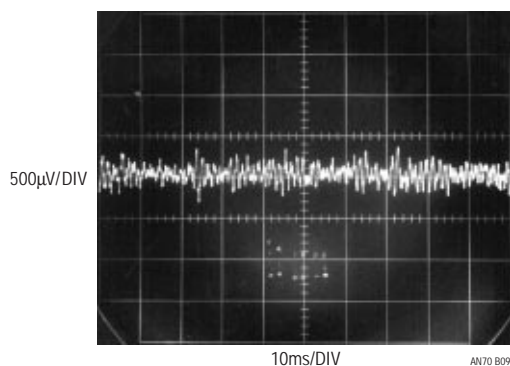


Figure B9. 1Hz to 3kHz Noise Using Standard Frequency Compensation. Almost All Noise Power Is Below 1kHz

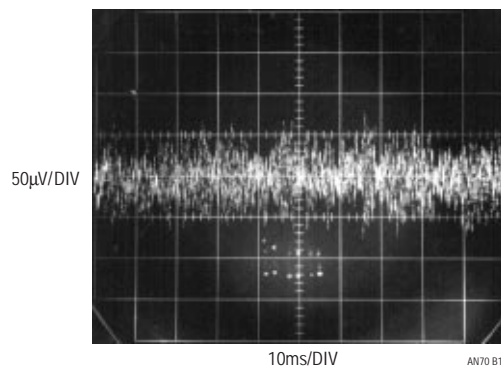


Figure B10. Feedback Lead Network Decreases Low Frequency Noise, Even as Measurement Bandwidth Expands to 100kHz

# Application Note 70

INSTRUMENT TYPE	MANUFACTURER	MODEL NUMBER	BANDWIDTH	MAXIMUM SENSITIVITY/GAIN	AVAILABILITY	COMMENTS
Amplifier	Hewlett-Packard	461A	150MHz	Gain = 100	Secondary Market	50Ω Input, Stand-Alone
Differential Amplifier	Tektronix	1A5	50MHz	1mV/DIV	Secondary Market	Requires 500 Series Mainframe
Differential Amplifier	Tektronix	7A13	100MHz	1mV/DIV	Secondary Market	Requires 7000 Series Mainframe
Differential Amplifier	Tektronix	11A33	150MHz	1mV/DIV	Secondary Market	Requires 11000 Series Mainframe
Differential Amplifier	Tektronix	P6046	100MHz	1mV/DIV	Secondary Market	Stand-Alone
Differential Amplifier	Preamble	1855	100MHz	Gain = 10	Current Production	Stand-Alone, Settable Bandstops
Differential Amplifier	Tektronix	1A7/1A7A	1MHz	10μV/DIV	Secondary Market	Requires 500 Series Mainframe, Settable Bandstops
Differential Amplifier	Tektronix	7A22	1MHz	10μV/DIV	Secondary Market	Requires 7000 Series Mainframe, Settable Bandstops
Differential Amplifier	Tektronix	5A22	1MHz	10μV/DIV	Secondary Market	Requires 5000 Series Mainframe, Settable Bandstops
Differential Amplifier	Tektronix	ADA-400A	1MHz	10μV/DIV	Current Production	Stand-Alone with Optional Power Supply, Settable Bandstops
Differential Amplifier	Preamble	1822	10MHz	Gain = 1000	Current Production	Stand-Alone, Settable Bandstops
Differential Amplifier	Stanford Research Systems	SR-560	1MHz	Gain = 50000	Current Production	Stand-Alone, Settable Bandstops, Battery or Line Operation

Figure B11. Some Applicable High Sensitivity, Low Noise Amplifiers. Trade-Offs Include Bandwidth, Sensitivity and Availability

## APPENDIX C

### PROBING AND CONNECTION TECHNIQUES FOR LOW LEVEL, WIDEBAND SIGNAL INTEGRITY

The most carefully prepared breadboard cannot fulfill its mission if signal connections introduce distortion. Connections to the circuit are crucial for accurate information extraction. The low level, wideband measurements demand care in routing signals to test instrumentation.

#### Ground Loops

Figure C1 shows the effects of a ground loop between pieces of line-powered test equipment. Small current flow between test equipment's nominally grounded chassis creates 60Hz modulation in the measured circuit output.

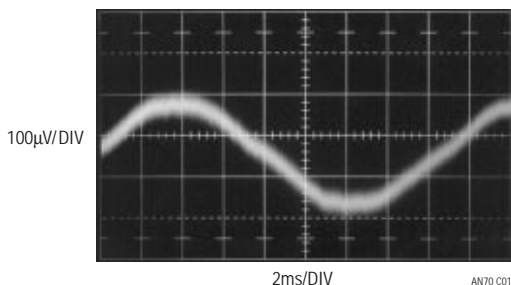


Figure C1. Ground Loop Between Pieces of Test Equipment Induces 60Hz Display Modulation

*This problem can be avoided by grounding all line powered test equipment at the same outlet strip or otherwise ensuring that all chassis are at the same ground potential. Similarly, any test arrangement that permits circuit current flow in chassis interconnects must be avoided.*

#### Pickup

Figure C2 also shows 60Hz modulation of the noise measurement. In this case, a 4-inch voltmeter probe at the feedback input is the culprit. *Minimize the number of test connections to the circuit and keep leads short.*

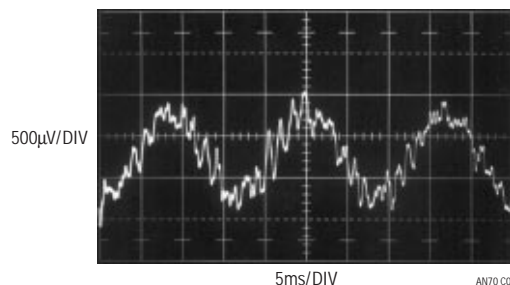


Figure C2. 60Hz Pickup Due to Excessive Probe Length at Feedback Node

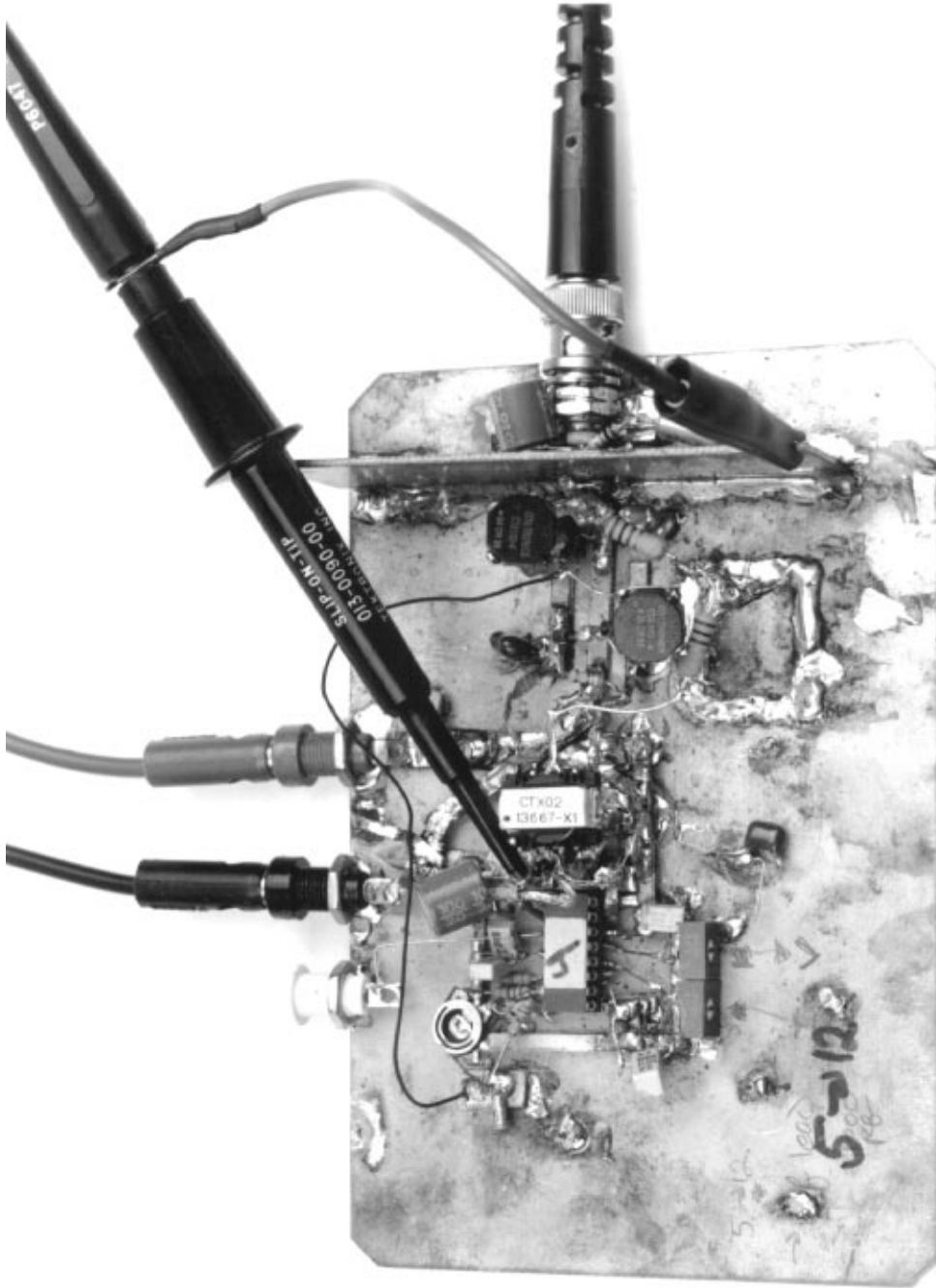


Figure C3. Poor Probing Technique. Trigger Probe Ground Lead Can Cause Ground Loop-Induced Artifacts to Appear in Display

# Application Note 70

## Poor Probing Technique

Figure C3's photograph shows a short ground strap affixed to a scope probe. The probe connects to a point which provides a trigger signal for the oscilloscope. Circuit output noise is monitored on the oscilloscope via the coaxial cable shown in the photo.

Figure C4 shows results. A ground loop on the board between the probe ground strap and the ground referred cable shield causes apparent excessive ripple in the display. *Minimize the number of test connections to the circuit and avoid ground loops.*

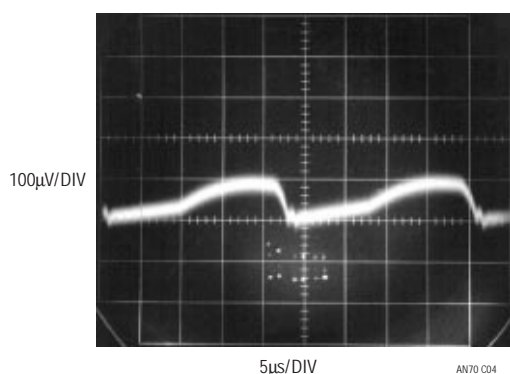


Figure C4. Apparent Excessive Ripple Results from Figure C3's Probe Misuse. Ground Loop on Board Introduces Serious Measurement Error

## Violating Coaxial Signal Transmission—Felony Case

In Figure C5, the coaxial cable used to transmit the circuit output noise to the amplifier-oscilloscope has been replaced with a probe. A short ground strap is employed as the probe's return. The error inducing trigger channel probe in the previous case has been eliminated; the 'scope is triggered by a noninvasive, isolated probe.<sup>1</sup> Figure C6 shows excessive display noise due to breakup of the coaxial signal environment. The probe's ground strap violates coaxial transmission and the signal is corrupted by RF. *Maintain coaxial connections in the noise signal monitoring path.*

## Violating Coaxial Signal Transmission—Misdemeanor Case

Figure C7's probe connection also violates coaxial signal flow, but to a less offensive extent. The probe's ground

strap is eliminated, replaced by a tip grounding attachment. Figure C8 shows better results over the preceding case, although signal corruption is still evident. *Maintain coaxial connections in the noise signal monitoring path.*

## Proper Coaxial Connection Path

In Figure C9, a coaxial cable transmits the noise signal to the amplifier-oscilloscope combination. In theory, this affords the highest integrity cable signal transmission. Figure C10's trace shows this to be true. The former examples aberrations and excessive noise have disappeared. The switching residuals are now faintly outlined in the amplifier noise floor. *Maintain coaxial connections in the noise signal monitoring path.*

## Direct Connection Path

A good way to verify there are no cable-based errors is to eliminate the cable. Figure C11's approach eliminates all cable between breadboard, amplifier and oscilloscope. Figure C12's presentation is indistinguishable from Figure C10, indicating no cable-introduced infidelity. *When results seem optimal, design an experiment to test them. When results seem poor, design an experiment to test them. When results are as expected, design an experiment to test them. When results are unexpected, design an experiment to test them.*

## Test Lead Connections

In theory, attaching a voltmeter lead to the regulator's output should not introduce noise. Figure C13's increased noise reading contradicts the theory. The regulator's output impedance, albeit low, is not zero, especially as frequency scales up. The RF noise injected by the test lead works against the finite output impedance, producing the 200µV of noise indicated in the figure. If a voltmeter lead must be connected to the output during testing, it should be done through a 10kΩ-10µF filter. Such a network eliminates Figure C13's problem while introducing minimal error in the monitoring DVM. *Minimize the number of test lead connections to the circuit while checking noise. Prevent test leads from injecting RF into the test circuit.*

Note 1: To be discussed. Read on.

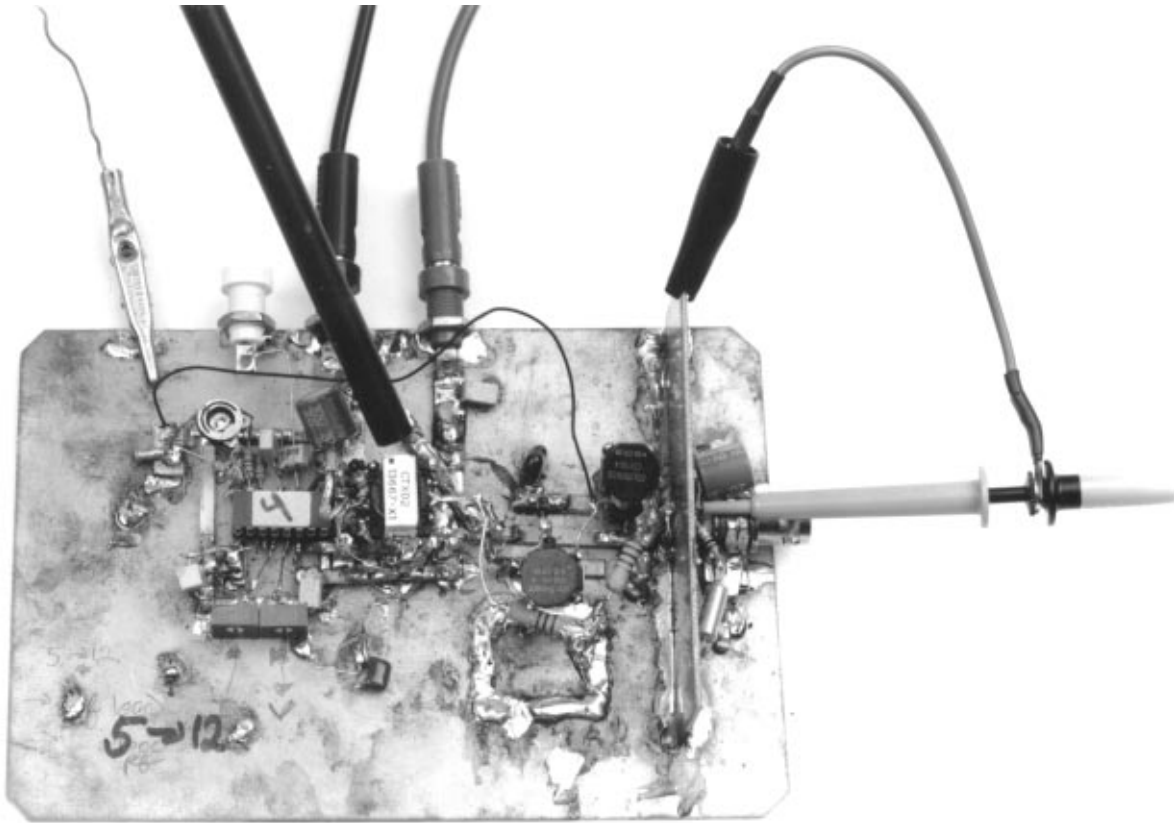


Figure C5. Floating Trigger Probe Eliminates Ground Loop, but Output Probe Ground Lead (Photo Upper Right) Violates Coaxial Signal Transmission

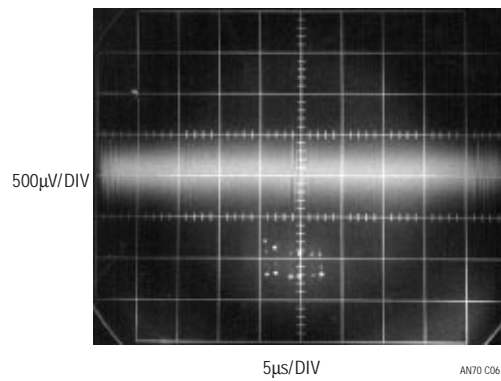


Figure C6. Signal Corruption Due to Figure C5's Noncoaxial Probe Connection



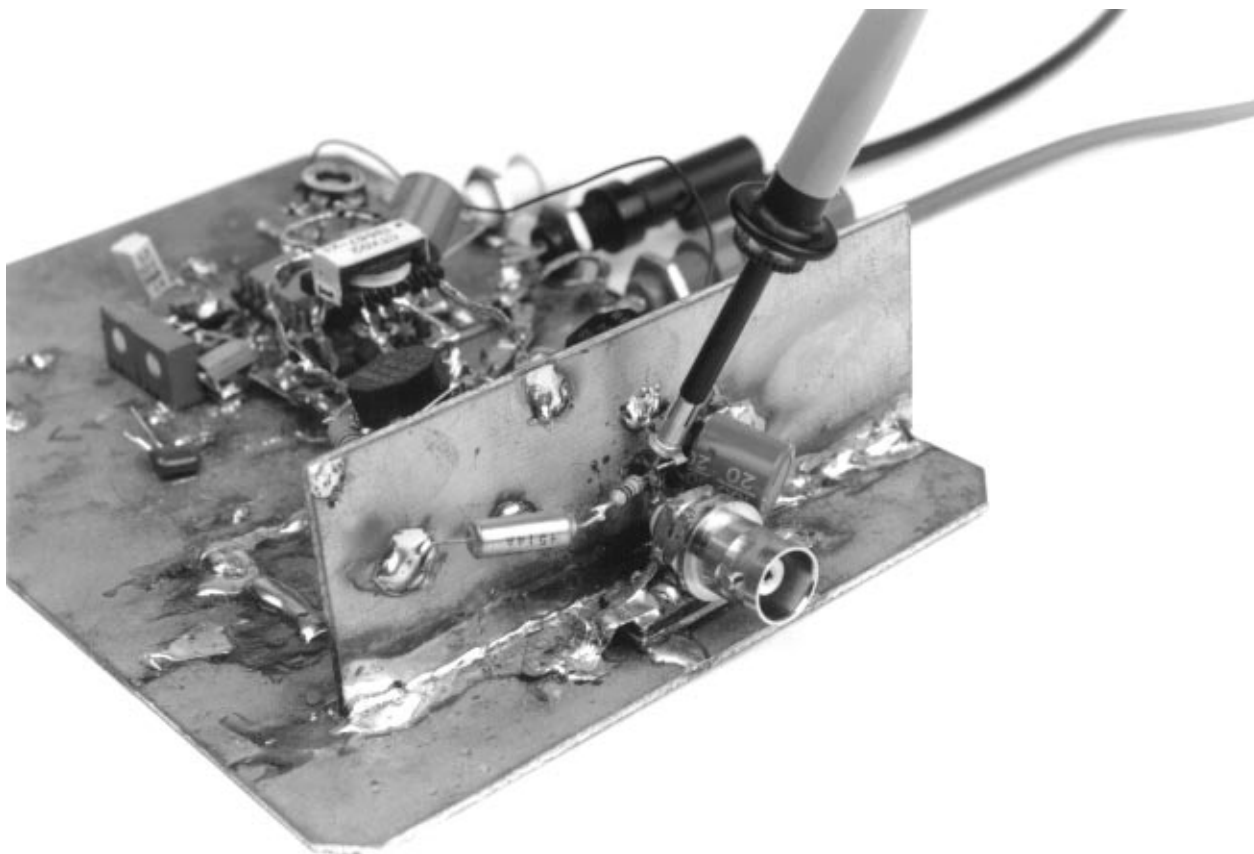


Figure C7. Probe with Tip Grounding Attachment Approximates Coaxial Connection

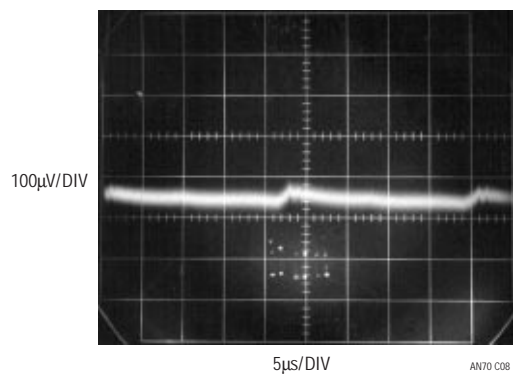


Figure C8. Probe with Tip Grounding Attachment Improves Results. Some Corruption Is Still Evident

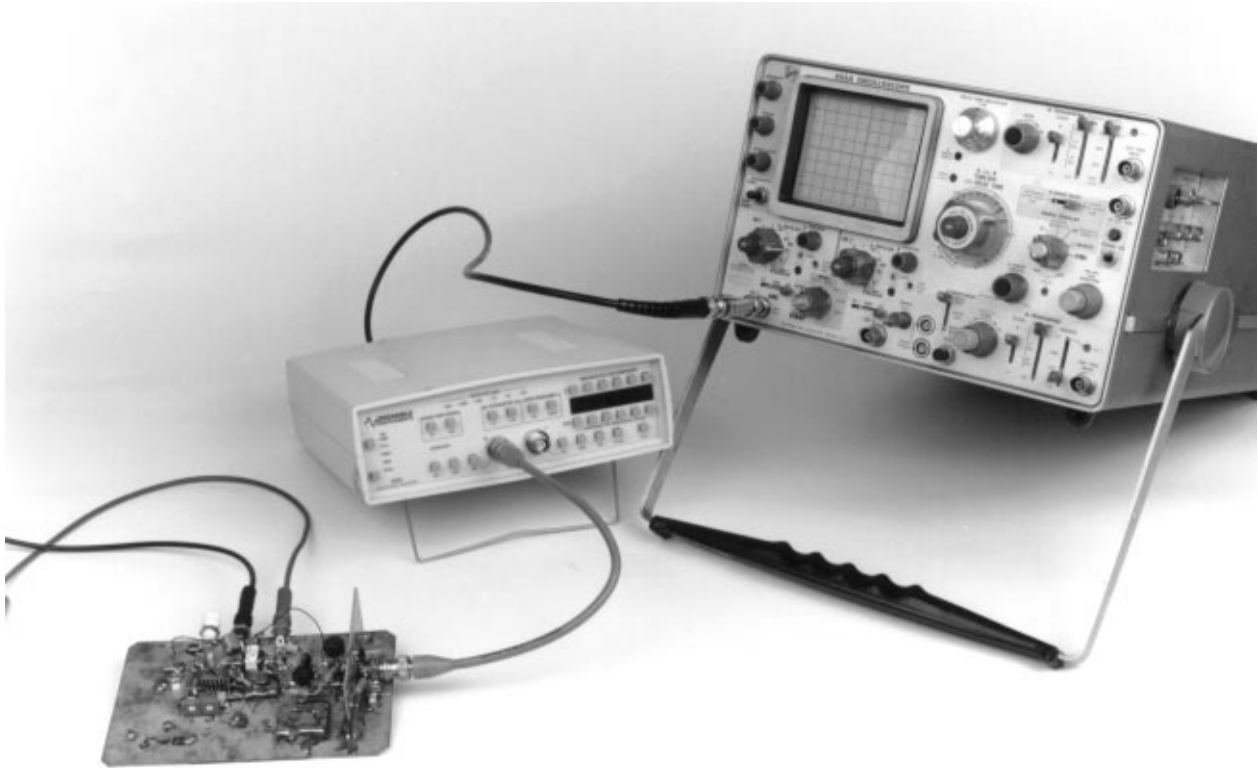


Figure C9. Coaxial Connection Theoretically Affords Highest Fidelity Signal Transmission

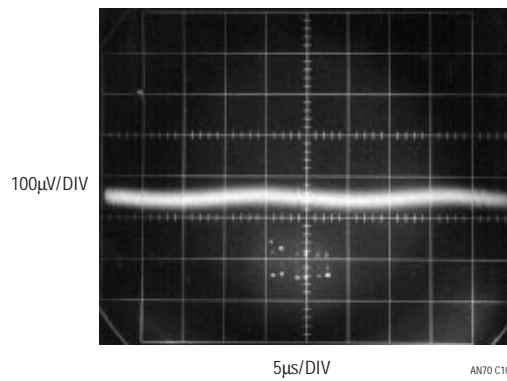


Figure C10. Life Agrees with Theory. Coaxial Signal Transmission Maintains Signal Integrity. Switching Residuals Are Faintly Outlined in Amplifier Noise



# Application Note 70

---

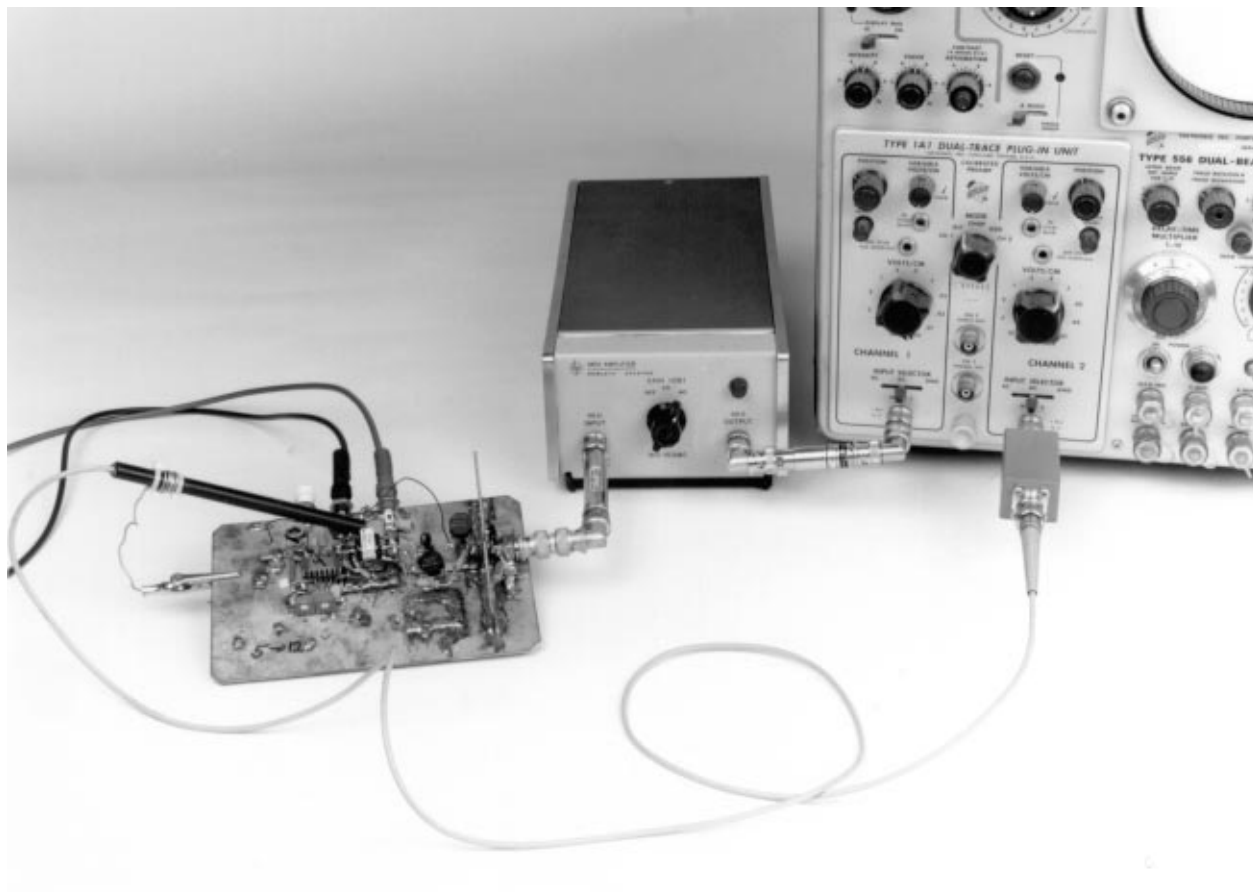


Figure C11. Direct Connection to Equipment Eliminates Possible Cable-Termination Parasitics, Providing Best Possible Signal Transmission

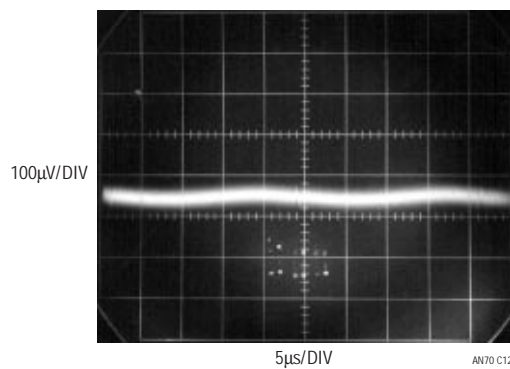


Figure C12. Direct Connection to Equipment Provides Identical Results to Cable-Termination Approach. Cable and Termination Are Therefore Acceptable

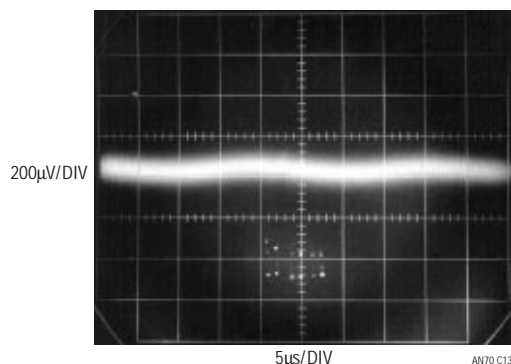


Figure C13. Voltmeter Lead Attached to Regulator Output Introduces RF Pickup, Multiplying Apparent Noise Floor

## Isolated Trigger Probe

The text associated with Figure C5 somewhat cryptically alluded to an “isolated trigger probe.” Figure C14 reveals this to be simply an RF choke terminated against ringing. The choke picks up residual radiated field, generating an isolated trigger signal. This arrangement furnishes a ‘scope trigger signal with essentially no measurement corruption. The probe’s physical form appears in Figure C15. For good results the termination should be adjusted for minimum ringing while preserving the highest possible amplitude output. Light compensatory damping produces Figure C16’s output, which will cause poor ‘scope triggering. Proper adjustment results in a more favorable output (Figure C17), characterized by minimal ringing and well-defined edges.

## Trigger Probe Amplifier

The field around the switching magnetics is small and may not be adequate to reliably trigger some oscilloscopes. In such cases, Figure C18’s trigger probe amplifier is useful. It uses an adaptive triggering scheme to compensate for variations in probe output amplitude. A stable 5V trigger output is maintained over a 50:1 probe output range. A1, operating at a gain of 100, provides wideband AC gain. The output of this stage biases a 2-way peak detector (Q1 through Q4). The maximum peak is stored in Q2’s emitter capacitor, while the minimum excursion is retained in Q4’s emitter capacitor. The DC value of the midpoint of A1’s

output signal appears at the junction of the 500pF capacitor and the 3MΩ units. This point always sits midway between the signal’s excursions, regardless of absolute amplitude. This signal-adaptive voltage is buffered by A2 to set the trigger voltage at the LT1116’s positive input. The LT1116’s negative input is biased directly from A1’s output. The LT1116’s output, the circuit’s trigger output, is unaffected by >50:1 signal amplitude variations. An X100 analog output is available at A1.

Figure C19 shows the circuit’s digital output (Trace B) responding to the amplified probe signal at A1 (Trace A).

Figure C20 is a typical noise testing setup. It includes the breadboard, trigger probe, amplifier, oscilloscope and coaxial components.

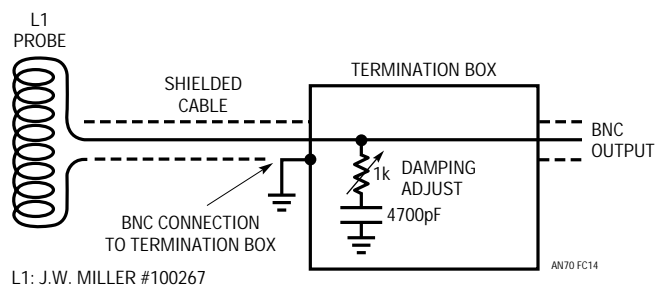


Figure C14. Simple Trigger Probe Eliminates Board Level Ground Loops. Termination Box Components Damp L1’s Ringing Response



Figure C15. The Trigger Probe and Termination Box. Clip Lead Facilitates Mounting Probe, Is Electrically Neutral

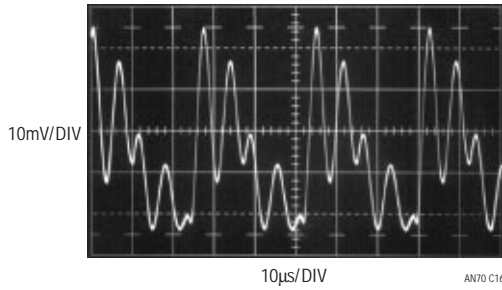


Figure C16. Misadjusted Termination Causes Inadequate Damping. Unstable Oscilloscope Triggering May Result

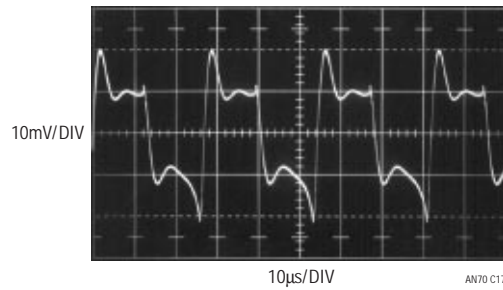


Figure C17. Properly Adjusted Termination Minimizes Ringing with Small Amplitude Penalty

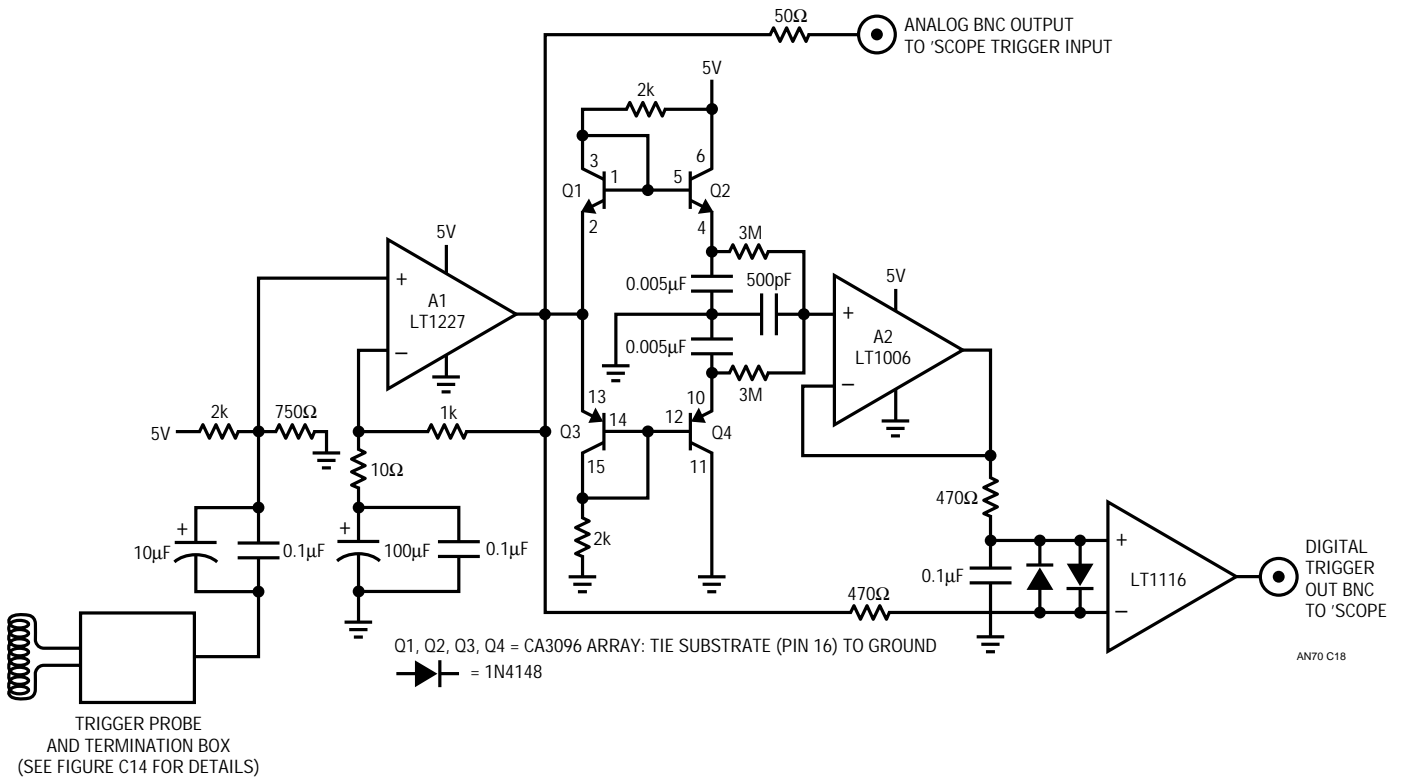


Figure C18. Trigger Probe Amplifier Has Analog and Digital Outputs. Adaptive Threshold Maintains Digital Output over 50:1 Probe Signal Variations

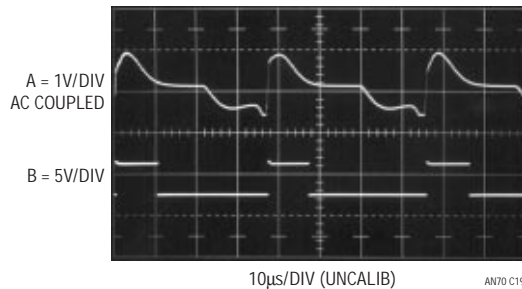


Figure C19. Trigger Probe Amplifier Analog (Trace A) and Digital (Trace B) Outputs

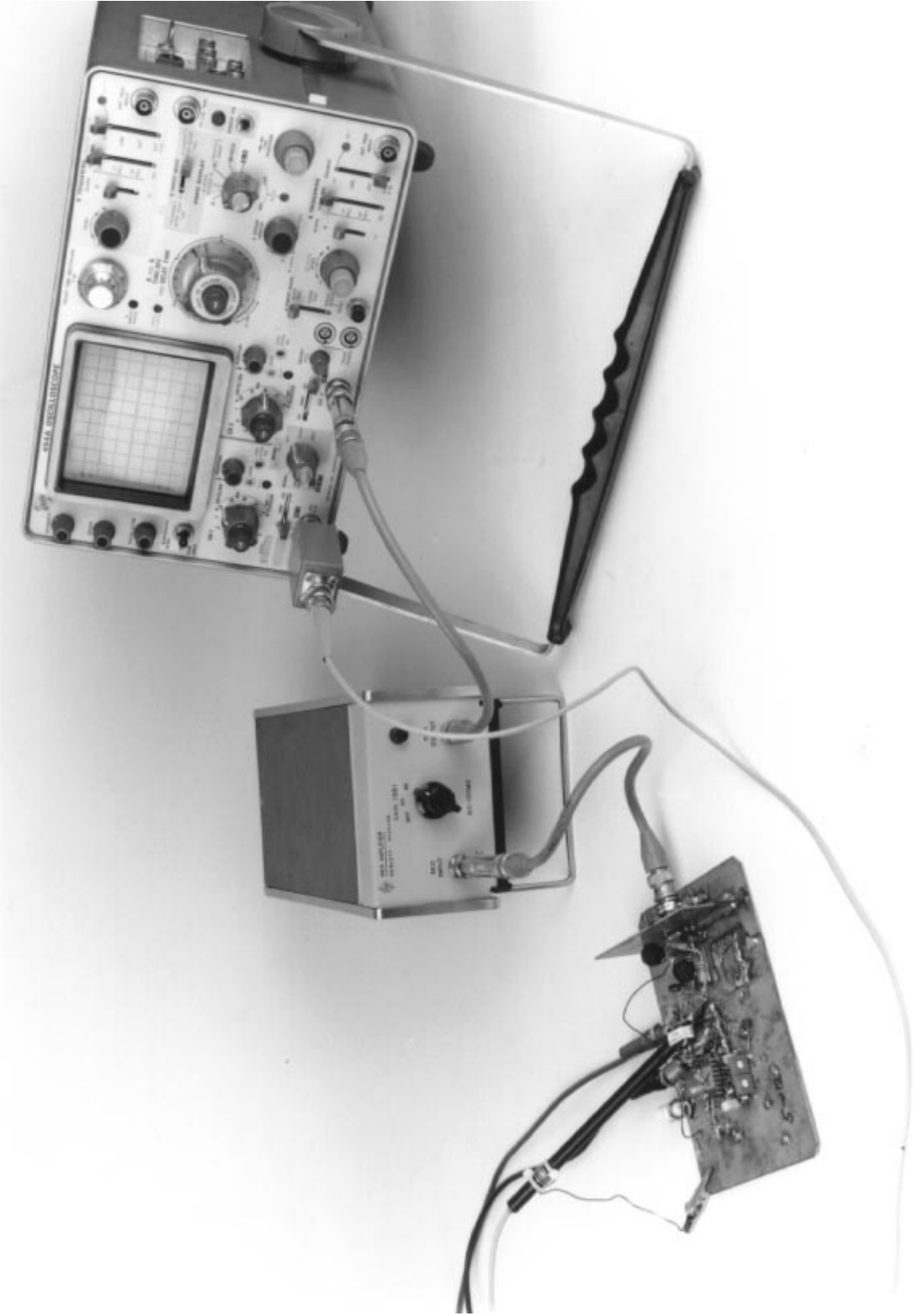


Figure C20. Typical Noise Test Setup Includes Trigger Probe, Amplifier, Oscilloscope and Coaxial Components

## APPENDIX D

### BREADBOARDING AND LAYOUT CONSIDERATIONS

LT1533-based circuit's low harmonic content allows their noise performance to be less layout sensitive than other switching regulators. However, some degree of prudence is in order. As in all things, cavaliness is a direct route to disappointment. Obtaining the absolute lowest noise figure requires care, but performance below 500 $\mu$ V is readily achieved. In general, lowest noise is obtained by preventing mixing of ground currents in the return path. Indiscriminate disposition of ground currents into a bus or ground plane will cause such mixing, raising observed output noise. The LT1533's restricted edge rates mitigate against corrupted ground path-induced problems, but best noise performance occurs in a "single-point" ground scheme. Single-point return schemes may be impractical in production PC boards. In such cases, provide the lowest possible impedance path to the power entry point from the inductor associated with the LT1533's power ground pin. (Pin 16). Locate the output component ground returns as close to the circuit load point as possible. Minimize return current mixing between input and output sections by restricting such mixing to the smallest possible common conductive area.

#### 5V to 12V Breadboard

Figure D1 shows text Figure 5's breadboard. In keeping with a breadboard's purpose, it is constructed to be fast and easy to modify. Single-point returns arrive separately

from the output area (right side of photo) and Pin 16 of the LT1533 (center left photo). The ground plane carries no current. The dummy load resistors are *not* terminated to the plane, but returned to the transformer's center tap. The center tap and plane are separately tied into the ground system at the power input common jack.

#### 5V to $\pm$ 15V Breadboard

Text Figure 24's breadboard appears in Figure D2. Layout considerations are similar to Figure D1, although the design's floating output mandates changes. The output load (photo's right, above BNC connector) returns directly to the transformer secondary, which floats from input (and plane) ground potential. The main ground plane is tied to input common at the power entry port (left banana jack). The floating output potentials are referred to a separate, smaller planed area (photo lower right) which is tied to the transformer secondary center tap.

#### Demonstration Board

Figure D3 enticingly portrays an LT1533 demonstration board. The board's practical layout is readily adaptable to production versions. This board is useful for observing LT1533 performance and as an example of a practical layout. Noise performance is similar to the text's breadboards.



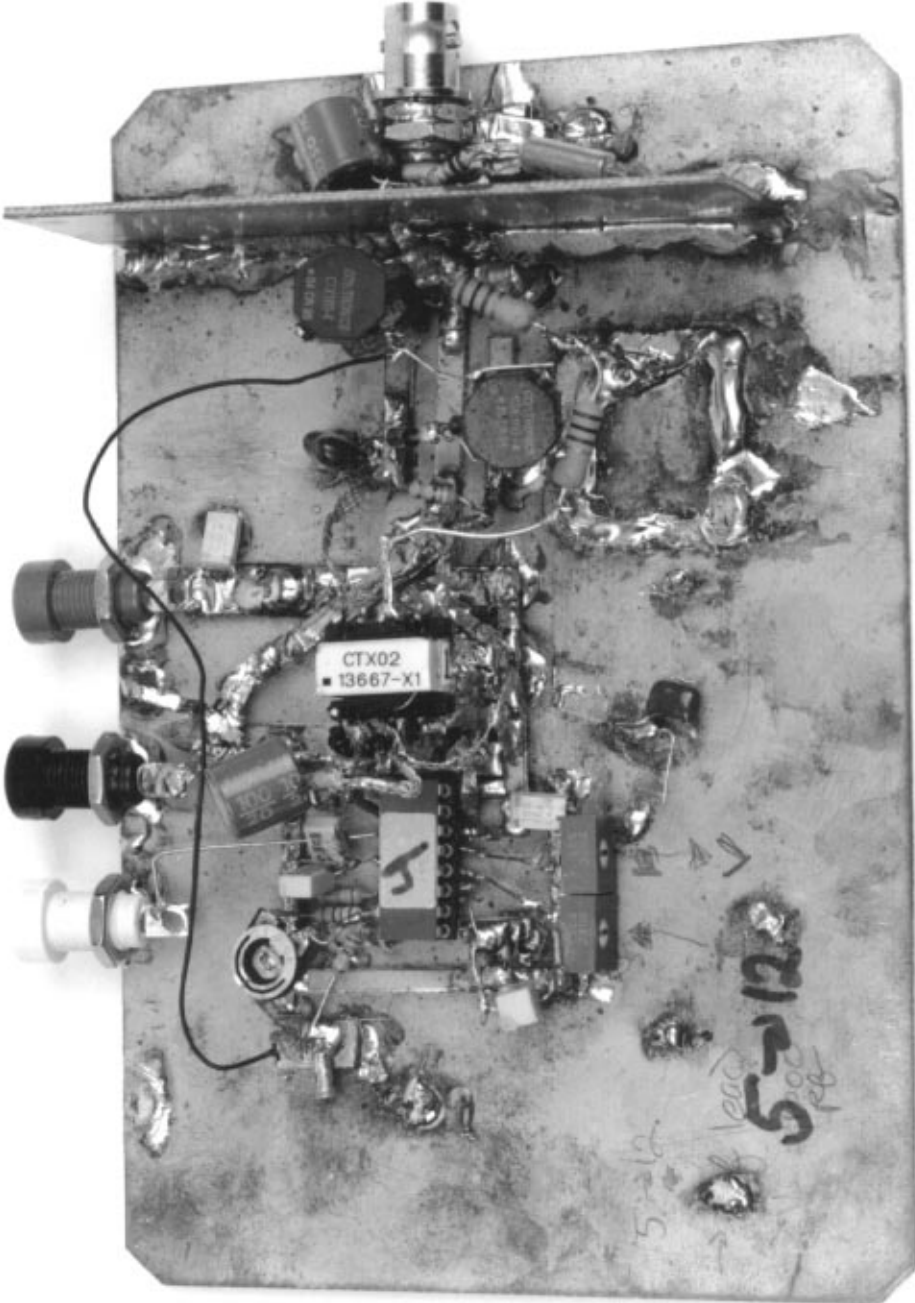


Figure D1. Text Figure 5's 5V-to-12V Converter Breadboard. Construction Is Easy to Change, Facilitating Experiments. Note Single-Point Ground Returns. Ground Plane Carries No Current, Is Tied to Input Common at Board Entry Point (Middle Banana Jack)



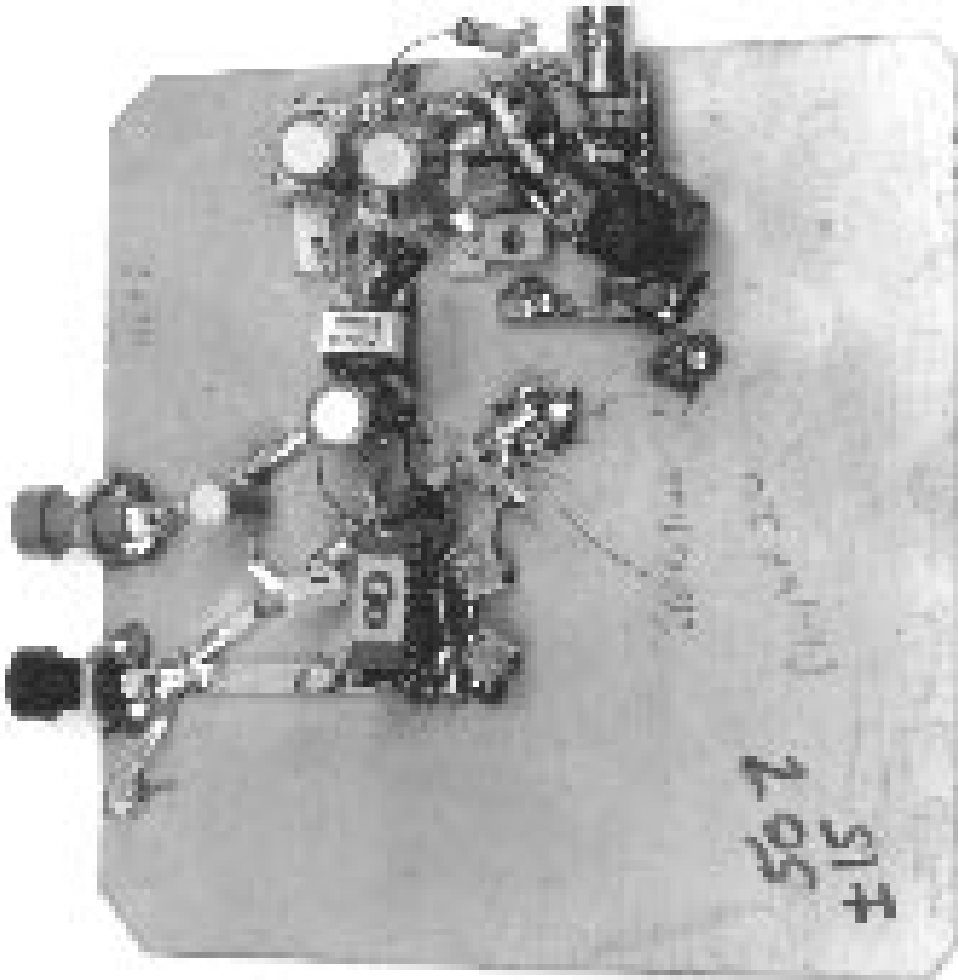


Figure D2. Text Figure 26's Breadboard with Linear Output Regulators. Construction Encourages Changes and Measurement. Layout Is Similar to Figure D1, Although Floating Output Necessitates Changes. Separate Planed Area (Photo Center Right) Maintains Low Impedance Between Output-Related Returns

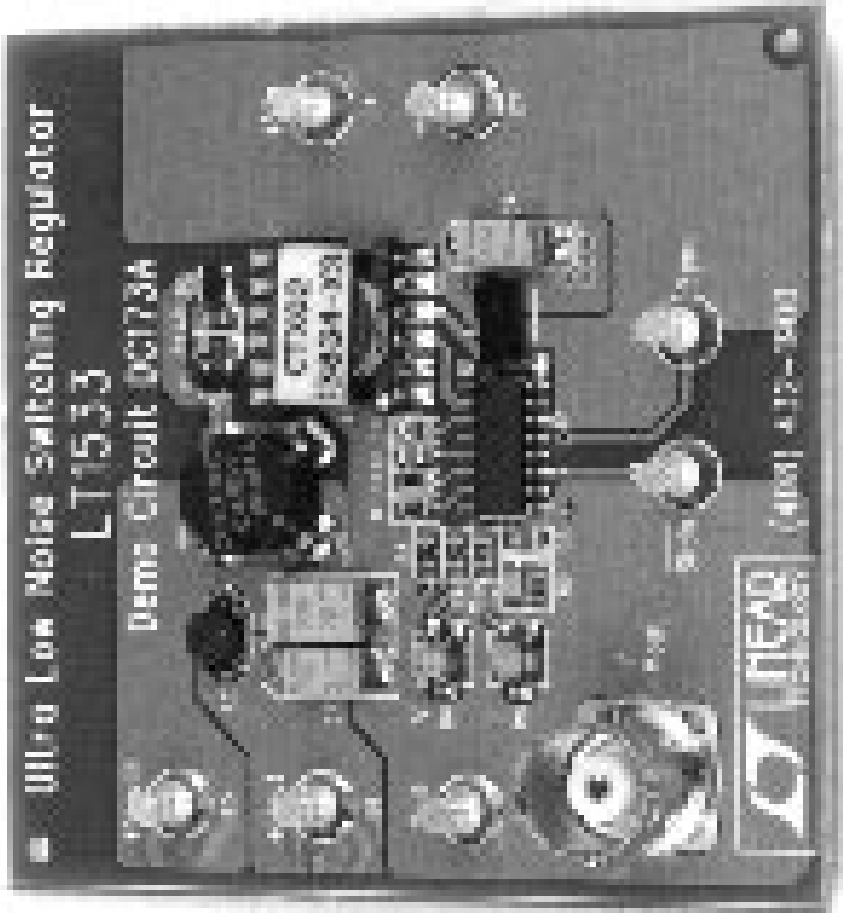


Figure D3. The Very Civilized LT1533 Demonstration Board in All Its Comely Splendor

## APPENDIX E

### SELECTION CRITERIA FOR LINEAR REGULATORS

Some applications, particularly floating output circuits, may require linear postregulators. Selection criteria include regulator output accuracy, dropout, ripple rejection and line regulation. Often, short-circuit protection is not needed because drive circuit output impedance and current limiting prevent destructive overload. In such cases, if relatively poor output load regulation and accuracy are acceptable, simple Zener diode-emitter follower-based regulation may suffice. LM78L/79L type devices offer 5% output accuracy and improved line regulation, although dropout is about 2V—significantly higher than a simple Zener-emitter follower regulator. Ripple rejection in LM78L/79L types degrades as they approach dropout, which is the desirable operating region for best efficiency. High performance regulators such as the LT1575 (negative) and LT1521 (positive) offer dropout voltages below 0.5V, tight line regulation, 1% accuracy and fully specified ripple rejection close to dropout.

It is usually desirable to operate close to dropout to maintain good overall efficiency. Because of this, regulator ripple rejection should be tested in this intended operating region. Additionally, cost, size and performance trade-offs of various filter components and regulators should be evaluated to determine the best solution for a particular application.

### Testing Ripple Rejection

Ripple rejection may be tested with Figure E1's arrangement. The generator should operate over the frequency range of interest and be capable of supplying the required output drive. In practice, the generator is set to supply the regulator input operating voltage at the expected LT1533 switching frequency. Comparison of different regulators and filter components under varying operating conditions is easily carried out.

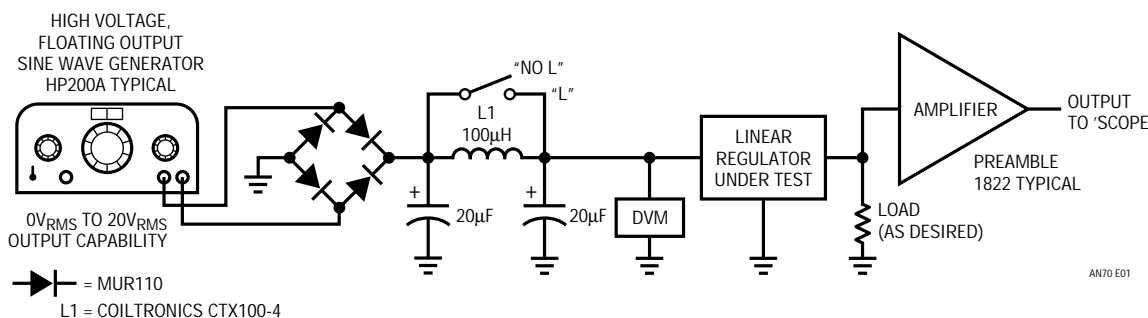


Figure E1. Ripple Rejection Test Setup for Linear Regulators. LC Combinations and Regulators May Be Evaluated



Figure E2. Ripple Rejection Test Setup Includes Sine Wave Generator, Breadboard, Amplifier and Oscilloscope

## APPENDIX F

### MAGNETICS CONSIDERATIONS

#### Transformers

The LT1533's symmetrical "push-pull" drive makes transformer behavior quite predictable. As such, transformers may usually be specified by indicating the operating frequency, power and desired input/output voltages. Figure F1 lists the transformers used in the text circuits along with some of their characteristics. These components, and variations on them, are available from Coiltronics, telephone #561-241-7876.

#### Inductors

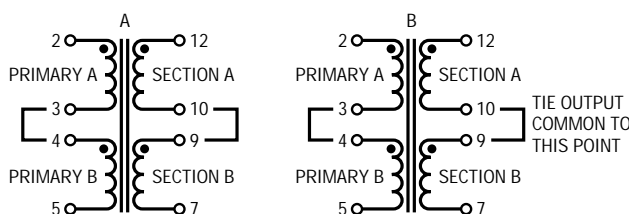
Inductors in LT1533 circuits do not have special characteristics. Text Figure 5's circuit, a "forward" type converter,<sup>1</sup> requires an inductor ahead of its filter capacitor, although additional LC filtering is optional. Figure 26's "50%" mode circuit has no output inductor requirement

unless heavily loaded (see text), although LC sections may be used for best possible ripple attenuation. In either case, inductor characteristics are not particularly critical. All circuits shown in the text use Coiltronics "Octa-Pak" type toroidal core-based inductors.

The 22nH inductor used in the LT1533's power ground return (Pin 16) is mandatory. It may take several forms, including trace inductance, a small coil of wire, a ferrite bead or the packaged inductor specified in the schematics. If coiled wire is employed, five turns of #28 is sufficient. An equivalent length of PC trace gives similar results. A ferrite bead (e.g., Ferronics #21-110J or equivalent) with one or two turns of wire also works well. An example of a packaged 22nH inductor is the Coilcraft B-07T which is specified in the test circuits.

Note 1: See References 16 and 17 for basic forward converter theory.

NOMINAL INPUT VOLTAGE	NOMINAL OUTPUT VOLTAGE AFTER LINEAR REGULATOR	OUTPUT POWER	COILTRONICS PART NUMBER	CONNECTION DIAGRAM
5V	12V	1.5W	CTX-02-13716-X1	A
5V	12V	3.0W	CTX-02-13665-X1	A
5V	±15V	1.5W	CTX-02-13713-X1	B
5V	±15V	3.0W	CTX-02-13664-X1	B
5V	12V	1.5W	CTX-02-13834-X3*	A
5V	12V	10W	CTX-02-13949-X1	A



☐ = TIED TOGETHER

\* = HIGH TURNS RATIO VERSION OF CTX-02-13716-X1. ACCOMMODATES LOW SUPPLY VOLTAGES OR HIGH DROPOUT REGULATORS

AN70 FF01

Figure F1. Transformer Types Used in Text Circuits. Variations for Specific Requirements Are Available from Coiltronics, 561-241-7876

# Application Note 70

## APPENDIX G

### WHY VOLTAGE AND CURRENT SLEW CONTROL?

Carl T. Nelson

The LT1533 gives dramatic reduction of high frequency noise by controlling both voltage and current slew rates in the switch. This technique also has the advantage of controlling noise in the other switching regulator components, namely, the catch diode and input and output capacitors.

Figure G1's block diagram shows the basic concepts for slew control. The switch Q1 is driven on and off with currents  $I_1$  and  $I_2$  switched via S1. These currents are large enough to drive the switch at very high slew rates. Actual slew rates are set by  $I_3$  for voltage slew and  $I_4$  for current slew.

During switch turn-on, the collector of Q1 is initially high and current is zero. Inductor current holds the switch high until switch current equals inductor current. The first limiting action occurs as current builds in Q1. Current is sensed by a fixed gain amplifier A3. The increasing current generates a current through C2 proportional to switch current slew rate. This current is compared to  $I_4$ , and the

difference is amplified by A2, which shunts away all excess  $I_1$  current to control switch current slew rate.

When switch current exceeds inductor current, Q1's collector would normally fall low at a speed limited only by diode and switch parasitic capacitance. To control voltage slew, the current through C1 is compared to  $I_3$ , and the difference is amplified by A1 to clamp the base current of Q1. This stops any further rise in switch current and forces switch voltage to fall at a controlled rate.

At switch turn-off, current and voltage must be controlled in the reverse order. Switch S1 is flipped to provide reverse base drive, and the polarity of  $I_3$  and  $I_4$  is reversed. Almost immediately, switch current falls slightly below inductor current. This would normally cause the switch voltage to slew up, limited only by diode and switch capacitance. Here, C1 senses voltage slew and A1 controls switch base drive to limit switch rise time. Switch current remains essentially constant during voltage slew.

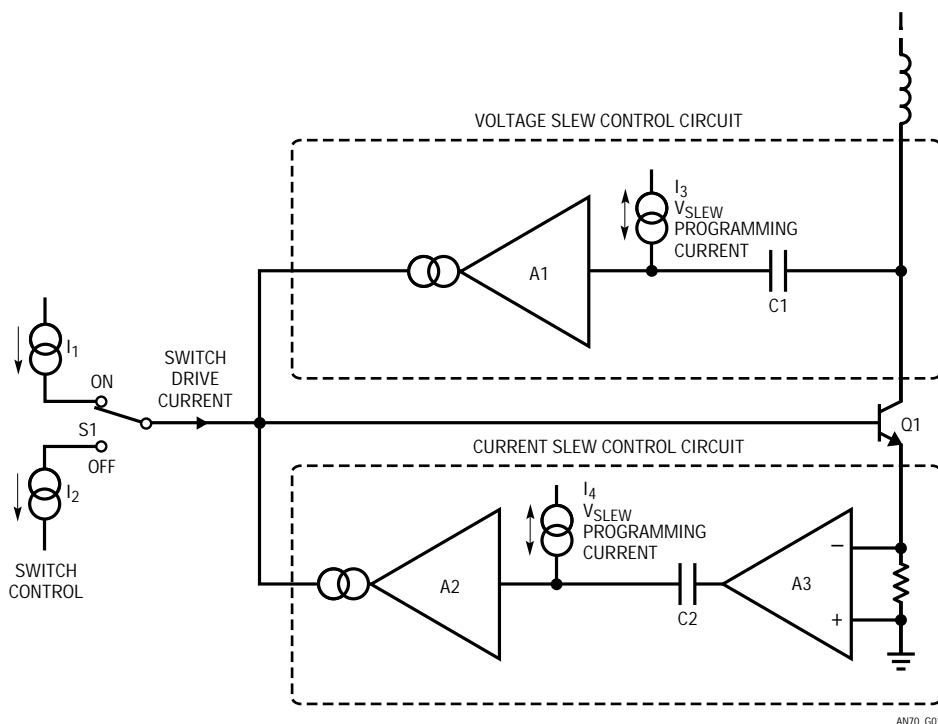


Figure G1. Slew Control Conceptual Block Diagram

When switch voltage reaches the level where the catch diode turns on, switch current would normally drop rapidly, creating fast B field transients around the switch, diode and output capacitor lines. A3 and C2 come into play here, sensing the decreasing switch current and controlling the base drive via A2 to force a controlled decrease in switch, diode and capacitor current.

Figure G2 shows switch, diode and output capacitor waveforms with controlled switch drive in operation. Note that current and voltage slew limiting do not occur simultaneously. One must take over when the first is complete. This requires very fast control circuitry to avoid crossover glitches that would create noise spikes.

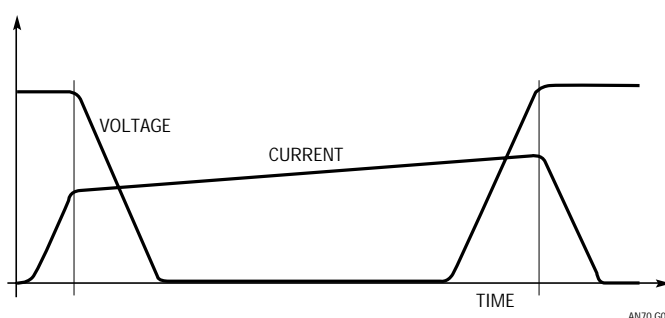


Figure G2. Switch Voltage and Current During Turn-On and Turn-Off

## APPENDIX H

### HINTS FOR LOWEST NOISE PERFORMANCE

The LT1533's controlled switching times allow extraordinarily low noise DC/DC conversion with surprisingly little design effort. Wideband output noise well below 500 $\mu$ V is easily achieved. In most situations this level of performance is entirely adequate. Applications requiring the lowest possible output noise will benefit from special attention to several areas.

#### Noise Tweaking

The slew time versus efficiency trace-off discussed in the text should be weighted towards lowest noise to the extent tolerable. Typically, slew times beyond 1.3 $\mu$ s result in "expensive" noise reduction in terms of lost efficiency, but the benefit is available. The issue is how much power is expendable to obtain incremental decreases in output noise. Similarly, the layout techniques discussed in Appendix D should be reviewed. Rigid adherence to these guidelines will result in correspondingly lower noise performance. The text's breadboards were originally constructed to provide the lowest possible noise levels, and then systematically degraded to test layout sensitivity. This approach allows experimentation to determine the best layout without expending fanatical attention to details that provide essentially no benefit.

The slow edge times greatly minimize radiated EMI, but experimentation with the component's physical orienta-

tion can sometimes improve things. Look at the components (yes, literally!) and try and imagine just what their residual radiated field impinges on. In particular, the optional output inductor may pick up field radiated by other magnetics, resulting in increased output noise. Appropriate physical layout will eliminate this effect, and experimentation is useful. The EMI probe described in Appendix J is a useful tool in this pursuit and highly recommended. Appendix I contributes hints on magnetics-based noise and is similarly recommended.

#### Capacitors

The filter capacitors used should have low parasitic impedance. Sanyo OS-CON types are excellent in this regard and contributed to the performance levels quoted in the text. Tantalum types are nearly as good. The input supply bypass capacitor, which should be located directly at the transformer center tap, needs similarly good characteristics. Aluminum electrolytics are not suitable for any service in LT1533 circuits.

#### Damper Network

Some circuits may benefit from a small (e.g., 330 $\Omega$ -1000pF) damper network across the transformer secondary if the absolutely lowest noise is needed. Extremely small (20 $\mu$ V to 30 $\mu$ V) excursions can briefly appear during



# Application Note 70

the switching interval when no energy is coming through the transformer. These events are so minuscule that they are barely measurable in the noise floor, but the damper will eliminate them.

## Measurement Technique

Strictly speaking, measurement technique is not a way to obtain lowest noise performance. Realistically, it is essen-

tial that measurement technique be trustworthy. Uncountable hours have been lost chasing “circuit problems” that in reality are manifestations of poor measurement technique. Please read Appendices B and C before pursuing solutions to circuit noise that isn’t really there.<sup>1</sup>

Note 1: I do not wax pedantic here. My guilt in this offense runs deep.

## APPENDIX I

### PROTECTION AGAINST MAGNETICS NOISE IS KNOWLEDGE AND GOOD COMMON SENSE

Jon Roman—Coiltronics, Inc.

#### Noise Test Data

For this test I chose four of the most common magnetics geometries that are currently in production use today. They are as follows: Pot Core, ER Core, E Core and the Toroid. The following test data was taken using the methods as described in the following paragraphs. The test circuit used to determine the amount of noise radiation is as shown in Figure I1 . The push-pull configuration, power ratings and turns ratios were chosen to align with the Jim Williams’ low noise designs presently under study. The distance chosen for the Sniffer Noise Probe<sup>1</sup> was set at 0.250 inches from the surface of the core structure. This distance was chosen as a result of preliminary testing to allow for a measurable reading on the smallest amount of flux lines coming from the quietest core structure. The measured worst-case full load noise is shown in Figure I2, for each of the four geometries chosen for this test. Note

that the noise is shown in millivolts rather than gauss, the conversion for gauss is:

$$V_{\text{PROBE}}(\text{mV}_{\text{P-P}}) = 2.88\text{mGauss}/\mu\text{s}^2$$

After taking the noise reading for each of the UUT’s under their full load conditions, the load resistor was removed to allow for observation of magnetizing flux noise. Then, using the same measurement techniques, the noise was measured a second time to determine the difference between the load noise and the magnetizing noise. The measured worst-case magnetizing noise is shown in Figure I3.

Note 1: See Appendix J.

Note 2: See Appendix J.

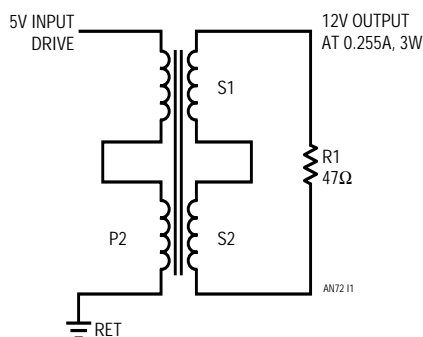


Figure I1. Test Circuit

GEOMETRY	FULL LOAD MAGNETIZING
Pot Core	20mV
ER Core	63mV
E Core	488mV
Toroid	860mV

Figure I2. Worst-Case Full Load Noise

GEOMETRY	FULL LOAD MAGNETIZING
Pot Core	16mV
ER Core	49mV
E Core	95mV
Toroid	91mV

Figure I3. Worst-Case Magnetizing Load Noise

## Pot Core

The Pot core tested was as predicted the quietest geometry of the ones tested. Just as expected the "Hot Spot" for noise was located at the window of the gap where the leads exit the core. Reference the waveform shown in Figure I4. Note the top waveform shows the voltage input, the middle waveform shows the noise as recorded using an amplifier and the bottom waveform is the current through the UUT.

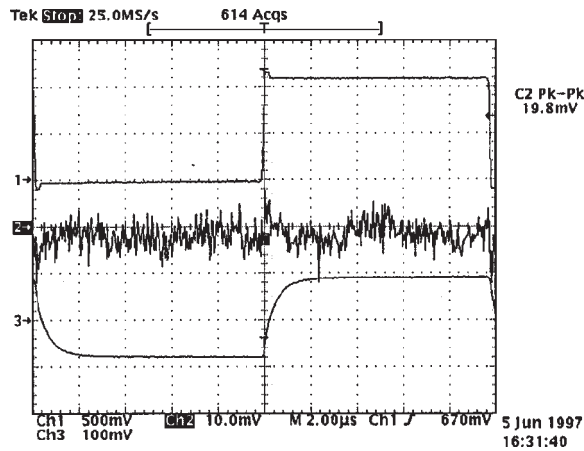
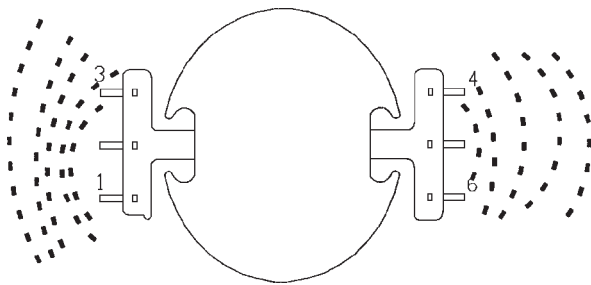


Figure I4

## ER Core

The ER core tested was the surprise of the group with a much lower noise reading than one would have originally thought possible. Reference the waveform shown in Figure I5. Note the top waveform shows the voltage input, the middle waveform shows the noise as recorded using an amplifier and the bottom waveform is the current through the UUT.

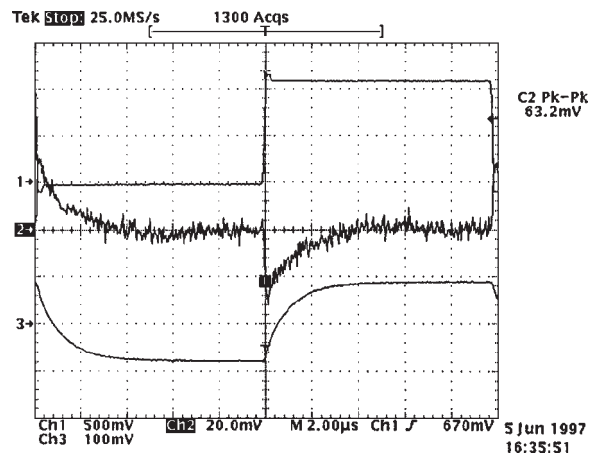
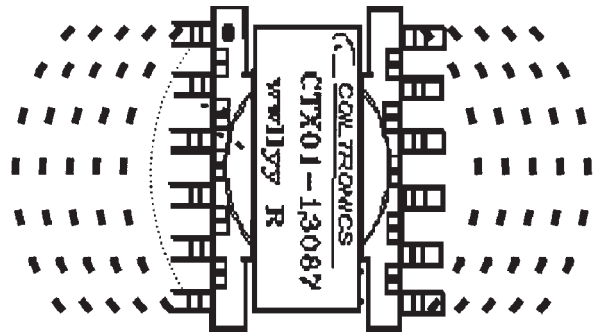


Figure I5

# Application Note 70

## Toroid

The Toroid core (Figure I6) tested showed a much higher electronic noise than was originally expected from a closed-path geometry. The worst-case noise came from the top of the core, with the winding placed as evenly on the core as possible. Note the top waveform shows the voltage input, the middle waveform shows the noise as recorded using an amplifier and the bottom waveform is the current through the UUT.

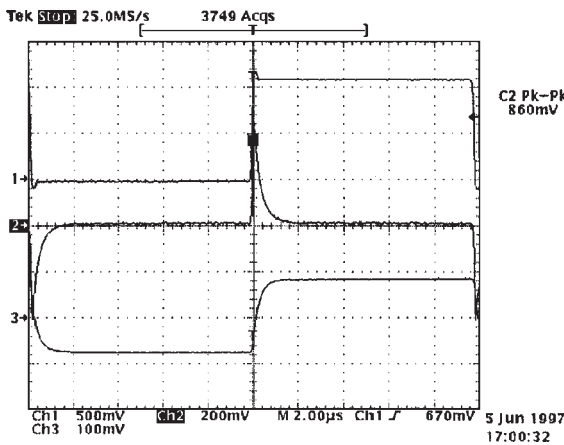
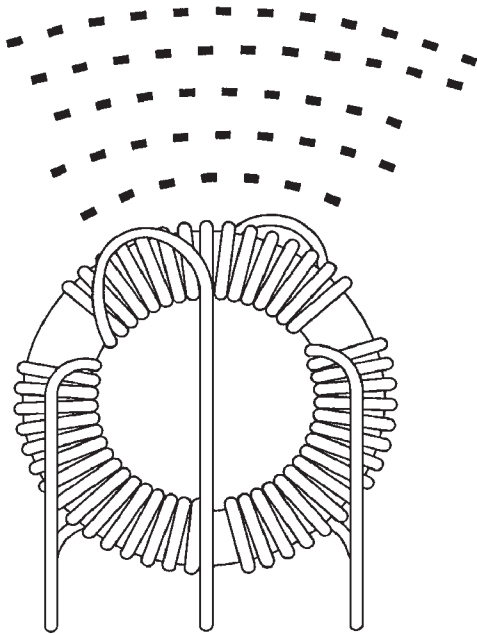


Figure I6

## E Core

The E-core (Figure I7) showed the highest concentration of noise just above the winding on the top center of the device. The noise on the surrounding sides was measurable but far below the field that was found directly above and below the part. Note the top waveform shows the voltage input, middle waveform shows the noise as recorded using an amplifier and the bottom waveform is the current through the UUT.

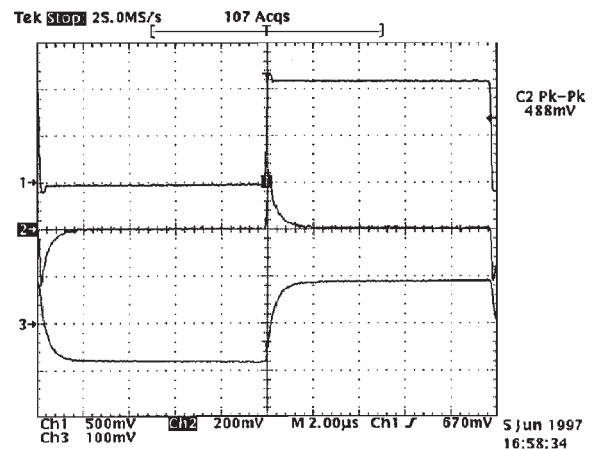
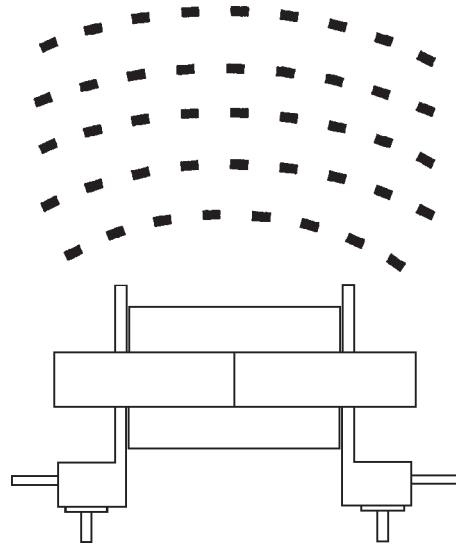


Figure I7

## Summary

Figure 18 is a graph showing the relative difference comparing the full load noise against the magnetizing load noise. It is recognized that closed core structures such as toroids in inductors produce less stray (leakage) flux than open structures like rod cores or bobbin cores. Some recent products offer “magnetic shields” or tubes of magnetic material around a bobbin-type core in an attempt to provide a “magnetic shunt” for the flux to follow. These structures offer very little reduction in noise because of the high reluctance in the air gap between the “shield” and the inner bobbin core. The reluctance in this gap is much higher than that of the magnetic material. The resultant leakage flux from the gap can defeat the purpose of the shield almost entirely! The best approach for reducing noise in inductors is to use true closed-field geometries, such as the toroid.

When designing for the lowest possible noise in transformer applications, it is important to observe the effects

of the load current, as opposed to the magnetizing current. The preceding test demonstrates that the traditional low noise structures (toroid) can radiate relatively high amounts of leakage flux due to the coupling characteristics between windings. The reflected load currents in both the primary and the secondary do not affect the magnetizing flux, but create a magnetic leakage field around the wire, if the coupling is less than perfect. This is, by definition, leakage flux. The size and shape of the window area can have an effect on coupling between windings, as well as the shape of the flux field emanating from the transformer.

Winding technique also has an effect on coupling and noise. Multifilar winding, as opposed to layer winding, can offer better coupling characteristics, which in turn, lowers noise by lessening leakage flux.

## Conclusion

Every *millivolt* counts.

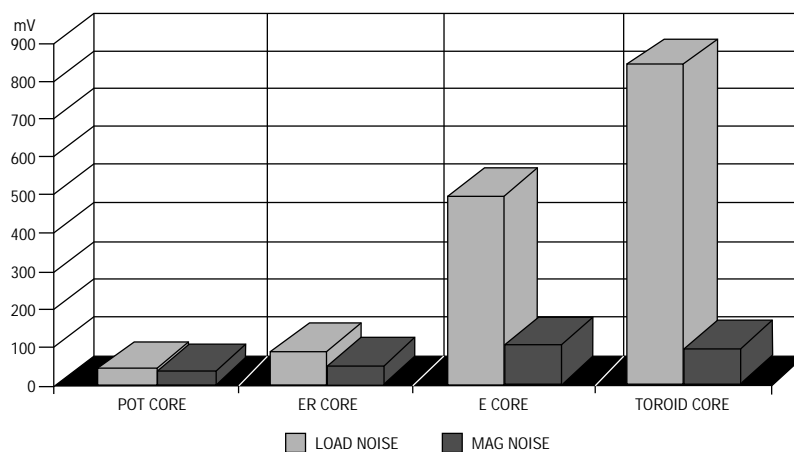


Figure 18

## APPENDIX J

### MEASURING EMI RADIATION

EMI (Electromagnetic Interference) is a form of switching regulator noise. It is a radiated, as opposed to conducted, phenomenon. LT1533-based circuits produce low amounts of EMI for the same reason they minimize conducted noise—controlled switching times. This appendix, guest written by Bruce Carsten, describes an excellent tool for

relative EMI measurement and how to use it.<sup>1</sup> Carsten’s methods not only show how to measure relative EMI, but how to identify and silence its source.

Note 1: Calibrated measurements are discussed in References 14 and 15.

# Application Note 70

---

APPLICATION NOTE E101: EMI "SNIFFER" PROBE  
Bruce Carsten Associates, Inc.  
6410 NW Sisters Place, Corvallis, Oregon 97330  
541-745-3935

The EMI Sniffer Probe<sup>2</sup> is used with an oscilloscope to locate and identify magnetic field sources of electromagnetic interference (EMI) in electronic equipment. The probe consists of a miniature 10 turn pickup coil located in the end of a small shielded tube, with a BNC connector provided for connection to a coaxial cable (Figure J1). The Sniffer Probe output voltage is essentially proportional to the rate of change of the ambient magnetic field, and thus to the rate of change of nearby currents.

The principal advantages of the Sniffer Probe over simple pickup loops are:

1. Spatial resolution of about a millimeter.
2. Relatively high sensitivity for a small coil.
3. A 50Ω source termination to minimize cable reflections with unterminated scope inputs.
4. Faraday shielding to minimize sensitivity to electric fields.

The EMI Sniffer Probe was developed to diagnose sources of EMI in switch mode power converters, but it can also be used in high speed logic systems and other electronic equipment.

## SOURCES OF EMI

Rapidly changing voltages and currents in electrical and electronic equipment can easily result in radiated and conducted noise. Most EMI in switch mode power converters is thus generated during switching transients when power transistors are turned on or off.

Conventional scope probes can readily be used to see dynamic voltages, which are the principal sources of common mode conducted EMI. (High  $dV/dt$  can also feed through poorly designed filters as normal mode voltage spikes and may radiate fields from a circuit without a conductive enclosure.)

Dynamic currents produce rapidly changing magnetic fields which radiate far more easily than electric fields as

they are more difficult to shield. These changing magnetic fields can also induce low impedance voltage transients in other circuits, resulting in unexpected normal and common mode conducted EMI.

These high  $dI/dt$  currents and resultant fields can not be directly sensed by voltage probes, but are readily detected and located with the Sniffer Probe. While current probes can sense currents in discrete conductors and wires, they are of little use with printed circuit traces or in detecting dynamic magnetic fields.

## PROBE RESPONSE CHARACTERISTICS

The Sniffer Probe is sensitive to magnetic fields only along the probe axis. This directionality is useful in locating the paths and sources of high  $dI/dt$  currents. The resolution is usually sufficient to locate which trace on a printed circuit board, or which lead on a component package, is conducting the EMI generating current.

For "isolated" single conductors or PC traces, the Probe response is greatest just to either side of the conductor where the magnetic flux is along with probe axis. (Probe response may be a little greater with the axis tilted towards the center of the conductor.) As shown in Figure J2, there is a sharp response null in the middle of the conductor, with a 180° phase shift to either side and a decreasing response with distance. The response will increase on the inside of a bend where the flux lines are crowded together, and is reduced on the outside of a bend where the flux lines spread apart.

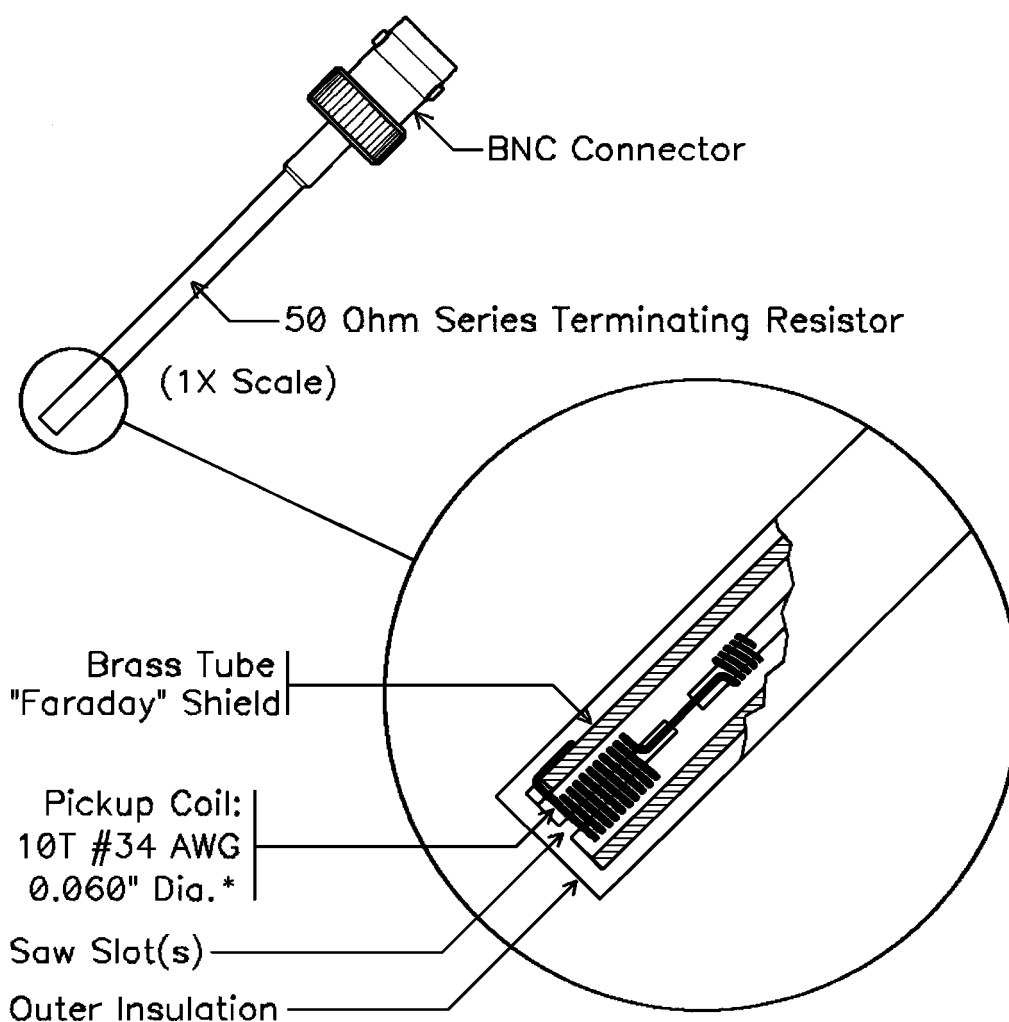
When the return current is in an adjacent parallel conductor, the Probe response is greatest between the two conductors as shown in Figure J3. There will be a sharp null and phase shift over each conductor, with a lower peak response outside the conductor pair, again decreasing with distance.

---

Note 2: The EMI Sniffer Probe is available from Bruce Carsten Associates at the address noted in the title of this appendix.

The response to a trace with a return current on the opposite side of the board is similar to that of a single isolated trace, except that the probe response may be greater with the Probe axis tilted away from the trace. A

"ground plane" below a trace will have a similar effect, as there will be a counter-flowing "image" current in the ground plane.



© 1997, Bruce Carsten Associates, Inc.

\* Approx. 160 $\mu$  Wire, 1.5mm Coil Dia.

Figure J1. Construction of the EMI "Sniffer Probe" for Locating and Identifying Magnetic Field Sources of EMI

# Application Note 70

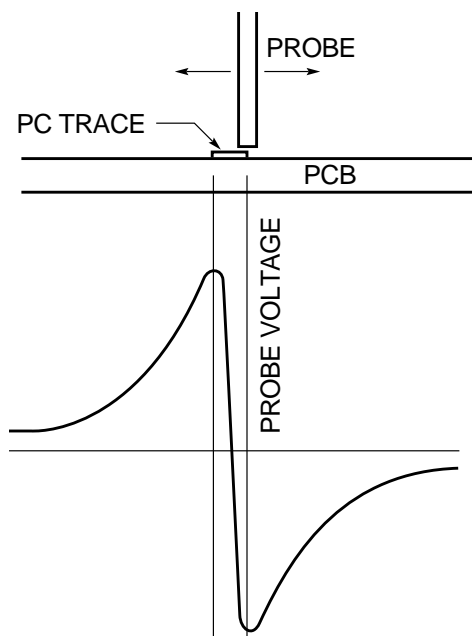


Figure J2. Sniffer Probe Response to Current in a Physically “Isolated” Conductor

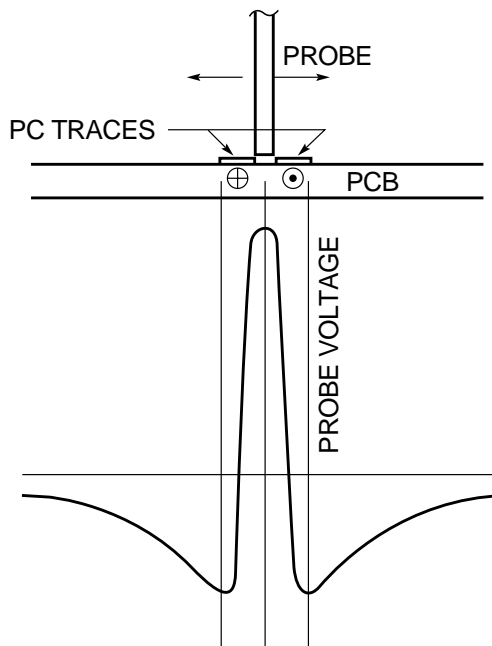


Figure J3. Sniffer Probe Response with Return Current in a Parallel Conductor

The Probe frequency response to a uniform magnetic field is shown in Figure J4. Due to large variations in field strength around a conductor, the Probe should be considered as a qualitative indicator only, with no attempt made to “calibrate” it. The response fall-off near 300MHz is due to the pickup coil inductance driving the coax cable impedance, and the mild resonant peaks (with a 1M $\Omega$  scope termination) at multiples of 80MHz are due to transmission line reflections.

## PRINCIPLES OF PROBE USE

The Sniffer Probe is used with at least a 2-channel scope. One channel is used to view the noise whose source is to be located (which may also provide the scope trigger) and the other channel is used for the Sniffer Probe. The probe response nulls make it inadvisable to use this scope channel for triggering.

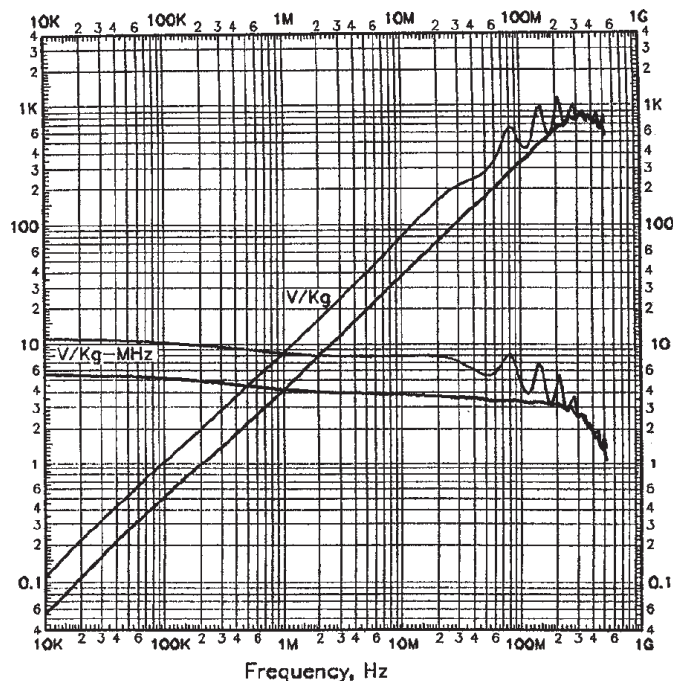
A third scope trigger channel can be very useful, particularly if it is difficult to trigger on the noise. Transistor drive waveforms (or their predecessors in the upstream logic) are ideal for triggering; they are usually stable, and allow immediate precursors of the noise to be viewed.

Start with the Probe at some distance from the circuit with the Probe channel at maximum sensitivity. Move the probe around the circuit, looking for “something happening” in the circuit’s magnetic fields at the same time as the noise problem. A precise “time domain” correlation between EMI noise transients and internal circuit fields is fundamental to the diagnostic approach.

As a candidate noise source is located, the Probe is moved closer while the scope sensitivity is decreased to keep the probe waveform on-screen. It should be possible to quickly bring the probe down to the PC board trace (or wiring) where the probe signal seems to be a maximum. This may not be near the point of EMI generation, but it should be near a PC trace or other conductor carrying the current from the EMI source. This can be verified by moving the probe back and forth in several directions; when the appropriate PC trace is crossed at roughly right angles, the probe output will go through a sharp null over the trace, with an evident phase reversal in probe voltage on each side of the trace (as noted above).

This EMI “hot” trace can be followed (like a bloodhound on the scent trail) to find all or much of the EMI generating current loop. If the trace is hidden on the back side (or





©1996, Bruce Carsten Associates, Inc.

Figure J4. Typical EMI "Sniffer" Probe Frequency Response Measured with 1.3m (51") of 50Ω Coax to Scope  
 Upper Traces: 1Meg Scope Input Impedance  
 Lower Traces: 50Ω Scope Input Impedance

inside) of the board, mark its path with a felt pen and locate the trace on disassembly, on another board or on the artwork. From the current path and the timing of the noise transient, the source of the problem usually becomes almost self-evident.

Several not-uncommon problems (all of which have been diagnosed with various versions of the Sniffer Probe) are discussed here with suggested solutions or fixes.

## TYPICAL DI/DT EMI PROBLEMS

### Rectifier Reverse Recovery

Reverse recovery of rectifiers is the most common source of di/dt-related EMI in power converters; the charge stored in P-N junction diodes during conduction causes a momentary reverse current flow when the voltage reverses. This reverse current may stop very quickly (<1ns) in diodes with a "snap" recovery (more likely in devices with a PIV rating of less than 200V), or the reverse current may

decay more gradually with a "soft" recovery. Typical Sniffer Probe waveforms for each type of recovery are shown in Figure J5.

The sudden change in current creates a rapidly changing magnetic field, which will both radiate external fields and induce low impedance voltage spikes in other circuits. This reverse recovery may "shock" parasitic L-C circuits into ringing, which will result in oscillatory waveforms with varying degrees of damping when the diode recovers. A series R-C damper circuit in parallel with the diode is the usual solution.

Output rectifiers generally carry the highest currents and are thus the most prone to this problem, but this is often recognized and they may be well-snubbed. It is not uncommon for unsnubbed catch or clamp diodes to be *more* of an EMI problem. (The fact that a diode in an R-C-D snubber may need its *own* R-C snubber is not always self-evident, for example).

# Application Note 70

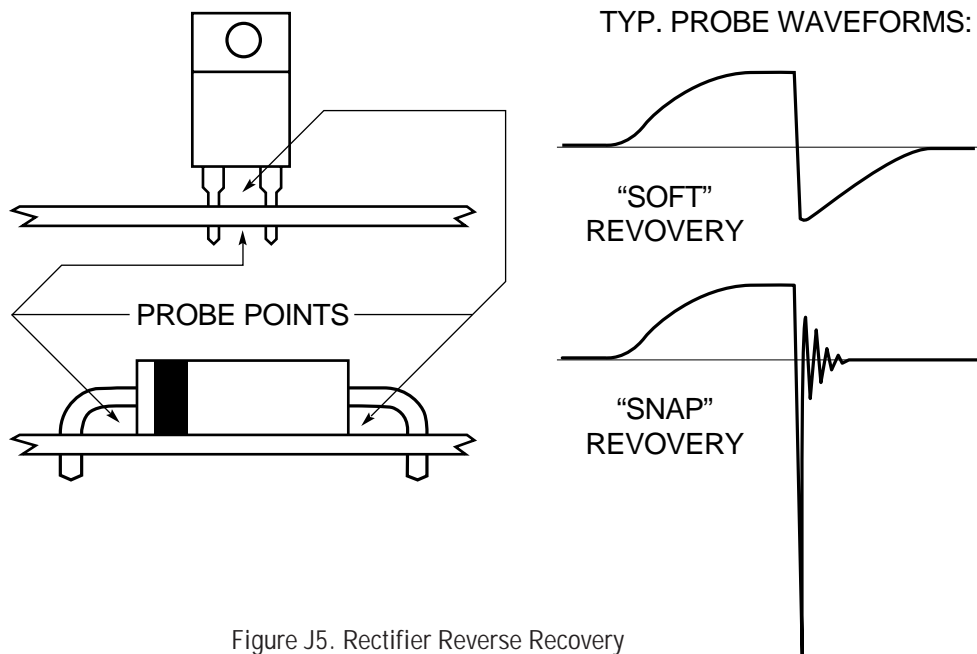


Figure J5. Rectifier Reverse Recovery  
Typical Fix: Tightly Coupled R-C Snubber

The problem can usually be identified by placing the Sniffer Probe near a rectifier lead. The signal will be strongest on the inside of a lead bend in an axial package, or between the anode and cathode leads in a TO-220, TO-247 or similar type of package, as shown in Figure J5.

Using “softer” recovery diodes is a possible solution and Schottky diodes are ideal in low voltage applications. However, it must be recognized that a P-N diode with soft recovery is also inherently lossy (while a “snap” recovery is not), as the diode simultaneously develops a reverse voltage while still conducting current: The fastest possible diode (lowest recovered charge) with a moderately soft recovery is usually the best choice. Sometimes a faster, slightly “snappy” diode with a tightly coupled R-C snubber works as well or better than a soft but excessively slow recovery diode.

If significant ringing occurs, a “quick-and-dirty” R-C snubber design approach works fairly well: increasingly large damper capacitors are placed across the diode until the ringing frequency is halved. We know that the total ringing capacity is now quadrupled or that the original ringing capacity is 1/3 of the added capacity. The damper resistance required is about equal to the capacitive reactance of

the original ringing capacity at the original ringing frequency. The “frequency halving” capacity is then connected in series with the damping resistance and placed across the diode, as tightly coupled as possible.

Snubber capacitors must have a high pulse current capability and low dielectric loss. Temperature stable (disc or multilayer) ceramic, silvered mica and some plastic film-foil capacitors are suitable. Snubber resistors should be noninductive; metal film, carbon film and carbon composition resistors are good, but wirewound resistors must be avoided. The maximum snubber resistor dissipation can be estimated from the product of the damper capacity, switching frequency and the square of the peak snubber capacitor voltage.

Snubbers on passive switches (diodes) or active switches (transistors) should always be coupled as closely as physically possible, with minimal loop inductance. This minimizes the radiated field from the change in current path from the switch to the snubber. It also minimizes the turn-off voltage overshoot “required” to force the current to change path through the switch-snubber loop inductance.

## Ringing in Clamp Zeners

A capacitor-to-capacitor ringing problem can occur when a voltage clamping Zener or TransZorb<sup>®</sup> is placed across the output of a converter for overvoltage protection (OVP). Power Zeners have a large junction capacity, and this can ring in series with the lead ESL and the output capacitors, with some of the ringing voltage showing up on the output. This ringing current can be most easily detected near the Zener leads, particularly on the inside of a bend as shown in Figure J6.

R-C snubbers have not been found to work well in this case as the ringing loop inductance is often as low or lower than the obtainable parasitic inductance in the snubber. Increasing the external loop inductance to allow damping is not advisable as this would limit dynamic clamping capability. In this case, it was found that a small ferrite bead on one or both of the Zener leads dampened the HF oscillations with minimal adverse side effects (a high permeability ferrite bead quickly saturates as soon as the Zener begins to conduct significant current).

TransZorb is a registered trademark of General Instruments, GSI.

## Paralleled Rectifiers

A less evident problem can occur when dual rectifier diodes in a package are paralleled for increased current capability, even with a tightly coupled R-C snubber. The two diodes seldom recover at exactly the same time, which can cause a very high frequency oscillation (hundreds of MHz) to occur between the capacities of the two diodes in series with the anode lead inductances, as shown in Figure J7. This effect can really only be observed by placing the probe between the two anode leads, as the ringing current exists almost nowhere else (the ringing is nearly “invisible” to a conventional voltage probe, like many other EMI effects that can be easily found with a magnetic field Sniffer Probe).

This “teeter-totter” oscillation has a voltage “null” about where the R-C snubber is connected, so it provides little or no damping (see Figure J7a). It is actually very difficult to insert a suitable damping resistance into this circuit.

The easiest way to dampen the oscillation is to “slit” the anode PC trace for an inch or so and place a damping resistor at the anode leads as shown in Figure J7b. This

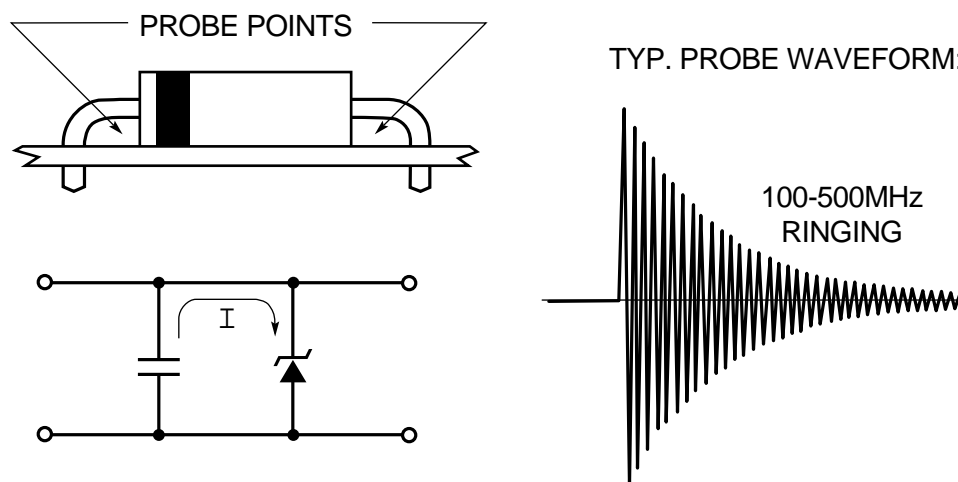


Figure J6. Ringing Between Clamp Zener and Capacitor  
Typical Fix: Small Ferrite Bead on Zener Lead(s)

# Application Note 70

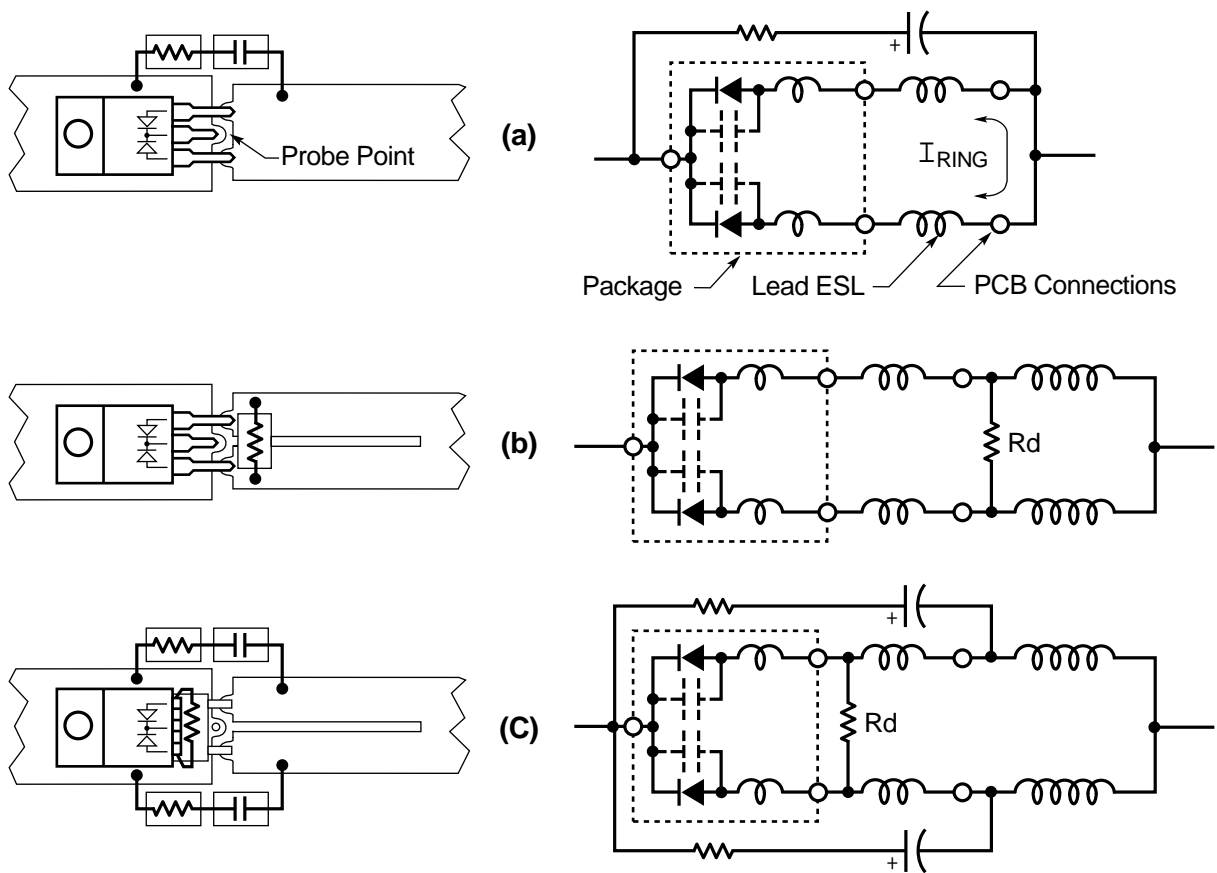


Figure J7. Ringing in Paralleled Dual Rectifiers

increases the inductance in series with the diode-diode loop external to the package and leads, while having minimal effect on the effective series inductance. Even better damping is obtained by placing the resistor across the anode leads at the entry point to the case, as shown in Figure J7c, but this violates the mindset of many production engineers.

It is also preferable to split the original R-C damper into two  $(2R) - (C/2)$  dampers, one on each side of the dual rectifier (also shown in Figure 7c). In practice, it is always preferable to use dual R-C dampers, one each side of the diode; loop inductance is cut about in half, and the external  $di/dt$  field is reduced even further due to the oppositely "handed" currents in the two snubber networks.

## Paralleled Snubber or Damper Caps

A problem similar to that with the paralleled diodes occurs when two or more low loss capacitors are paralleled and driven with a sudden current change. There is a tendency for a current to ring between the two capacitors in series with their lead inductances (or ESL), as shown in Figure J8a. This type of oscillation can usually be detected by placing the Sniffer Probe between the leads of the paralleled capacitors. The ringing frequency is much lower than with the paralleled diodes (due to the larger capacity), and the effect *may* be benign if the capacitors are sufficiently close together.

If the resultant ringing *is* picked up externally, it can be damped in a similar way as with the parallel diodes as shown in Figure J8b. In either case, the dissipation in the damping resistor tends to be relatively small.

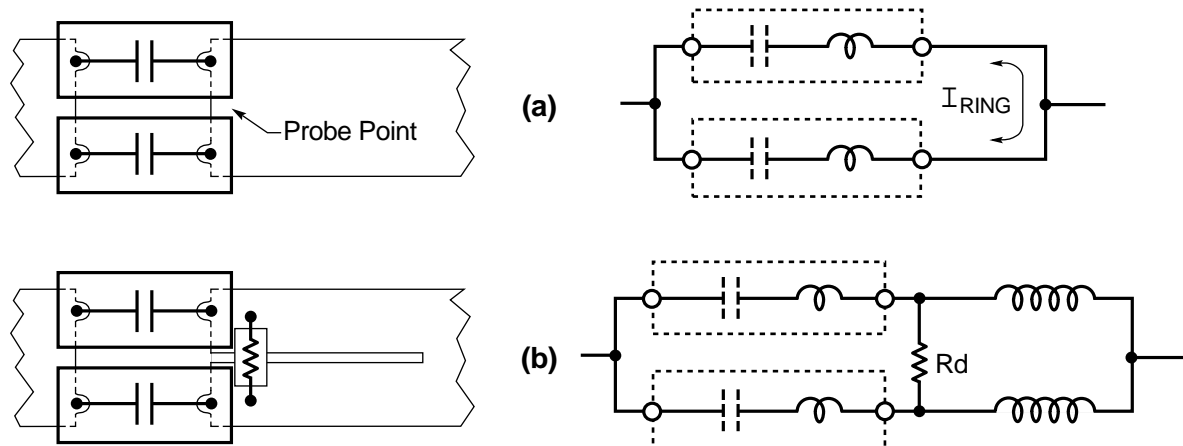


Figure J8. Ringing in Paralleled “Snubber” Capacitors

## Ringling in Transformer Shield Leads

The capacity of a transformer shield to other shields or windings ( $C_S$  in Figure J9) forms a series resonant circuit with its “drain wire” inductance ( $L_S$ ) to the bypass point. This resonant circuit is readily excited by typical square wave voltages on windings, and a poorly damped oscillatory current may flow in the drain wire. The shield current may radiate noise into other circuits, and the shield voltage will often show up as common mode conducted noise. The shield voltage is very difficult to detect with a voltage probe in most transformers, but the ringing shield current can be observed by holding the Sniffer Probe near the shield drain wire (Figure J10), or the shield current’s return path in the circuit.

This ringing can be dampened by placing a resistor  $R_D$  in series with the shield drain wire, whose value is approximately equal to the surge impedance of the resonant circuit, which may be calculated from the formula in Figure J9.

The shield capacitance ( $C_S$ ) can readily be measured with a bridge (as the capacity from the shield to all facing shields and/or windings), but  $L_S$  is usually best calculated from  $C_S$  and the ringing frequency (as sensed by the Sniffer Probe). This resistance is typically on the order of tens of ohms.

One or more small ferrite beads can also be placed on the drain wire instead to provide damping. This option may be preferable as a late “fix” when the PC board has already been laid out.

In either case, the damper losses are typically quite small. The damper resistor has a moderately adverse impact on shield effectiveness below the shield and drain wire resonant frequency; damper beads are superior in this respect as their impedance is less at lower frequencies. The drain wire connection should also be as short as possible to the circuit bypass point, both to minimize EMI and to raise the shield’s maximum effective (i.e., resonant) frequency.

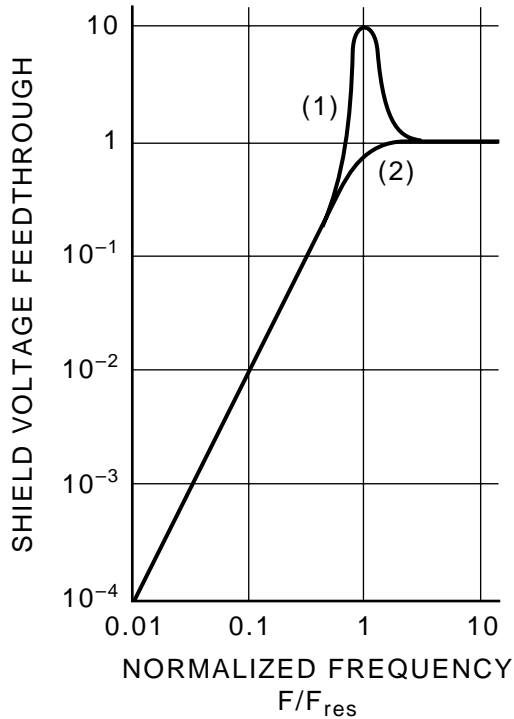
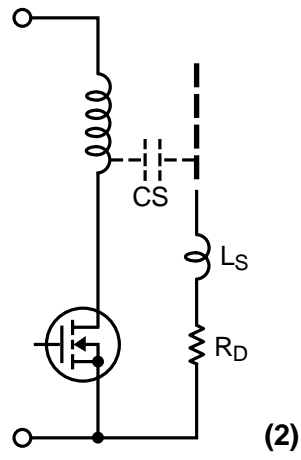
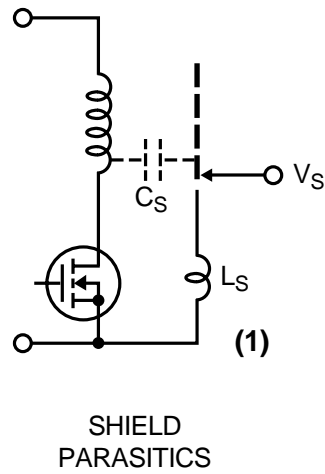
## Leakage Inductance Fields

Transformer leakage inductance fields emanate from between primary and secondary windings. With a single primary and secondary, a significant dipole field is created, which may be seen by placing the Sniffer Probe near the winding ends as shown in Figure J11a. If this field is generating EMI, there are two principal fixes:

1. Split the Primary *or* Secondary in two, to “sandwich” the other winding, and/or:
2. Place a shorted copper strap “electromagnetic shield” around the *complete-core and winding* assembly as shown in Figure J12. Eddy currents in the shorted strap largely cancel the external magnetic field.

The first approach creates a “quadrupole” instead of a dipole leakage field, which significantly reduces the distant field intensity. It also reduces the eddy current losses in any shorted strap electromagnetic shield used, which may or may not be an important consideration.

# Application Note 70



SHIELD RESONANCE  
CAN BE DAMPED WITH  
A RESISTOR "R<sub>D</sub>" OR A  
SMALL FERRITE BEAD:

$$R_D \cong \sqrt{\frac{L_S}{C_S}}$$

Figure J9. Shield Effectiveness at High Frequencies Is Limited by Shield Capacity and Lead Inductance



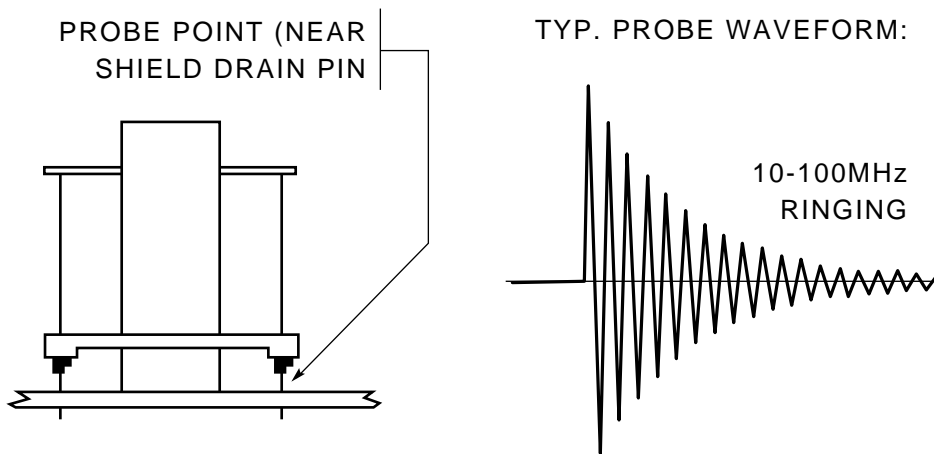


Figure J10. Transformer Shield Ringing  
 Typical Fix:  $10\Omega$  to  $100\Omega$  Resistor  
 (or Ferrite Bead in Drain Wire)

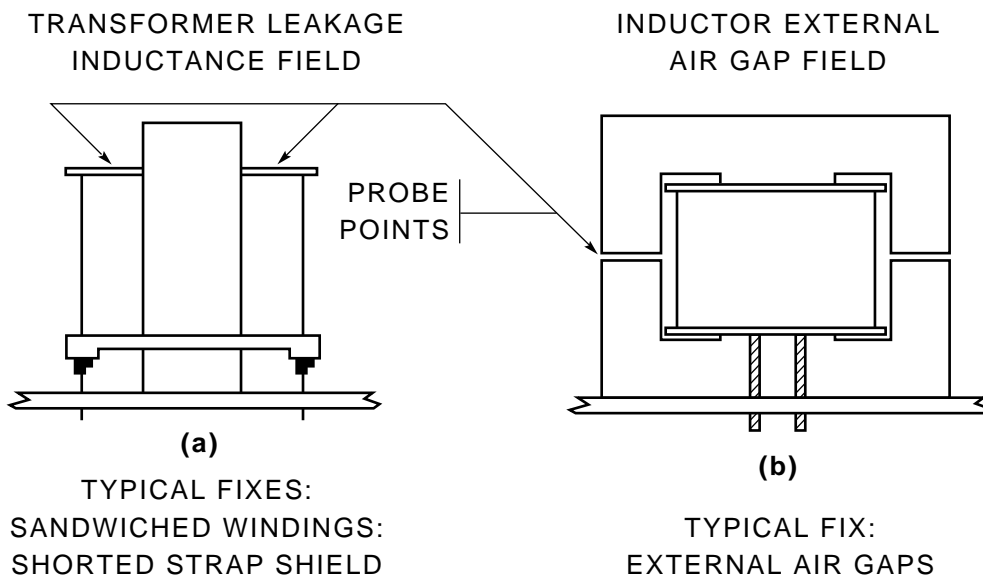


Figure J11. Probe Voltages Resemble the Transformer and Inductor Winding Waveforms

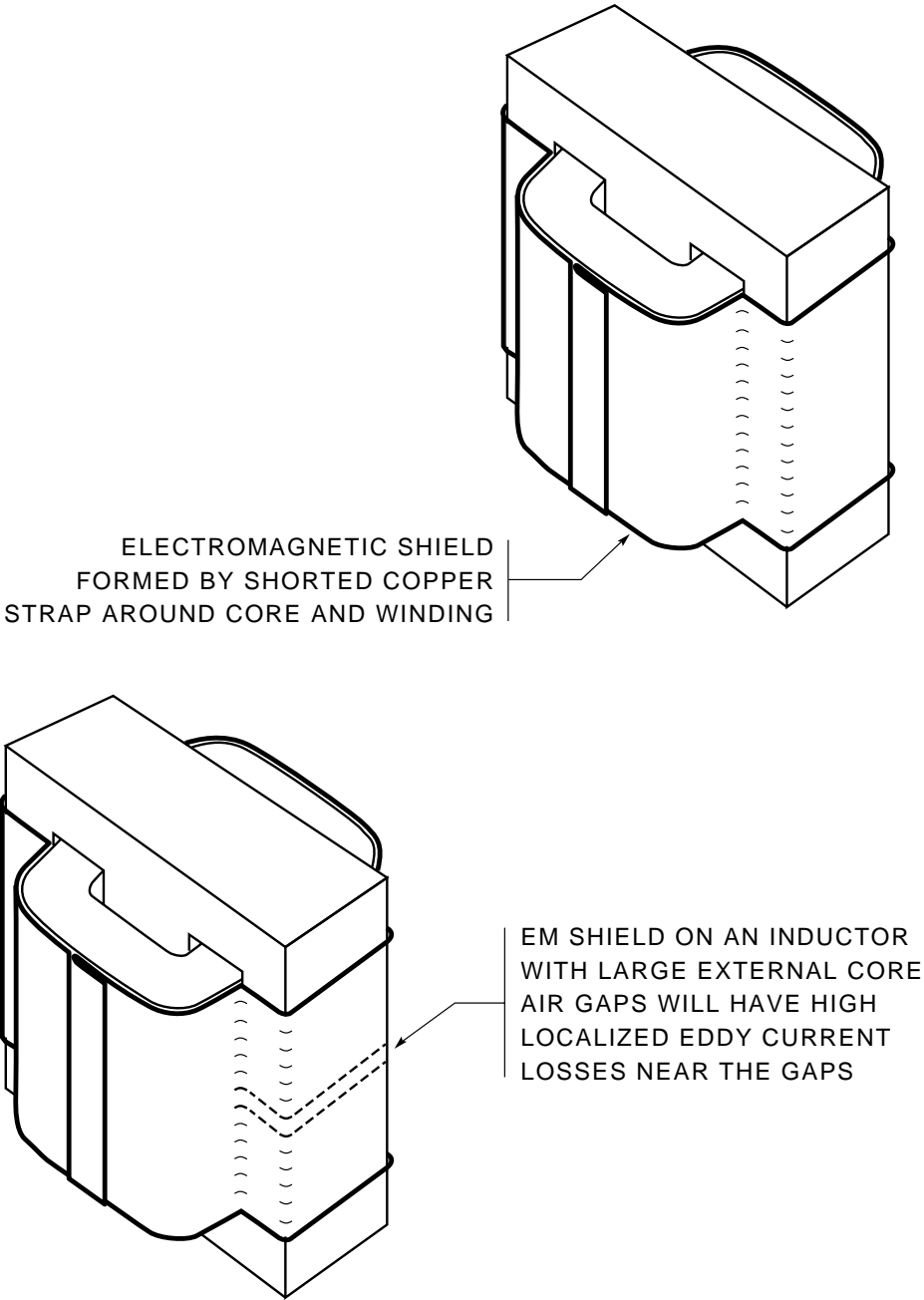


Figure J12. A "Sandwiched" PRI-SEC Transformer Winding Construction Reduces Electromagnetic Shield Eddy Current Losses

### External Air Gap Fields

External air gaps in an inductor, such as those in open “bobbin core” inductors or with “E” cores spaced apart (Figure J11b), can be a major source of external magnetic fields when significant ripple or AC currents are present. These fields can also be easily located with the Sniffer Probe; response will be a maximum near an air gap or near the end of an open inductor winding.

“Open” inductor fields are not readily shielded and if they present an EMI problem the inductor must usually be redesigned to reduce external fields. The external field around spaced E cores can be virtually eliminated by placing all of the air gap in the center leg. Fields due to a (possibly intentional) residual or minor outside air gap can be minimized with the shorted strap electromagnetic shield of Figure J12, if eddy current losses prove not to be too high.

A less obvious problem may occur when inductors with “open” cores are used as second stage filter chokes. The minimal ripple current may not *create* a significant field, but such an inductor can “pick up” external magnetic fields and convert them to noise voltages or be an EMI *susceptibility* problem.<sup>3</sup>

### Poorly Bypassed High Speed Logic

Ideally, all high speed logic should have a tightly coupled bypass capacitor for each IC and/or have power and ground distribution planes in a multilayer PCB.

At the other extreme, I have seen *one* bypass capacitor used at the power entrance to a logic board, with power and ground led to the ICs from opposite sides of the board. This created large spikes on the logic supply voltage and produced significant electromagnetic fields around the board.

With a Sniffer Probe, I was able to show which pins of which ICs had the larger current transients *in synchronism* with the supply voltage transients. (The logic design engineers were accusing the power supply vendor of creating the noise. I found that the supplies were fairly quiet; it was the poorly designed logic power distribution system that was the problem.)

### Probe Use with a “LISN”

A test setup using the Sniffer Probe with a Line Impedance Stabilization Network (LISN) is shown in Figure J13. The optional “LISN AC LINE FILTER” reduces AC line voltage feedthrough from a few 100mV to microvolt levels, simplifying EMI diagnosis when a suitable DC voltage source is not available or cannot be used.

### TESTING THE SNIFFER PROBE

The Sniffer Probe can be functionally tested with a jig similar to that shown in Figure J14, which is used to test probes in production.

---

Note 3: Ed Note. See Appendix H for additional commentary.

# Application Note 70

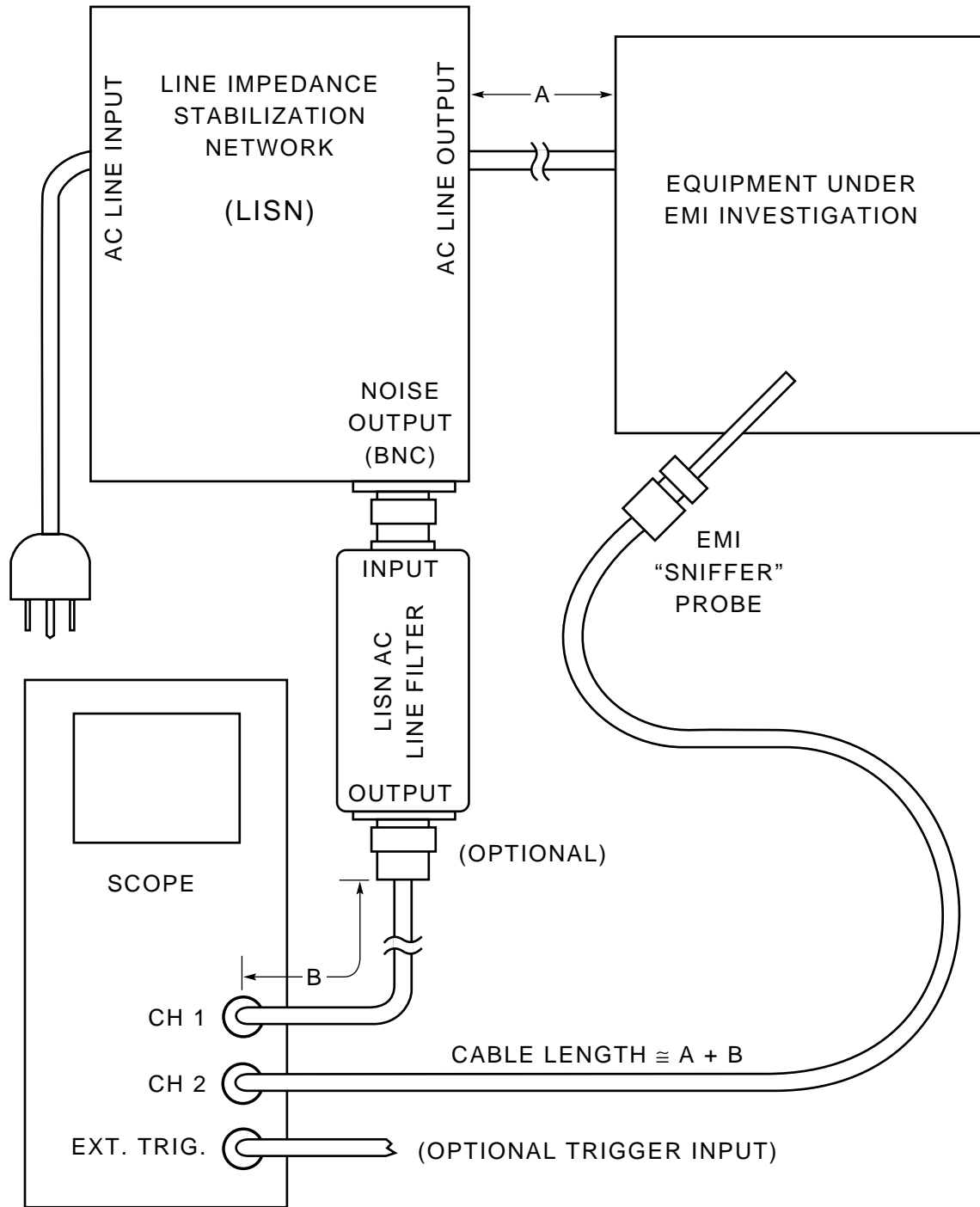
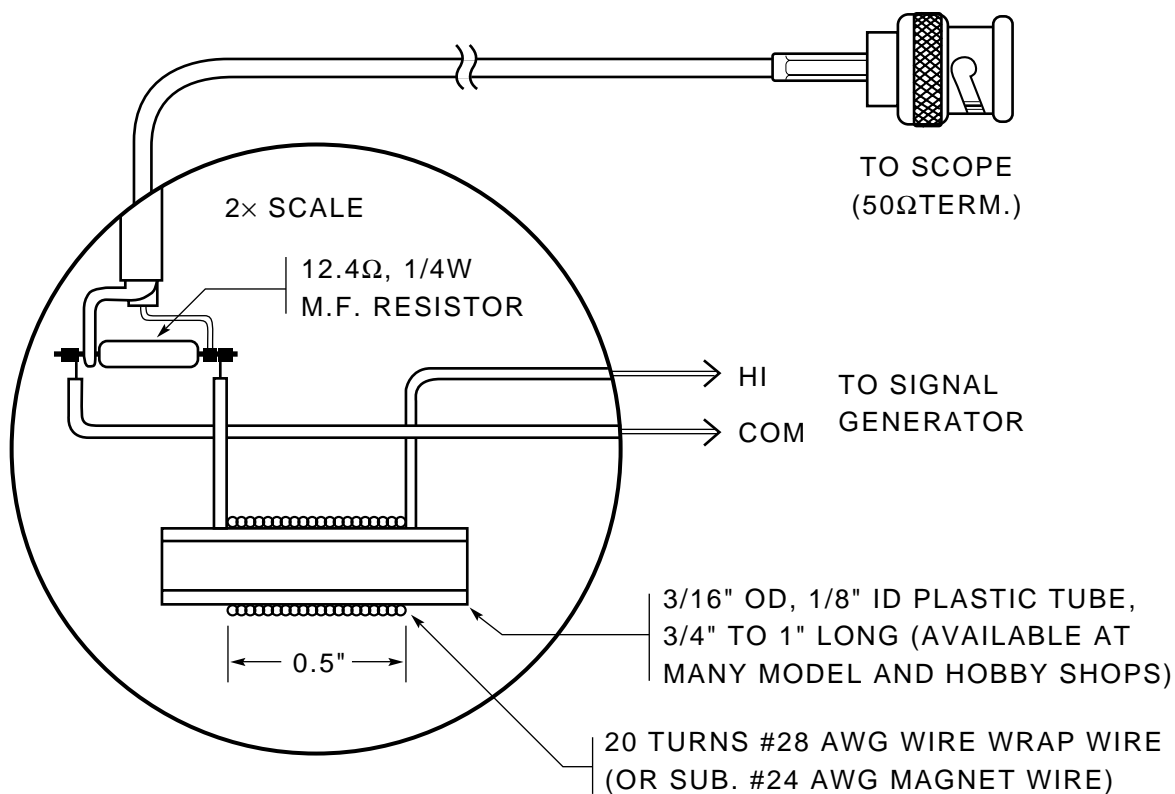


Figure J13. Using the Probe with a "LISN"



The Sniffer Probe Tip is centered inside the test coil where the Probe voltage is greatest. The approximate flux density in the middle of a coil can be calculated from the formula:

$$B = H = 1.257 NI/I \quad (\text{CGS Units})$$

For the 1.27cm long, 20-turn test coil, the flux density is about 20 Gauss per amp. At 1MHz, the Sniffer Probe voltage is 19mV<sub>P-P</sub> (±10%) per 100mA<sub>P-P</sub> for a 1MΩ load impedance, and half that for a 50Ω load.

Figure J14. EMI "Sniffer" Probe Test Coil

# Application Note 70

---

## CONCLUSION

The Sniffer Probe is a simple, but very fast and effective means to locate  $di/dt$  sources of EMI. These EMI sources are very difficult to locate with conventional voltage or current probes.

## SUMMARY

A summarized procedure for using the EMI "Sniffer" Probe appears in Figure J15.

- 1) Use a 2-channel scope, preferably one with an external trigger.
- 2) One scope channel is used for the Sniffer Probe, which is not to be used for triggering.
- 3) The second channel is used to view the noise transient whose source is to be located, which may also be used for triggering if practical.
- 4) More stable and reliable triggering is achieved with an "external trigger" ( or a 3rd channel) on a transistor drive waveform (or preceding logic transition), allowing immediate precursors to the transient to be viewed. (Nearly all noise transients occur during, or just after, a power transistor turn-on or turn-off.
- 5) Start with the Probe at some distance from the circuit with maximum sensitivity and "sniff around" for something happening in *precise sync* with the noise transient. The Probe waveform will not be identical to the noise transient, but will usually have a strong resemblance.
- 6) Move the Probe closer to the suspected source while decreasing sensitivity. The conductor carrying the responsible current is located by the sharp response null on top of the conductor with inverted polarity on each side.
- 7) Trace out the noise current path as much as possible. Identify the current path on the schematic.
- 8) The source of the noise transient is usually evident from the current path and the timing information.

© 1997, BRUCE CARSTEN ASSOCIATES, Inc.

Figure J15. EMI "Sniffer" Probe Procedure Outline



## SNIFFER PROBE AMPLIFIER

Figure J16 shows a 40MHz amplifier for the Sniffer Probe. A gain of 200 allows an oscilloscope to display probe output over a wide range of sensed inputs. The amplifier is built into a small aluminum box. The probe should connect to the amplifier via BNC cable, although the 50Ω

termination does not have to be a high quality coaxial type. The probe's uncalibrated, relative output means high frequency termination aberrations are irrelevant. A simple film resistor, contained in the amplifier box, is adequate. Figure J17 shows the Sniffer Probe and the amplifier.

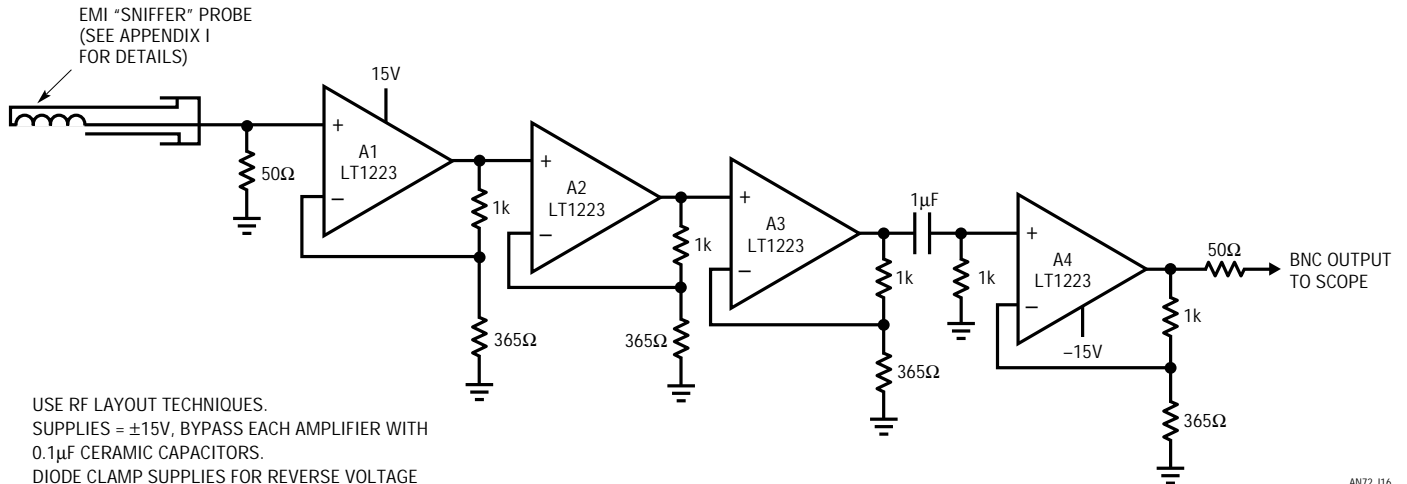


Figure J16. 40MHz Amplifier for EMI Probe

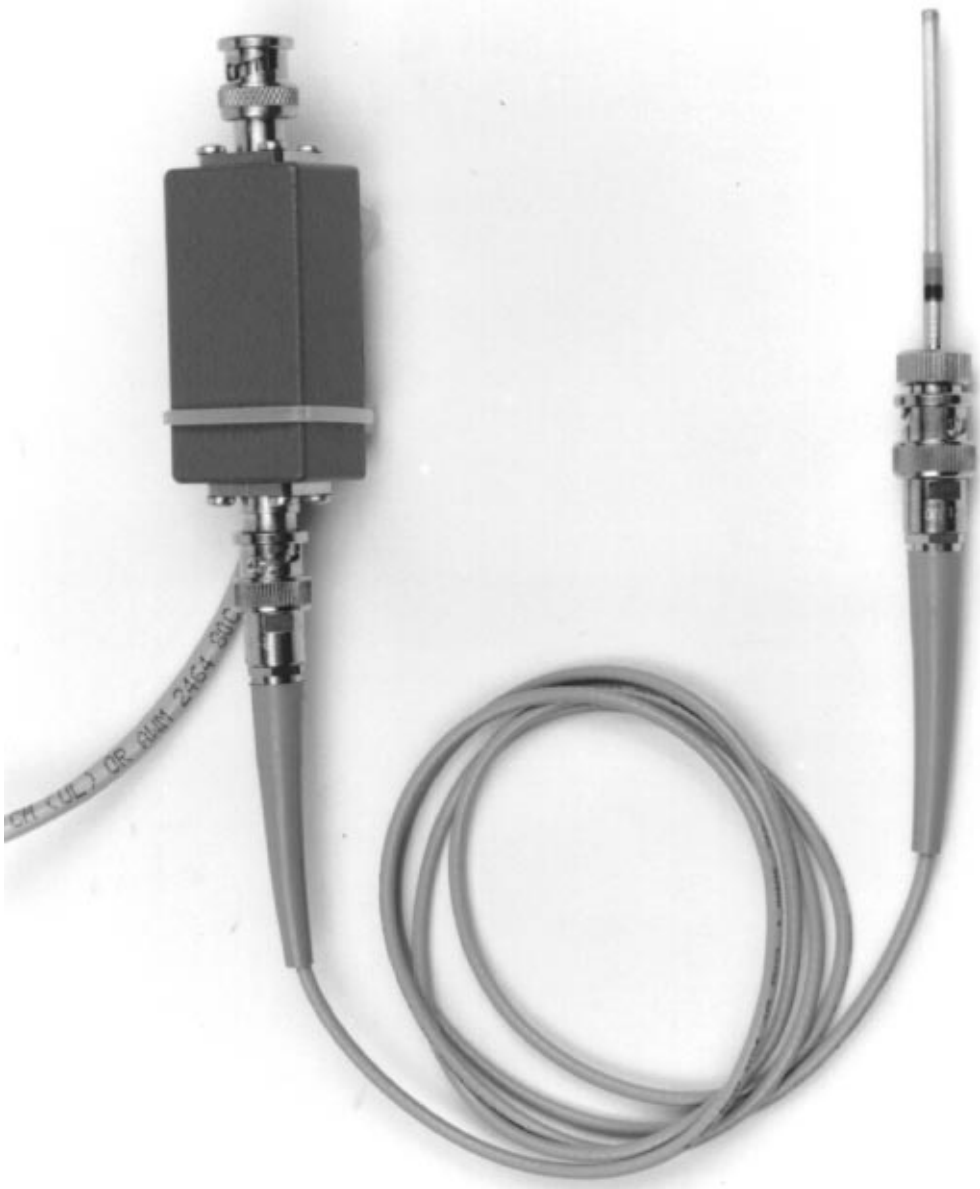


Figure J17. Sniffer Probe and Amplifier. Note All BNC-Based Signal Transmission.  
±15V Power Enters Box via Separate Cable

## APPENDIX K

### SYSTEM-BASED NOISE "MEASUREMENT"

The ultimate test of switching regulator noise is its effect on the system being powered. The data below was taken using an LT1533 powering an LT1605 16-bit A/D converter. Crossplots for integral and differential nonlinearity

are shown for bench supply vs LT1533 supply powered operation. The difference is within the test systems limit-of-error.

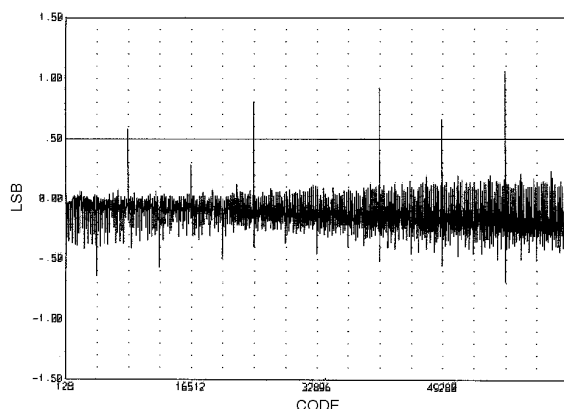


Figure K1. Differential Nonlinearity Using Bench Supply

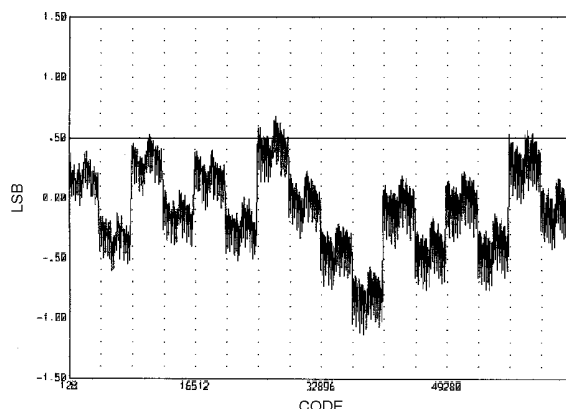


Figure K4. Integral Nonlinearity Using Bench Supply

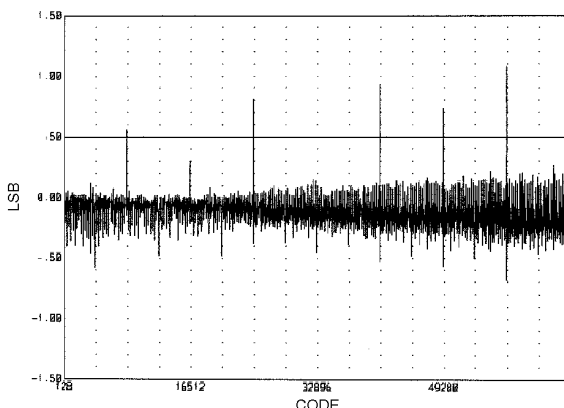


Figure K2. Differential Nonlinearity Using LT1533 Supply

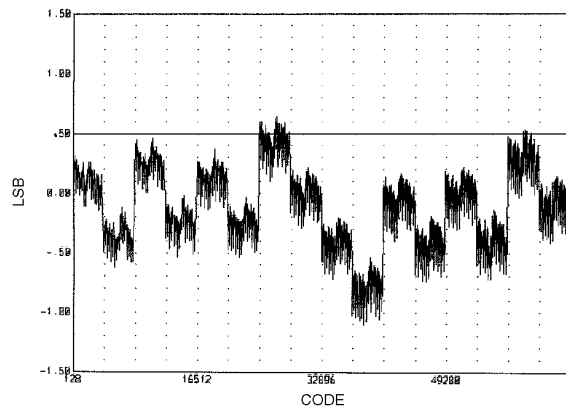


Figure K5. Integral Nonlinearity Using LT1533 Supply

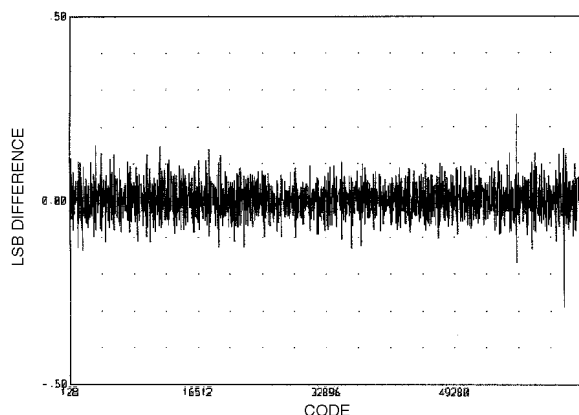


Figure K3. Subtraction of Above Plots. Residual Error Is Test System Limited

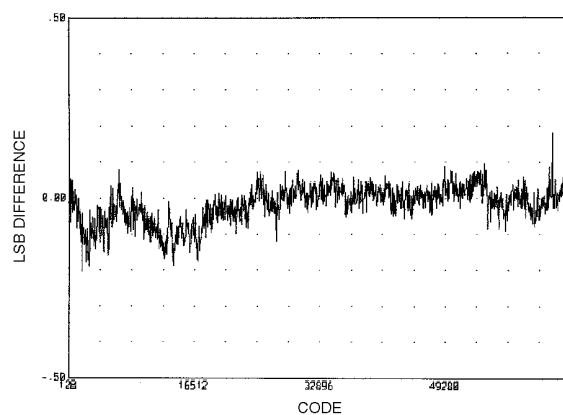


Figure K6. Subtraction of Above Plots. Residual Error Is Test System Limited

# Application Note 70

